

Cover Page



Universiteit Leiden



The handle <http://hdl.handle.net/1887/18947> holds various files of this Leiden University dissertation.

Author: Wit-van der Veen, Berlinda Jantina de

Title: Quantitative nuclear cardiology using SPECT : evaluation of perfusion, function and innervation

Date: 2012-05-15

QUANTITATIVE NUCLEAR CARDIOLOGY USING SPECT

Evaluation of perfusion, function and innervation

Berlinda Jantina de Wit – van der Veen

ISBN/EAN: 9789461082916

Production

Cover and layout by B.J. de Wit - van der Veen

Printed by Gildeprint (Enschede)

Copyrights

© 2011 B.J. de Wit-van der Veen, no part of this thesis may be reproduced, stored, or transmitted in any form, or by any means, without prior permission from the author.

Chapter 2 European Journal of Nuclear Medicine and Molecular Imaging

Chapter 3 Clinical Nuclear Medicine

Chapter 4 Journal of Nuclear Cardiology

Chapter 5 European Journal of Nuclear Medicine and Molecular Imaging

Chapter 6 Nuclear Medicine Communications

Chapter 7 Journal of Nuclear Cardiology

The financial support provided by **VANDERWILT techniques**, **GE Healthcare** and **Invia Medical Imaging Solutions** for the costs associated with the publication of this thesis is gratefully acknowledged.

QUANTITATIVE NUCLEAR CARDIOLOGY USING SPECT

Evaluation of perfusion, function and innervation

PROEFSCHRIFT

ter verkrijging van
de graad van Doctor aan de Universiteit Leiden,
op gezag van de Rector Magnificus prof.mr. P.F. van der Heijden,
volgens besluit van het College voor Promoties
te verdedigen op 15 mei 2012
klokke 15.00 uur

door

Berlinda Jantina de Wit – van der Veen

geboren te Vries
in 1984

Promotor: Prof. dr. A. de Roos

Copromotor: Dr. M.P.M. Stokkel

(Nederlands Kanker Instituut – Antoni van Leeuwenhoek Ziekenhuis)

Commissieleden: Prof. dr. P.P. van Rijk

Prof. dr. ir. B.P.F. Lelieveldt

Prof. dr. E.E. van der Wall

Dr. A.J.H.A. Scholte

Dr. H.J. Verberne

(Academisch Medisch Centrum – Universiteit van Amsterdam)

The research described in this thesis was carried out at the Department of Radiology (head: prof. dr. J.L. Bloem), section Nuclear Medicine of the Leiden University Medical Centre.

Financial support by the **Dutch Heart Foundation** for the publication of this thesis is gratefully acknowledged.

To my husband and my parents

TABLE OF CONTENTS

<i>Chapter 1</i>	<i>General introduction and outline</i>	9
------------------	---	---

Part I. Gated Myocardial Perfusion Scintigraphy

<i>Chapter 2</i>	<i>The impact of a new software package</i>	27
------------------	---	----

The consequences of a new software package for the quantification of gated-SPECT myocardial perfusion studies.

<i>Chapter 3</i>	<i>Relevance of the injection-acquisition time interval</i>	47
------------------	---	----

The effects of early and late scanning on image quality and functional parameters in myocardial perfusion imaging.

<i>Chapter 4</i>	<i>Transient Ischemic Dilatation</i>	61
------------------	--------------------------------------	----

Transient Ischemic Dilatation ratio derived from myocardial perfusion scintigraphy; What are we looking at?

<i>Chapter 5</i>	<i>Ventricular dyssynchrony</i>	79
------------------	---------------------------------	----

Ventricular dyssynchrony assessed by gated myocardial perfusion SPECT using a geometrical approach: a feasibility study.

Part II. Myocardial Innervation Scintigraphy

<i>Chapter 6</i>	<i>Quantitative parameters of planar I-123 MIBG studies</i>	99
------------------	---	----

Mathematical methods to determine quantitative parameters of myocardial I -123 MIBG studies: a review of the literature.

<i>Chapter 7</i>	<i>Volumetric quantification of I-123 MIBG SPECT</i>	<i>123</i>
	Assessment of global cardiac I-123 MIBG uptake and washout using volumetric quantification of SPECT acquisitions.	
<i>Chapter 8</i>	<i>Summary and conclusions</i>	<i>143</i>
	<i>Nederlandse samenvatting en conclusies</i>	<i>151</i>
	<i>Curriculum vitae and publications</i>	<i>159</i>
	<i>Acknowledgements</i>	<i>165</i>

Chapter 1

General introduction and outline

Cardiovascular diseases and ischemic heart diseases in particular, are a major health problem in the westernized countries. Still, a considerable number of the morbidity and mortality incidences as a result from these diseases could be prevented. Therefore, cardiovascular medicine has concentrated on prevention, early diagnosis and risk stratification in the recent years.¹⁻² Non-invasive imaging techniques are an essential tool in realising this approach. The application of nuclear imaging for non-invasive assessment of various cardiovascular diseases is nowadays well established. Myocardial perfusion scintigraphy, which is the most frequently performed study in the nuclear cardiology, is considered an accurate, safe and cost-effective method for diagnosing and evaluating ischemic heart diseases.³⁻⁷ A normal MPS study is associated with an annual risk for myocardial infarction of less than 1%, making it also an very valuable technique for riskstratification.⁷

Although the visual assessment of myocardial perfusion will remain the mainstay of cardiovascular nuclear medicine for some time, the field is changing. Advancements in device technology, processing techniques and radiopharmaceuticals has shifted the field beyond assessment of perfusion alone.⁸ The following paragraphs will provide an overview of this ongoing evolution within nuclear cardiology.

A HISTORICAL VIEW ON PERFUSION IMAGING

Radioactive tracers have been used since the late 1940's to study biochemical processes within the human body. The clinical use of nuclear medicine underwent an unparalleled growth in the 1950's due to the increasing knowledge on radionuclides and the introduction of new methods to detect radioactivity. The field of quantitative nuclear cardiology has its roots in the early seventies when perfusion protocols using ionic tracers such as Thallium-201 (Tl-201) became available.⁹⁻¹² Today, acquisition protocols similar to these early protocols are still being used to visually discriminate between normal, ischemic or infarcted myocardium.¹³ However, in the 1980's two advances were introduced that had a major impact on the quantification; the Technetium-99m (Tc-99m) labelled perfusion tracers and single photon emission computer tomography (SPECT).

Perfusion tracers

Both Tl-201 and Tc-99m labelled tracers are usable for scintigraphic imaging, though the physical properties of Tc-99m make it more suitable for imaging than Tl-201. The main

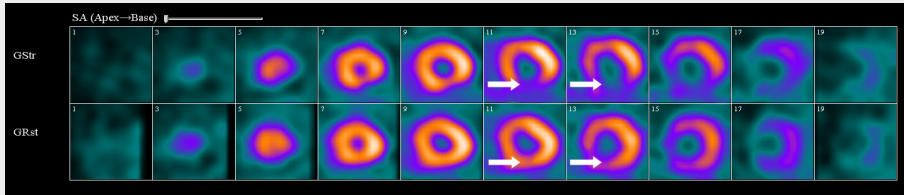


Figure 1. Short axis images obtained after a stress/rest protocol. The upper images show the stress acquisition, in which a heterogeneous distribution pattern is apparent with several perfusion defects (arrows). The lower images represent the rest acquisition where the distribution is more homogenous and the defects are largely filled (arrows). This combination of perfusion defects in the stress acquisition and a near normal perfusion pattern in the rest acquisitions advocates for myocardial ischemia.

advantages of Tc-99m include; a short half-life of approximately six hours, widespread availability from a molybdenum generator and a photon energy of 140 keV which is ideal for scintigraphic imaging.¹⁴ The first Tc-99m labelled perfusion tracer to be approved for clinical use was 2-methoxy-isobutylisonitrile (also known as sestamibi).¹⁴⁻¹⁶ Later on, Tc-99m labelled tetrofosmin was introduced as an alternative for sestamibi. Both tetrofosmin and sestamibi are currently approved and are widely used in clinical practice. Given that both radiotracers have a positive charge, they are trapped within the mitochondria by the relative negative transmembrane potential of the cardiomyocytes. This property ensures that the distribution of Tc-99m within the myocardium will remain roughly the same over time. Tl-201, on the other hand, is a potassium analogue that is not retained within cardiomyocytes and is constantly exchanged between the intra- and extracellular space. This so called redistribution of Tl-201 has been used to study the dynamic properties of cardiac perfusion.^{15, 16}

Single photon emission computer tomography

SPECT is the second important advancement that was introduced. Despite the fact that the mathematical principles for this technology were already developed years before, it was not until the late seventies that tomographic perfusion imaging was first applied.¹⁸⁻²⁰ Tomographic imaging uses a detector system that rotates around the patient acquiring images from different directions. Mathematical algorithms are applied to reconstruct the set of projection images into a three-dimensional dataset. These data are visualized in the standard views for cardiac imaging, which are the vertical long axis, the horizontal long

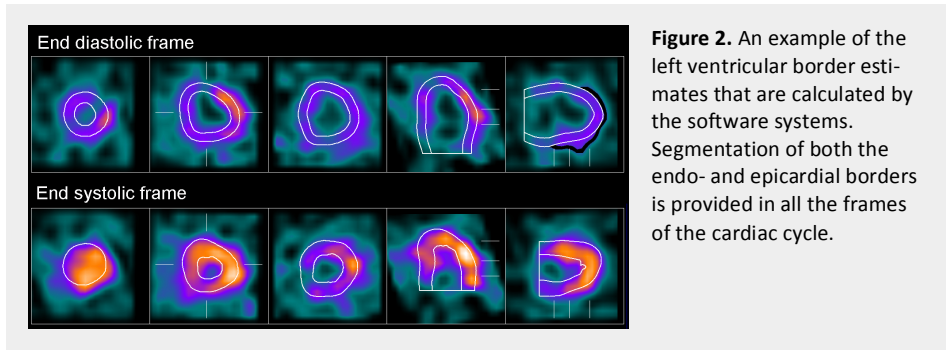
axis and the short axis. Figure 1 shows short axis images of both normal and abnormal perfusion patterns for a standard post-stress/rest MPS imaging protocol.

Basic principles of perfusion imaging

Despite all these developments, the underlying principles of perfusion imaging remained more or less unchanged. Myocardial tracer uptake is related to the coronary blood flow, so when the vascular bed is able to provide adequate flow, tracer uptake is homogenous throughout the myocardium.¹⁷ In the presence of coronary artery disease (CAD), the ability of the vascular bed to provide sufficient flow is inversely related to the severity of a stenosis. To visualise perfusion abnormalities more clearly, physical stress is applied. Stress induces an augmentation of coronary flow in order to meet the increased oxygen demand of the myocytes. In CAD, augmentation of the blood flow will be inadequate resulting in a reduced or absent tracer uptake in areas distal to a stenosis. To distinguish between normal, ischemic and infarcted regions, images acquired at rest and post-stress are compared. If the tracer distribution is abnormal after stress and restores to normal in rest, myocardial ischemia is present (also known as *reversible* perfusion defect). Often medical therapies like percutaneous coronary intervention or revascularization surgery are considered in these patients. Defects that remain unchanged in the post-stress and rest images represent areas of severe myocardial ischemia or scarring (also known as *persistent* perfusion defects).^{6,7}

Early quantification techniques

The perfusion images were initially assessed by visual interpretation alone. Even up to this day, visual assessment of perfusion remains an important aspect of MPS.⁸ Still, in the late seventies researchers started to obtain quantitative measures from the MPS.²¹ Initially, only planar images were used for quantification. Tracer uptake was quantified by creating linear count profiles along pre-defined paths.^{22, 23} Later on, an automated method was introduced that constructs circumferential count profiles along paths radiating from the centre of the left ventricle in short axis SPECT images.^{24, 25} Rendering these count profiles into so called '*polarmaps*' resulted in a simple two-dimensional visualization of the tracer distribution, that is unaffected by anatomical variations (see Figure 2). The principle of polarmaps is still being used today to quantify and display various aspects of cardiac perfusion and innervation.



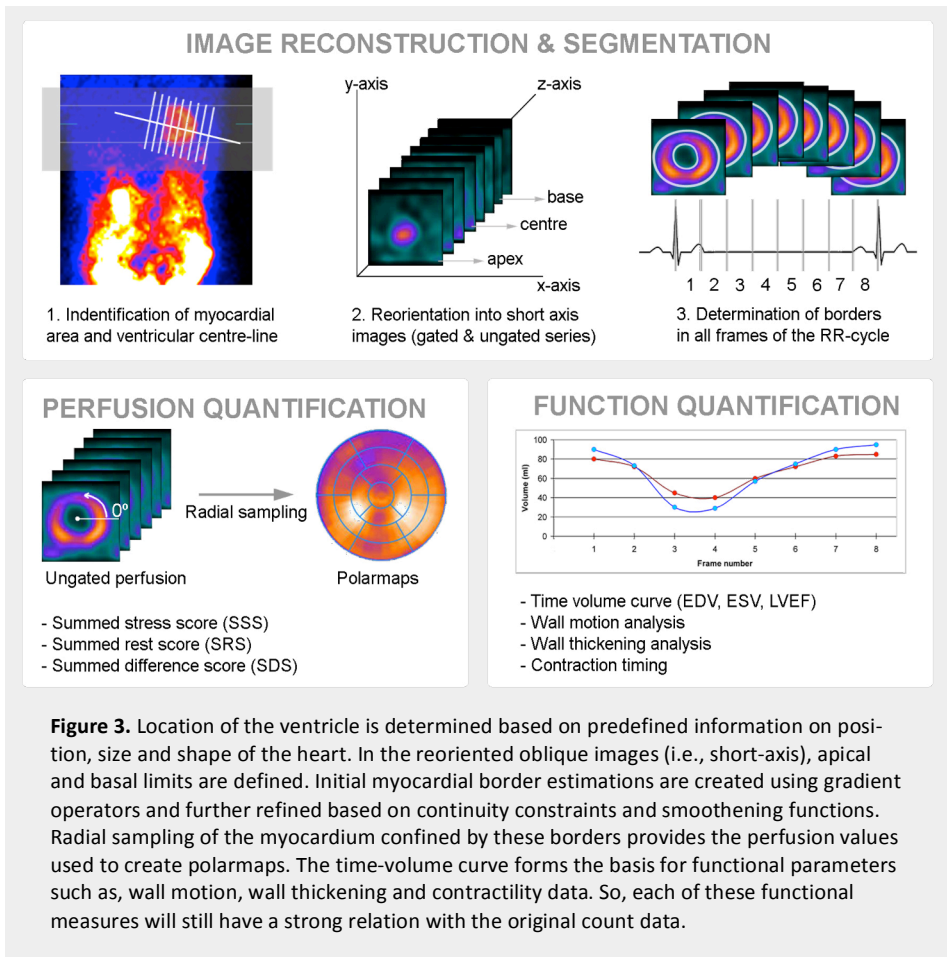
CONTEMPORARY QUANTITATIVE NUCLEAR CARDIOLOGY

Both hardware and software to obtain and process MPS have considerably improved since these early attempts. The addition of the time-based electrocardiogram (ECG) signal to the SPECT acquisition has stimulated the development of new quantification methods. At present, entirely automated software systems are available that integrate information from different cardiac studies and add easy quantification of perfusion, function and innervation to the visual findings.

Functional evaluation by gated SPECT

The majority of nuclear cardiac imaging today is performed using ECG-gated SPECT. Though different acquisition protocols are described in the recent guidelines, they all deduce to the same basic principle.²⁶ An ECG is recorded during SPECT acquisition and allows for allocation of the measured counts into specific intervals within the cardiac cycle (this acquisition method is called *frame-mode*). Most often, the cardiac cycle is divided into either 8 or 16 'frames'. Because all projection images are reconstructed into transaxial images, a four-dimensional dataset (i.e. time, x, y, z) is created.²⁷⁻²⁹

The addition of a time-based signal allows for evaluation of cardiac function by determining indices such as time-volume curves, wall motion, wall thickening and contraction timing. Frequently, an increased specificity of gated SPECT is reported which can be assigned to the more effective characterisation of true perfusion defects.³⁰⁻³¹ Additionally, multiple studies indicate an added prognostic value and improved risk-stratification when functional parameters are used in combination with visual interpreta-



tion of perfusion patterns.³²⁻³⁵ Furthermore, the reproducibility of quantitative indices is generally considered equivalent or better than the visual analysis.^{36, 37}

Modern quantitative software systems

Various commercial and non-commercial systems are nowadays available, each applying their own algorithms and characteristics. Still, the fundamental operations in most tools include; 1) localization of the heart, 2) extraction of the midventricular axis, basal and apical limits, 3) determination of the myocardial borders, and, 4) calculation of parameters.³⁸⁻⁴¹ Due to the relatively limited camera resolution compared to the thickness of the myocardial wall, it is difficult to delineate the wall exactly. Therefore,

automated algorithms use predefined information on the shape, continuity and average wall thickness to estimate the myocardial contours in one cardiac frame. This initial estimate is scaled, with preservation of volume, to the other frames.

Though many software tools were traditionally developed to display perfusion images, they also allow assessment of myocardial function, viability and innervation. Modern tools will also depict SPECT images in combination with anatomical information from computer tomography (CT) or magnetic resonance imaging (MRI), thus providing a true platform for integrated nuclear cardiology. This development was further encouraged by the addition of hybrid scanners to the field of nuclear cardiology. These cameras combine fast acquisition protocols with new reconstruction algorithms and are able to assess anatomy, function and perfusion. Based on these advances the new focus of nuclear cardiology is now on the reduction of dose and acquisition time.⁴²⁻⁴⁵

Imaging cardiac nervous function

The assessment of sympathetic innervation within the heart is also gradually becoming an important technology. At present, I-123 labelled meta-iodobenzylguanidine (MIBG) is the only valid SPECT radiopharmaceutical to assess cardiac adrenergic nerve function. This specific technique has been around since 1980's, but is still not considered a routine clinical imaging method.

I-123 MIBG resembles the neurotransmitter norepinephrine with respect to its molecular structure, synaptic uptake and intracellular storage. The main difference is that, unlike norepinephrine, I-123 MIBG does not participate in signalling processes nor in the enzymatic degradation pathways, making it a suitable radiotracer to assess nervous function.^{49, 50} Figure 4 provides a schematic overview of the kinetics of both norepinephrine and I-123 MIBG. Normal individuals have a fairly homogenous distribution of adrenergic fibres, and accordingly I-123 MIBG uptake, throughout the myocardium. Abnormalities in the adrenergic nerve function can result from various diseases.⁴⁶⁻⁴⁸ Figure 5 shows an example of the planar images of a normal I-123 MIBG distribution.

An I-123 MIBG acquisition protocol usually consists of one image obtained within minutes after tracer injection (*early*) and one obtained several hours after tracer injection (*delayed*).⁵¹ Anterior planar images are acquired to assess global I-123 MIBG uptake and washout (i.e., the difference between early and delayed accumulation) from the cardiac region in relation to the non-specific I-123 MIBG uptake. It is thought that the early heart-to-mediastinum (HM) ratio reflects the initial uptake of I-123 MIBG by the

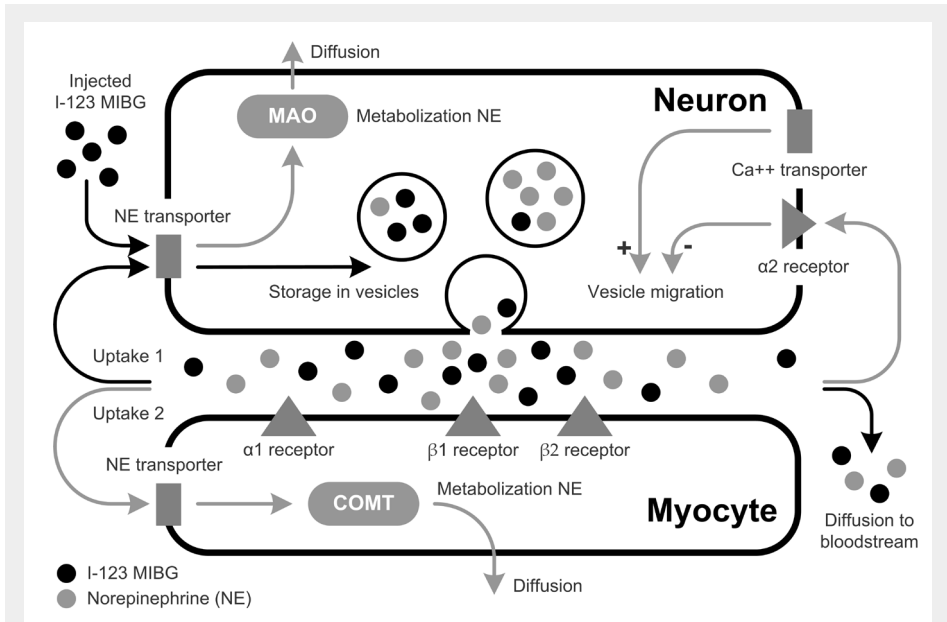
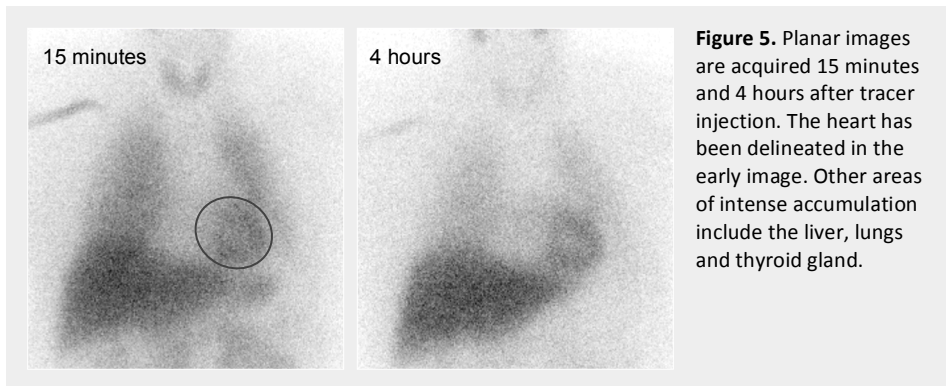


Figure 4. This diagram schematically displays the uptake, storage and degradation of norepinephrine (NE). The pathways shared by both NE and I-123 MIBG are shown in black. NE is synthesized within postganglionic neurons by a series of enzymatic steps and eventually stored in vesicles. Once released, NE will either interact with adrenergic receptors, enter the neuron ('Uptake 1'), enter the myocyte ('Uptake 2') or diffuse to the bloodstream. Intravenous injected MIBG disperses through the bloodstream and will enter the neuron by the Uptake-1 pathway. I-123 MIBG does not participate in the signalling processes, or in the enzymatic degradation, instead it is stored in the NE vesicles and co-released with NE during nerve excitement. Similar to NE, I-123 MIBG will partly diffuse through the bloodstream or for a second time enter the neuron through the Uptake-1 mechanism. These processes will result in a physiological washout of I-123 MIBG from the neurons over time.

Uptake-1 mechanism, whereas the washout rate is considered a measure for the integrity and activity of the neurons. The addition of a I-123 MIBG SPECT acquisition to an imaging protocol allows for visual assessment of the regional innervation patterns, which may be advantageous in diseases where the cardiac innervation is affected in a heterogeneous manner.⁵²

CLINICAL CONSIDERATIONS OF QUANTIFICATION

All aforementioned advances have contributed greatly to the shift from evaluating perfusion abnormalities alone, towards describing perfusion in conjunction with



function and/or innervation. Both acquisition and interpretation of the MPS acquisitions are, to a large extent, standardized and described in guidelines.^{13,26} For cardiac innervation imaging, on the other hand, there are currently no guidelines available. Still, acquisition, processing and evaluation of SPECT remain complex procedures. While improvements in automated quantification have increased the diagnostic accuracy, there are various factors that may induce inaccuracies. Commonly, errors are induced by patient motion, attenuation, scatter, camera defects or processing problems.⁵³ Even though these factors are known to limit the visual interpretation of both MPS and I-123 MIBG studies, they may also affect the reliability of the quantitative analysis. Previous studies have already shown that factors like the heart size, gender, age, filter-settings, method of stress induction and radiopharmakon can influence volumetric indices of MPS.⁵⁴⁻⁶⁰ As quantitative nuclear cardiology is becoming more important in a clinical setting, it is important to better understand the factors that may influence the functional evaluation of perfusion, function and innervation.

OBJECTIVE AND OUTLINE OF THE THESIS

Despite extensive research in the field of nuclear cardiology, ambiguities in the SPECT-based quantification remain. The dependence of functional MPS indices on, for example, the software package or the injection-acquisition time interval, are indistinct. Also the meaning of recently introduced functional parameters and their relation to other MPS indices remain unclear. For innervation imaging, the lack of standardization regarding acquisition and processing still affects the clinical applicability of this technology. All these ambiguities of SPECT quantification are addressed in this thesis.

Part 1 will cover new aspects of perfusion and function quantification based on MPS. The effects of the software system on quantification of SPECT perfusion studies will first be described in *Chapter 2*. Two widely used commercial software systems are compared with respect to their linearity, performance on clinical data and normal values. The effects of the time interval between tracer injection and acquisition on image quality, perfusion scores and functional parameters are discussed in *Chapter 3*.

In *Chapter 4* and *Chapter 5* two recently introduced MPS parameters, transient ischemic dilation (TID) and ventricular dyssynchrony, are evaluated. Post-stress dilatation is considered an important indicator of severe CAD; however, the mechanisms behind this dilatation remain indistinct. Accordingly, *Chapter 4* will focus on the relation between TID and the other functional parameters. Myocardial contractility, and dyssynchrony in particular, can also be studied using gated MPS. In *Chapter 5* the feasibility of a new geometrical approach to calculate dyssynchrony indices is evaluated.

Part 2 will focus on sympathetic innervation in both planar and SPECT acquisitions. Various acquisition protocols and quantification methods are described to assess cardiac innervation. *Chapter 7* presents the results of a systematic literature study on the various protocols and methods to quantify innervation in planar images. SPECT imaging, although less frequently used, may also be suitable for quantification of global I-123 MIBG uptake. A simple volumetric method to quantify I-123 MIBG uptake in SPECT images is introduced in *Chapter 8*.

REFERENCE LIST

- (1) World Health Organization. Prevention of Cardiovascular Diseases: Guidelines for assessment and management of cardiovascular risk. *WHO Press*; 2007.
- (2) Allender S, Scarborough P, Peto V, Rayner M. *European cardiovascular disease statistics*. British Heart Foundation; 2008.
- (3) Clark AN, Beller GA. The present role of nuclear cardiology in clinical practice. *Q J Nucl Med Mol Imaging* 2005;49(1):43-58.
- (4) Des Prez RD, Shaw LJ, Gillespie RL et al. Cost-effectiveness of myocardial perfusion imaging: a summary of the currently available literature. *J Nucl Cardiol* 2005;12(6):750-9.
- (5) Marcassa C, Bax JJ, Bengel F et al. Clinical value, cost-effectiveness, and safety of myocardial perfusion scintigraphy: a position statement. *Eur Heart J* 2008;29:557-63.
- (6) Underwood SR, Anagnostopoulos C, Cerqueira M et al. Myocardial perfusion scintigraphy: the evidence. *Eur J Nucl Med Mol Imaging* 2004;3:261-91.
- (7) Hachamovitch R, Berman DS. The use of nuclear cardiology in clinical decision making. *Semin Nucl Med* 2005;35(1):62-72.
- (8) Ficaro EP, Corbett JR. Advances in quantitative perfusion SPECT imaging. *J Nucl Cardiol* 2004;11:62-70.
- (9) Strauss HW, Harrison K, Langan JK, Lebowitz E, Pitt B. Thallium-201 for myocardial imaging. Relation of thallium-201 to regional myocardial perfusion. *Circulation* 1975;51:641-5.
- (10) Zaret BL, Strauss HW, Martin ND, Wells HP, Jr., Flamm MD, Jr. Noninvasive regional myocardial perfusion with radioactive potassium. Study of patients at rest, with exercise and during angina pectoris. *N Engl J Med* 1973;288:809-12.
- (11) Lebowitz E, Greene MW, Fairchild R et al. Thallium-201 for medical use. I. *J Nucl Med* 1975;16:151-5.
- (12) Zaret BL, Stenson RE, Martin ND et al. Potassium-43 myocardial perfusion scanning for the non-invasive evaluation of patients with false-positive exercise tests. *Circulation* 1973;48:1234-41.
- (13) Hansen CL, Goldstein RA, Akinboboye OO et al. Myocardial perfusion and function: single photon emission computed tomography. *J Nucl Cardiol* 2007 November;14(6):e39-e60.
- (14) Heo J, Iskandrian AS. Technetium-labeled myocardial perfusion agents. *Cardiol Clin* 1994;12:187-98.
- (15) Baggish AL, Boucher CA. Radiopharmaceutical agents for myocardial perfusion imaging. *Circulation* 2008;118:1668-74.
- (16) Beller GA, Bergmann SR. Myocardial perfusion imaging agents: SPECT and PET. *J Nucl Cardiol* 2004;11:71-86.
- (17) Taillefer R. Kinetics of Myocardial Perfusion Imaging Radiotracers. *Nuclear Cardiac Imaging: Principles and Applications*. 3 ed. Oxford University Press; 2003.

- (18) Muehllehner G. A tomographic scintillation camera. *Physics in Medicine and Biology* 1971;16:87-96.
- (19) Kuhl DE, Edwards RQ. Image separation radioisotope scanning. *Radiology* 1963;80:653-62.
- (20) Vogel RA, Kirch DL, LeFree MT, Rainwater JO, Jensen DP, Steele PP. Thallium-201 myocardial perfusion scintigraphy: results of standard and multi-pinhole tomographic techniques. *Am J Cardiol* 1979;43:787-93.
- (21) Strauss HW, Pitt B. Evaluation of cardiac function and structure with radioactive tracer techniques. *Circulation* 1978 April;57:645-54.
- (22) Meade RC, Bamrah VS, Horgan JD, Ruetz PP, Kronenwetter C, Yeh EL. Quantitative methods in the evaluation of thallium-201 myocardial perfusion images. *J Nucl Med* 1978;19:1175-8.
- (23) Gould KL. Quantitative imaging in nuclear cardiology. *Circulation* 1982;66(6):1141-6.
- (24) Garcia E, Maddahi J, Berman D, Waxman A. Space/time quantitation of thallium-201 myocardial scintigraphy. *J Nucl Med* 1981;22:309-17.
- (25) Garcia EV, Van TK, Maddahi J et al. Quantification of rotational thallium-201 myocardial tomography. *J Nucl Med* 1985;26:17-26.
- (26) Hesse B, Tagil K, Cuocolo A et al. EANM/ESC procedural guidelines for myocardial perfusion imaging in nuclear cardiology. *Eur J Nucl Med Mol Imaging* 2005;32:855-97.
- (27) Cullom SJ, Case JA, Bateman TM. Electrocardiographically gated myocardial perfusion SPECT: technical principles and quality control considerations. *J Nucl Cardiol* 1998;5:418-25.
- (28) Paul AK, Nabi HA. Gated myocardial perfusion SPECT: basic principles, technical aspects, and clinical applications. *J Nucl Med Technol* 2004;32:179-87.
- (29) Abidov A, Germano G, Hachamovitch R, Berman DS. Gated SPECT in assessment of regional and global left ventricular function: major tool of modern nuclear imaging. *J Nucl Cardiol* 2006;13:261-79.
- (30) Taillefer R, DePuey EG, Udelson JE, Beller GA, Latour Y, Reeves F. Comparative diagnostic accuracy of Tl-201 and Tc-99m sestamibi SPECT imaging (perfusion and ECG-gated SPECT) in detecting coronary artery disease in women. *J Am Coll Cardiol* 1997;29:69-77.
- (31) Smanio PE, Watson DD, Segalla DL, Vinson EL, Smith WH, Beller GA. Value of gating of technetium-99m sestamibi single-photon emission computed tomographic imaging. *J Am Coll Cardiol* 1997;30:1687-92.
- (32) Thomas GS, Miyamoto MI, Morello AP, III et al. Technetium 99m sestamibi myocardial perfusion imaging predicts clinical outcome in the community outpatient setting. The Nuclear Utility in the Community (NUC) Study. *J Am Coll Cardiol* 2004;43:213-23.
- (33) Petix NR, Sestini S, Coppola A et al. Prognostic value of combined perfusion and function by stress technetium-99m sestamibi gated SPECT myocardial perfusion imaging in patients with suspected or known coronary artery disease. *Am J Cardiol* 2005;95:1351-7.

- (34) Sharir T, Germano G, Kang X et al. Prediction of myocardial infarction versus cardiac death by gated myocardial perfusion SPECT: risk stratification by the amount of stress-induced ischemia and the post-stress ejection fraction. *J Nucl Med* 2001;42:831-7.
- (35) Travin MI, Heller GV, Johnson LL et al. The prognostic value of ECG-gated SPECT imaging in patients undergoing stress Tc-99m sestamibi myocardial perfusion imaging. *J Nucl Cardiol* 2004;11:253-62.
- (36) Hsu CC, Chen YW, Hao CL et al. Comparison of automated 4D-MSPECT and visual analysis for evaluating myocardial perfusion in coronary artery disease. *Kaohsiung J Med Sci* 2008;24:445-52.
- (37) Xu Y, Hayes S, Ali I et al. Automatic and visual reproducibility of perfusion and function measures for myocardial perfusion SPECT. *J Nucl Cardiol* 2010;17:1050-7.
- (38) Ficaro EP, Lee BC, Kritzman JN, Corbett JR. Corridor4DM: the Michigan method for quantitative nuclear cardiology. *J Nucl Cardiol* 2007;14:455-65.
- (39) Liu YH. Quantification of nuclear cardiac images: the Yale approach. *J Nucl Cardiol* 2007;14:483-91.
- (40) Germano G, Kavanagh PB, Slomka PJ, Van Kriekinge SD, Pollard G, Berman DS. Quantitation in gated perfusion SPECT imaging: the Cedars-Sinai approach. *J Nucl Cardiol* 2007;14:433-54.
- (41) Garcia EV, Faber TL, Cooke CD, Folks RD, Chen J, Santana C. The increasing role of quantification in clinical nuclear cardiology: the Emory approach. *J Nucl Cardiol* 2007;14(4):420-32.
- (42) Petretta M, Costanzo P, Acampa W et al. Noninvasive assessment of coronary anatomy and myocardial perfusion: going toward an integrated imaging approach. *J Cardiovasc Med* 2008;9:977-86.
- (43) Patton JA, Townsend DW, Hutton BF. Hybrid imaging technology: from dreams and vision to clinical devices. *Semin Nucl Med* 2009;39:247-63.
- (44) Flotats A, Knuuti J, Gutberlet M et al. Hybrid cardiac imaging: SPECT/CT and PET/CT. A joint position statement by the European Association of Nuclear Medicine (EANM), the European Society of Cardiac Radiology (ESCR) and the European Council of Nuclear Cardiology (ECNC). *Eur J Nucl Med Mol Imaging* 2011;38:201-12.
- (45) Slomka PJ, Berman DS, Germano G. Applications and software techniques for integrated cardiac multimodality imaging. *Expert Rev Cardiovasc Ther* 2008;6:27-41.
- (46) Henneman MM, Bengel FM, van der Wall EE, Knuuti J, Bax JJ. Cardiac neuronal imaging: application in the evaluation of cardiac disease. *J Nucl Cardiol* 2008;15:442-55.
- (47) Ji SY, Travin MI. Radionuclide imaging of cardiac autonomic innervation. *J Nucl Cardiol* 2010;17:655-66.

- (48) Nagamatsu H, Momose M, Kobayashi H, Kusakabe K, Kasanuki H. Prognostic value of 123I-metaiodobenzylguanidine in patients with various heart diseases. *Ann Nucl Med* 2007;21:513-20.
- (49) Carrio I. Cardiac neurotransmission imaging. *J Nucl Med* 2001;42:1062-76.
- (50) Iversen LL. Role of transmitter uptake mechanisms in synaptic neurotransmission. *Br J Pharmacol* 1971;41:571-91.
- (51) Flotats A, Carrio I, Agostini D et al. Proposal for standardization of 123I-metaiodobenzylguanidine (MIBG) cardiac sympathetic imaging by the EANM Cardiovascular Committee and the European Council of Nuclear Cardiology. *Eur J Nucl Med Mol Imaging* 2010;37:1802-12.
- (52) Yamashina S, Yamazaki J. Neuronal imaging using SPECT. *Eur J Nucl Med Mol Imaging* 2007;34:939-50.
- (53) Burrell S, MacDonald A. Artifacts and pitfalls in myocardial perfusion imaging. *J Nucl Med Technol* 2006;34:193-211.
- (54) Ababneh AA, Sciacca RR, Kim B, Bergmann SR. Normal limits for left ventricular ejection fraction and volumes estimated with gated myocardial perfusion imaging in patients with normal exercise test results: influence of tracer, gender, and acquisition camera. *J Nucl Cardiol* 2000;7:661-8.
- (55) Knollmann D, Winz OH, Meyer PT et al. Gated myocardial perfusion SPECT: algorithm-specific influence of reorientation on calculation of left ventricular volumes and ejection fraction. *J Nucl Med* 2008;49:1636-42.
- (56) Peace RA, Adams PC, Lloyd JJ. Effect of sex, age, and weight on ejection fraction and end-systolic volume reference limits in gated myocardial perfusion SPECT. *J Nucl Cardiol* 2008;15:86-93.
- (57) Dorbala S, Crugnale S, Yang D, Di Carli MF. Effect of body mass index on left ventricular cavity size and ejection fraction. *Am J Cardiol* 2006 1;97:725-9.
- (58) Sharir T, Kang X, Germano G et al. Prognostic value of poststress left ventricular volume and ejection fraction by gated myocardial perfusion SPECT in women and men: gender-related differences in normal limits and outcomes. *J Nucl Cardiol* 2006;13:495-506.
- (59) De Bondt P., Van de Wiele C., De Sutter J., De Winter F., De Backer G., Dierckx RA. Age- and gender-specific differences in left ventricular cardiac function and volumes determined by gated SPET. *Eur J Nucl Med* 2001;28:620-4.
- (60) DePuey EG, Parmett S, Ghesani M, Rozanski A, Nichols K, Salensky H. Comparison of Tc-99m sestamibi and Tl-201 gated perfusion SPECT. *J Nucl Cardiol* 1999;6:278-85.

Part 1

Myocardial Perfusion Scintigraphy

Chapter 2

Impact of a new software system

B.J. van der Veen, A.J. Scholte, P. Dobbets-Schneider, M.P. Stokkel,

The consequences of a new software package for the quantification
of gated-SPECT myocardial perfusion studies.

Eur J Nucl Med Mol Imaging 2010; 37(9):1736-1744

ABSTRACT

Background: (Semi-) quantitative analysis of myocardial perfusion scintigraphy (MPS) has reduced inter- and intraobserver variability, and enables researchers to compare parameters in the same patient over time, or between groups of patients. There are several software packages available that are designed to process MPS and quantify parameters. In this study, the performances of two systems, quantitative gated SPECT (QGS) and 4D-MSPECT, in the processing of clinical patient data and phantom data were compared.

Methods: The clinical MPS data of 148 consecutive patients were analysed using QGS and 4D-MSPECT to determine the end-diastolic volume, end-systolic volume and left ventricular ejection fraction. Patients were divided into groups based on gender, body mass index, heart size, stressor type and defect type. The AGATE dynamic heart phantom was used to provide reference values for the left ventricular ejection fraction.

Results: Although the correlations were excellent (correlation coefficients 0.886 to 0.980) for all parameters, significant differences ($p < 0.001$) were found between the systems. Bland-Altman plots indicated that 4D-MSPECT provided overall higher values than QGS. These differences between the systems were not significant in patients with small heart sizes (end-diastolic volume < 70 ml). Other clinical factors had no direct influence on the relation. Additionally, the phantom data indicated good linear responses of both systems.

Conclusion: The discrepancies between these software packages were clinically relevant, and influenced by heart size. The possibility of such discrepancies should be taken into account when a new quantitative software system is introduced, or when multiple software systems are used in the same institution.

Keywords: Myocardial perfusion scintigraphy ▪ Quantitative software packages ▪ End-diastolic volume ▪ End-systolic volume ▪ Left ventricular ejection fraction

INTRODUCTION

In addition to visual interpretation of myocardial perfusion scintigraphy (MPS), quantitative software packages are used to supply (semi-)quantitative analysis of the data. Generally, these tools provide volumetric parameters such as left ventricle ejection fraction (LVEF), end-systolic volume (ESV) and end-diastolic volume (EDV). Additionally regional parameters, such as wall thickening, wall motion, and perfusion scores can be produced by most software packages. The introduction of these quantitative parameters has enabled researchers to compare parameters in one patient over time, or between groups of patients.¹

Although quantitative analysis improves accuracy and reduces inter- and intraobserver variability, there are also some important factors that can influence the performance of these software packages. For instance, the ability of a software tool to produce accurate and reproducible parameter values relies predominantly on its ability to determine the myocardial borders. In acquisitions in healthy humans, detection of the myocardial border is challenging because of relatively low resolution of the gamma camera, compared to the thickness of the myocardium. Additionally, factors such as Compton photon scatter, attenuation, extracardiac activity, and natural variations in orientation of the heart contribute to the complexity of border detection. Acquisitions in patients can also include extensive perfusion and functional abnormalities. Thus, a quantitative software package should provide a robust framework that produces correct estimations of the various parameter values in almost all situations.

Within the Nuclear Department of the Leiden University Medical Centre two software systems, quantitative gated SPECT (QGS) of Cedars-Sinai Medical Centre² and Corridor 4D-MSPECT of Invia Medical Solutions³ are available. Both quantitative software tools are commonly used and are well validated for their clinical use.⁴⁻⁷ Although previous studies have indicated good correlation for EDV, ESV and LVEF between these two packages, it seems that values are not exchangeable. So, the main objective of this study was to compare the two software packages with respect to their performances on clinical patient data. In order to study the differences between the two software packages, various clinical factors were identified that could influence the relation between the packages. A phantom study was performed to provide an absolute reference frame to compare the two systems with respect to linearity.

MATERIALS AND METHODS

Patient population

Consecutive patients referred for Tc-99m tetrofosmin MPS with adenosine- or exercise-induced stress during the period November 2008 to January 2009 were prospectively included ($n = 150$). All acquisitions were analysed by the QGS and 4D-MSPECT packages. Post-stress and rest acquisitions were also evaluated visually and scored either 'normal', 'reversible', 'persistent' or 'combined reversible and persistent'. Clinical characteristics with respect to relevant medication, risk factors and reason for MPS were also gathered.

Gated-SPECT acquisition and analysis

In the present study a 2-day stress/rest protocol was used, with the stress test performed in day 1 and the rest test performed on day 2. Patients were instructed to stop β -blockers and calcium antagonists 48 hours, and caffeine-containing products 12 hours before stress testing. The patients underwent physical exercise limited by symptoms, or, when contraindications to exercise were present, adenosine-induced stress using a standard infusion rate of 140 $\mu\text{g}/\text{kg}$ per minute. Injection of the radiopharmaceutical was done at peak exercise, or in the third minute of pharmacological stress induction. Acquisitions, both post-stress and rest, were performed with a triple-headed camera system (Toshiba, CGA 9300, Tokyo, Japan) 45 minutes after injection of approximately 500 MBq Tc-99m tetrofosmin. Images were acquired over 360 degrees (6 degrees/direction, 40 seconds/direction). Automated ECG gating was applied on the R-R interval with 16 frames per cardiac cycle, with a tolerance window of 50%.

Data were prefiltered using a Butterworth filter (eight order, cut-off frequency 0.26 cycles/pixel), and reconstructed as transaxial images using a filtered back-projection algorithm. No attenuation or scatter correction was applied. Acquisitions were projected as tomographic slices in short-axis and vertical/horizontal long-axis directions for visual evaluation. Quantitative values were automatically generated for EDV, ESV and LVEF by QGS (Version 2.0 revA) and Corridor 4D-MSPECT (Version 5.2 SP 2). Heart size was estimated using the left ventricular end-diastolic volume.

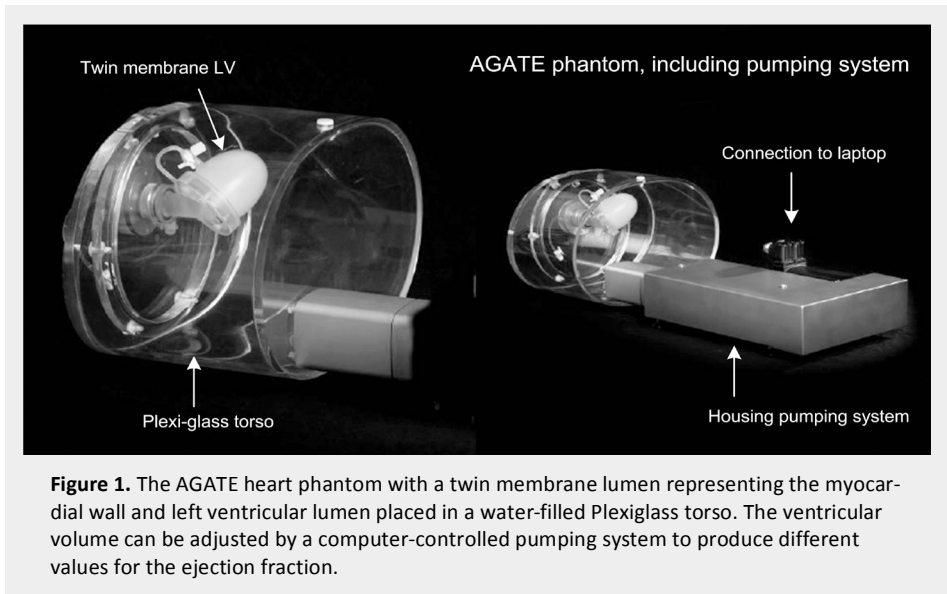


Figure 1. The AGATE heart phantom with a twin membrane lumen representing the myocardial wall and left ventricular lumen placed in a water-filled Plexiglass torso. The ventricular volume can be adjusted by a computer-controlled pumping system to produce different values for the ejection fraction.

Phantom study

The Amsterdam gated (AGATE) dynamic cardiac phantom (Model 830.100, vanderWilt Techniques, The Netherlands) was used as a reference for the LVEF (Figure 1). The phantom consists of a water filled torso in which a twin membrane lumen filled with water and 10MBq Tc-99m pertechnetate is placed. The cardiac volume is automatically regulated by a computer-controlled pumping system (Figure 1). The system produces ECG signals in agreement with the diastolic and systolic phases of the heart. In this study, the cardiac output was varied at a constant heart rate of 80 beats per minute to provide a range of LVEF values. The MPS acquisitions of the phantom were analysed by the QGS and 4D-MSPECT packages.

Statistical methods

All statistical analyses were performed using SPSS v16.0. Differences in EVD, ESD and LVEF between the packages were tested for significance using paired Student's *t*-tests, with $p < 0.05$ considered significant. The agreement between the systems was evaluated using Bland-Altman graphs. Linear regression analysis was performed on the phantom data to provide information about the linearity between the two software packages over a range of LVEF values. Multiple linear regression analysis was performed to identify

TABLE 1. PATIENT CHARACTERISTICS

Risk factors and medication use		Reason for MPS	
Age (years)	60.6 ± 10.2	Chest pain	24 (16.2)
BMI (kg/m ³)	27.6 ± 4.4	CAD or infarction	85 (57.4)
Gender: n (%) male	105 (70.9)	Abnormal ECG or stress test	15 (10.2)
Smoker	57 (38.5)	Stem cell protocol	10 (6.8)
Alcohol	14 (9.5)	Preoperative screening	7 (4.7)
Hypercholesteremia	57 (38.5)	Other reason	7 (4.7)
Hypertension	81 (54.7)		
Positive family history	50 (33.7)	MPS results	
Diabetic	33 (22.2)	Stressor type: n (%) exercise	77 (52.0)
CAD or infarction	83 (56.1)	Normal scan	31 (20.9)
Beta-blocker	107 (72.3)	Average rest ESV (ml)	72.0 ± 65.7
Calcium antagonist	13 (8.8)	Average rest EDV (ml)	138.2 ± 71.7
ACE inhibitor	67 (45.2)	Average rest LVEF (%)	54.6 ± 15.9

ACE, angiotensin-converting enzyme; BMI, body mass index; CAD, coronary artery disease; EDV, end-diastolic volume; ESV, end-systolic volume; LVEF, left ventricular ejection fraction

the main factors explaining differences in ESV, EDV and LVEF derived by the two software packages. Significant factors were used to further identify the relation between the QGS and 4D-MSPECT packages.

RESULTS

One patient had to be excluded during the study because 4D-MSPECT could not provide accurate border detection, and another patient had to be excluded because neither package was able to provide accurate border detection. Details regarding the included patient population ($n = 148$) can be found in Table 1.

Differences and agreement based on clinical patient data

The clinical patient dataset was used to calculate the EVD, ESV and LVEF using 4D-MSPECT and QGS (Table 2). Mean parameter values are shown, supplemented with the results of a paired Student's *t*-test calculating the mean differences between the values calculated by the two packages (4D-MSPECT – QGS). Although the correlations were high (PCC ranging from 0.886 to 0.980 for the different parameters), the EDV, ESV and

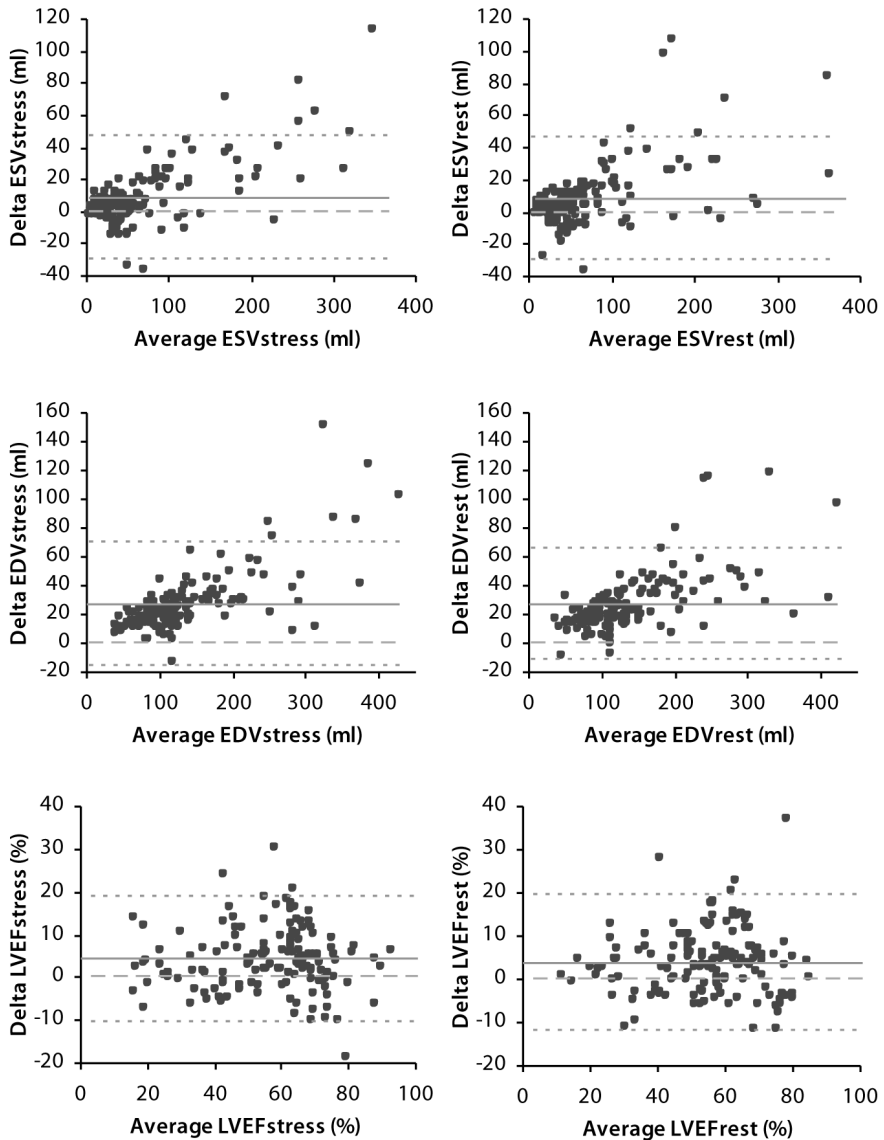


Figure 2. Bland-Altman analyses for the EDV, ESV and LVEF calculated by the two software systems for both rest and post-stress acquisitions. The analysis indicates the difference (4DM-QGS) in the values obtained by the two systems against the average of these estimates. The dotted lines (± 1.96 standard deviations) represent the Bland-Altman limits; the solid lines represent the mean differences and the striped lines represent the line of equality.

TABLE 2. EDV, ESV AND LVEF CALCULATED BY 4DM AND QGS

	Rest acquisitions			Post-stress acquisitions		
	Mean	Difference	<i>p</i> -value	Mean	Difference	<i>p</i> -value
EDV QGS (ml)	124.6 ± 66.2	27.3 ± 19.5	<0.001*	122.1 ± 66.8	27.2 ± 21.3	<0.001*
EDV 4DM (ml)	151.9 ± 78.0			149.3 ± 82.0		
ESV QGS (ml)	67.7 ± 61.0	8.8 ± 19.1	<0.001*	65.6 ± 62.2	8.5 ± 19.1	<0.001*
ESV 4DM (ml)	76.4 ± 71.3			74.1 ± 75.5		
LVEF QGS (%)	52.6 ± 16.0	4.0 ± 7.9	<0.001*	54.0 ± 17.5	4.3 ± 7.4	<0.001*
LVEF 4DM (%)	56.6 ± 16.7			58.3 ± 17.6		

Paired Student's *t*-test, with * indicating significance of <0.05. EDV, end-diastolic volume; ESV, end-systolic volume; LVEF, left ventricular ejection fraction

LVEF calculated by both software packages differ significantly ($p < 0.001$). Additionally, a Bland-Altman analysis is produced for rest and post-stress acquisitions (Figure 2). The limits for EDV, ESV and LVEF at rest acquisitions were -11.8 – 66.4ml (mean 27.3ml), -29.3 – 46.9ml (mean 8.8ml), and -11.7 – 19.7% (mean 4.0ml), respectively. The limits for EDV, ESV and LVEF in the post-stress acquisitions were -15.3 – 69.7ml (mean 27.2ml), -29.7 – 47.3ml (mean 8.5ml), and -10.5 – 19.1% (mean 4.3ml), respectively. A positive shift of the mean-line from the line of equality is apparent in all figures, indicating that 4D-MSPECT provides higher values than QGS for all parameters. Furthermore, differences between the software packages increased with increasing average heart size.

Multivariate analysis

Stepwise multiple regression analysis identified the most important factors explaining the differences in EDV, ESV and LVEF between the packages. Factors included in the analysis were relevant risk factors, reason for MPS, stressor type and average volumetric measurements. The average volumetric measurements were determined by calculating the means of the QGS and 4D-MSPECT values. The factors that were able to explain the difference between the ESV values determined by the two packages were average ESV_{rest} ($p < 0.001$), gender ($p = 0.034$) and BMI (rest $p = 0.036$ and post-stress $p = 0.018$). The difference in the EDV values was explained by BMI (rest $p = 0.002$ and post-stress $p = 0.005$) and average ESV_{rest} ($p < 0.001$). The difference in LVEF values was explained by average ESV_{rest} ($p = 0.012$), average EDV_{rest} ($p = 0.048$), small heart size (rest $p = 0.001$

TABLE 3. INFLUENCE OF VARIOUS FACTORS ON DIFFERENCES IN EDV, ESV AND LVEF

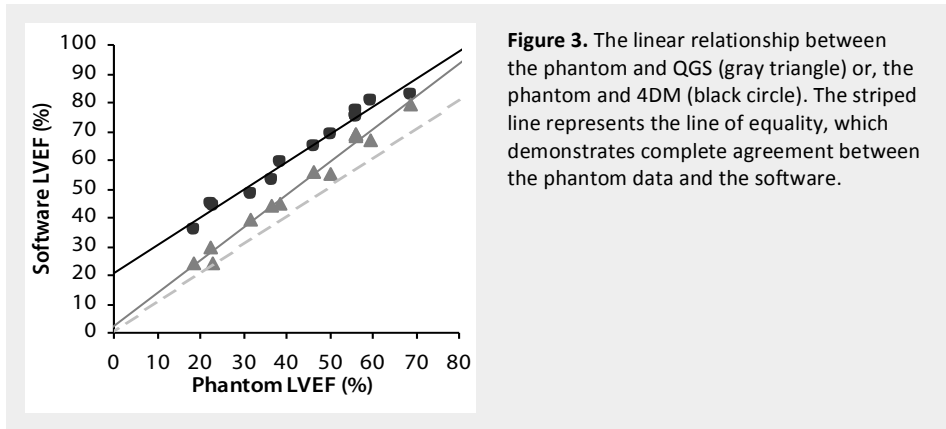
	Difference EDV (ml)		Difference ESV (ml)		Difference LVEF (%)		
	Mean	p-value	Mean	p-value	Mean	p-value	
Gender	Male rest	28.8 ± 21.0	<0.001	9.6 ± 20.7	<0.001	4.6 ± 7.2	<0.001
	Female rest	23.9 ± 15.1	<0.001	6.8 ± 14.5	0.003	2.5 ± 9.2	0.073*
	Male stress	29.3 ± 23.5	<0.001	9.9 ± 20.7	<0.001	4.7 ± 6.5	<0.001
	Female stress	22.2 ± 13.7	<0.001	5.3 ± 14.5	0.020	3.3 ± 9.2	0.022
Defect	Normal rest	19.5 ± 10.4	<0.001	2.0 ± 8.7	0.216*	3.2 ± 11.0	0.116*
	Reversible rest	22.8 ± 10.4	<0.001	3.7 ± 6.9	0.059*	4.4 ± 7.1	0.032
	Persistent rest	31.4 ± 24.6	<0.001	13.4 ± 24.7	<0.001	3.6 ± 6.7	<0.001
	Combination rest	28.7 ± 16.6	<0.001	8.6 ± 15.8	0.002	5.2 ± 6.9	<0.001
	Normal stress	17.9 ± 11.1	<0.001	0.8 ± 9.3	0.633*	4.1 ± 9.5	0.024
	Reversible stress	22.8 ± 8.8	<0.001	2.5 ± 8.6	0.272*	5.5 ± 7.2	0.010
	Persistent stress	31.5 ± 28.1	<0.001	13.5 ± 24.2	<0.001	3.7 ± 6.7	<0.001
	Combination stress	29.2 ± 14.8	<0.001	8.8 ± 16.0	0.001	5.0 ± 6.7	<0.001
Stressor	Adenosine rest	29.1 ± 14.8	<0.001	8.8 ± 20.9	<0.001	4.9 ± 8.8	<0.001
	Exercise rest	25.4 ± 16.4	<0.001	8.7 ± 16.9	<0.001	3.1 ± 6.7	<0.001
	Adenosine stress	30.4 ± 25.5	<0.001	10.6 ± 22.8	<0.001	4.8 ± 8.8	<0.001
	Exercise stress	23.8 ± 14.8	<0.001	6.2 ± 13.8	<0.001	3.7 ± 6.2	<0.001
Heart size	EDV ≤70ml rest	15.1 ± 5.3	<0.001	3.1 ± 4.6	0.005	-1.2 ± 10.3	0.647*
	EDV >70ml rest	28.7 ± 19.9	<0.001	9.3 ± 20.0	<0.001	4.6 ± 7.4	<0.001
	EDV ≤70ml stress	14.5 ± 5.4	<0.001	3.1 ± 4.6	0.020	-0.2 ± 7.7	0.901*
	EDV >70ml stress	28.6 ± 22.0	<0.001	9.1 ± 20.0	<0.001	4.8 ± 7.2	<0.001
BMI	BMI < 30 rest	24.6 ± 17.3	<0.001	6.8 ± 18.2	<0.001	4.7 ± 8.4	<0.001
	BMI ≥ 30 rest	33.9 ± 23.0	<0.001	13.6 ± 20.4	<0.001	2.3 ± 6.2	0.013
	BMI < 30 stress	26.2 ± 23.3	<0.001	7.5 ± 20.7	<0.001	5.1 ± 7.8	<0.001
	BMI ≥ 30 stress	29.7 ± 15.3	<0.001	11.0 ± 14.3	<0.001	2.3 ± 5.8	0.017

Paired Student's *t*-test, with * indicating **non-significant** differences. BMI, body mass index; EDV, end-diastolic volume; ESV, end-systolic volume; LVEF, left ventricular ejection fraction

and post-stress $p = 0.002$) and stressor type ($p = 0.032$). These factors were used to produce subgroups for further analysis.

Influence of various factors

Previous studies have shown that QGS overestimates LVEF in smaller hearts (EDV <70ml), so the study population patients was subdivided using the cut-off value.^{8,9} The



eventual distribution of the population resulted in the following subgroups; gender (104 male, 44 female), stressor type (77 adenosine, 71 exercise), heart size (15 EDV \leq 70ml, 133 EDV $>$ 70ml), defect type (31 normal, 15 reversible, 63 persistent, 39 combination) and BMI (105 BMI $<$ 30 kg/m², 43 BMI \geq 30 kg/m²). The paired differences between the values in each group determined by the two packages are presented in Table 3. Since the observed differences were significant over the entire population, the nonsignificant differences ($p > 0.05$) are marked within this table, as they indicate a deviation from the observed trend. Overall, we found a significant between EDV values ($p < 0.001$) determined by the two packages in all subgroups, and in both rest and post-stress acquisitions. A relatively smaller difference was found between the values determined by the two packages in the groups with a small heart size (EDV_{rest} 15.1 ± 5.3 ml, EDV_{stress} 14.5 ± 5.4 ml), as well as in the group with normal perfusion (EDV_{rest} 19.5 ± 10.4 ml, EDV_{stress} 17.9 ± 11.1 ml), when compared to the difference in the overall population (EDV_{rest} 27.3 ± 19.5 ml, EDV_{stress} 27.2 ± 21.3 ml).

Regarding ESV, the difference between the values determined by QGS and 4D-MSPECT was not significant in the normal and reversible perfusion subgroups. In addition, we found a smaller difference in ESV values between the groups with a small heart (ESV_{rest} and ESV_{stress} 3.1 ± 4.6 ml), compared to the overall population (ESV_{rest} 8.8 ± 19.1 ml, ESV_{stress} 8.5 ± 19.1 ml). Finally, the LVEF values determined by the two packages were significantly different in almost all groups, with the exception of the group with a small heart size, normal perfusion and female gender.

Phantom study

There was a strong linear relationship between the software packages estimates and the phantom data over the entire range of volumes, as is shown in Figure 3. Regression between the phantom (P) and 4D-MSPECT for the LVEF was $1.041P + 15.976$ (R^2 0.968). Regression between the phantom and the QGS values for the LVEF was $1.140P + 2,344$ (R^2 0.985). The relationship between the LVEF data determined by the two software packages was also linear, with a regression for $QGS = 1.057 \text{ 4D-MSPECT} - 12.932$ (R^2 0.947). The mean difference in LVEF between the 4D-MSPECT and QGS estimates was 9.61 ± 4.35 ($p < 0.001$).

DISCUSSION

In contrast to QGS, which has been compared frequently to other imaging techniques such as blood-pool imaging and magnetic resonance imaging (MRI), 4D-MSPECT seems to be a less well validated tool. In the present study the performances of QGS and 4D-MSPECT on both clinical patient data and phantom data were studied to gain better understanding of the relationship between these software packages.

The degree of association

A high degree of correlation and linearity between the estimates derived by the two software packages has been found in other studies and by the manufactures.^{7,10-13} These high correlation values have sometimes been incorrectly interpreted as a measure of inter-changeability between QGS and 4D-MSPECT. Therefore, it has to be stated that correlation is a direct measure of association rather than of agreement between the packages. If two methods are compared within a population with large variation between individuals which is present in our data, correlation analysis should be used with caution. When the variation between two methods is small compared to the variation between individuals, the correlation is mainly determined by the variation within the patient population. So, in addition to the correlation analysis, a Bland-Altman analysis is performed to provide visual representation of the level of agreement and the presence of a bias.^{14,15} If two systems or methods share total agreement, all measured values should be situated on the mean line in a Bland-Altman graph, and this line should coincide with the line of equality. For excellent, but not total, agreement, the measured values should be located around the mean-line within a narrow 95%

confidence interval. In the Bland-Altman graphs of the agreement between QGS and 4D-MSPECT the mean-line was located above the line of equality ($4D-MSPECT = QGS$) for all parameters, indicating higher parameter estimates by 4D-MSPECT than for QGS. The high level of correlation found in earlier studies can be explained by the distribution of the calculated values within wide 95% confidence intervals.

Relationship between QGS and 4D-MSPECT

There were excellent linear relationships between the estimates from the two software packages, and between the software estimates and the phantom data. Linearity over an entire range of LVEF values is an important characteristic of a robust software package. The phantom study further indicated overestimations of LVEF by both QGS and 4D-MSPECT, which was more profound in the 4D-MSPECT data.

In a study by Lipke et al.⁷ both 4D-MSPECT and QGS were compared with cardiac MRI. They found a significant underestimation of EDV by 4D-MSPECT, and an even higher degree of underestimation by the QGS. However, they found no significant difference between the software estimates and cardiac MRI for the ESV values. This result may be explained by the effects of improved count statistics in systole due to wall thickening. For the LVEF values, there was a minimal nonsignificant deviation between 4D-MSPECT and cardiac MRI, whereas QGS provided a significant underestimation. These results are supported by the studies of Stegger et al.¹³ and Schaefer et al.¹¹. Comparing the two packages with each other, Lipke et al. found significant differences for the EDV values between the packages, but only small, insignificant differences for the ESV values. In this study there was a high correlation between the packages for all three parameters, which is also in agreement with the studies of Stegger et al.¹³ and Schaefer et al.¹¹. Nakajima et al.¹⁶ compared data from both a mathematical model of the myocardium and gated blood pool studies with MPS data obtained by QGS and 4D-MSPECT. Although high correlations between the software-determined values and gated blood pool studies were found for LVEF and EDV, no clear significant differences were demonstrated between 4D-SPECT and QGS values. These results are in contrast with our findings and those of Lipke et al., but may be explained by the relatively small number of patients included ($n = 30$) and the relatively small heart sizes of these patients.

Important differences between the software algorithms

The general trend of higher estimates provided by 4D-MSPECT than by QGS found in this study may be explained by the underlying differences between the software algorithms. To provide an insight into the differences, we briefly discuss the basic principles of operation for the QGS software. This algorithm consists of three main steps: (1) segmentation of myocardium, (2) extracting the mid-myocardial line, and (3) determining the myocardial borders. During segmentation the 3-dimensional position of the LV within the ungated SPECT acquisition is located, and a binary mask is made of the heart. A mask is a rough black and white model indicating the location of the myocardium in a 3-D space. This binary mask is then used to locate the mid-myocardial line (the line with the highest count distribution). An ellipsoid model is fitted and adjusted to the mid-myocardial line so that it resembles the myocardial shape. The eventual ellipsoid will serve as a sampling profile for processing the individual intervals with an asymmetric Gaussian count profile. For every image in the cardiac cycle the LV cavity is confined by the mitral valve plane, which is estimated at a 25% threshold of heart activity in each frame. Eventually an estimate of myocardial borders containing holes that represent the valve plane is obtained for each frame. A more detailed description of the QGS algorithms is beyond the scope of this manuscript, but more information can be found in the literature.¹⁷⁻¹⁹

The 4D-MSPECT software uses the same basic principles of segmentation, determining the mid-myocardium and border estimation as are used by QGS; however, there are also some crucial differences.^{3,20-22} First, 4D-MSPECT uses a cylindrical sampling profile within the basal and mid-ventricular parts of the myocardium and a spherical profile in the apical part, whereas QGS uses the ellipsoidal profile throughout the myocardium. This difference may account for deviations in the estimated LV shape, especially within the basal regions. Second, 4D-MSPECT defines the valve plane perpendicular to the long axis, thus enclosing a part of the outflow tract to the LV volume. QGS, on the other hand, allows for a somewhat oblique valve plane towards the septum on the long axis, thus excluding a part of the LV volume near the septum. Additionally, 4D-MSPECT also allows a basal plane motion of 5-20mm towards the apex in systole, whereas the QGS uses a fixed basal plane with a maximum motion that is confined to one slice. These differences may account for the overestimation of LVEF, and the relatively smaller difference between the two software packages during the systolic phase.

Effects of heart size

The multivariate analysis indicated that the factors gender, BMI, stressor type, average EDV_{rest} and average ESV_{rest} could explain the differences in parameter values between the software packages. For this reason the factors gender, BMI, defect type, heart size and stressor type were used to create subgroups within the population.

In this study, BMI and stressor type had no particular effect on the relationship between the two software packages. The factors that did influence the relationship were gender, defect type and heart size. In the subgroups female gender, normal perfusion, reversible perfusion defects and small heart, the differences in LVEF between QGS and 4D-MSPECT were smaller than in the other subgroups tested, but still significant. This result could possibly be explained by the smaller sizes of these subgroups. Nonetheless, it remains apparent that all these subgroups had a relatively smaller heart size than the other groups. Overall, patients with a smaller heart size showed a reduced, but still significant, difference for EDV and ESV, and a small nonsignificant difference in LVEF, between the two packages. This may indicate that size affects the calculation of parameter values differently in both software packages.

The effects of a small heart size on the values determined by the QGS software package have also been reported in other studies.^{8,9,23} The subdivision of the population in the present study was based on a heart size (EDV <70ml) and the presence or absence of perfusion defects. Although the distribution method differed from our classification, Lum and Coel¹⁰ also did not find significant mean differences between the values determined by the two software packages among patients with a small heart. In the groups with present or absent perfusion defects, a significant overestimation of values calculated by 4D-MSPECT in comparison with those calculated by QGS was found, as in this study.

The partial volume effect, in which one voxel that should only describe the myocardial wall will in fact contain a mixture of myocardial, left ventricle and extra-cardiac values, is an important factor in small hearts. The combination of all these voxels will result in an overestimation of the actual size of the myocardial wall, reducing the estimated size of the left ventricle cavity. As EDV, and especially the ESV, are underestimated, a significant overestimation of LVEF values will occur with decreasing heart size. Factors such as photon scatter and the relatively low camera resolution may limit the ability to obtain good border estimates by many software packages, especially in smaller hearts. In small heart each voxel will represent a substantial part of the myocardial wall,

particularly during the systolic phase. Photon scatter also affects the image quality in both small and larger hearts resulting in blurring of the myocardial borders. Observations of Hambye et al. indicate that the presence of scattered photons in the main photo peak is of greater importance in smaller hearts than in large hearts.²⁴ So scatter compensation techniques such as methods based on the energy window, deconvolution or reconstruction are especially useful for improving image quality in smaller hearts.²⁵

Clinical consequences

Quantitative functional parameters are generally used to classify a patient with a normal or abnormal myocardial function within the clinical setting. Some studies have provided normal limits for QGS, but there are few studies that provide these limits for 4D-MSPECT. Normal limits for LVEF calculated by QGS are, according to Lomsky et al. and Ababneh et al.^{26,27}, in the range of 51-53% for women, and 43-47% for men. Based on our findings, 4D-MSPECT overestimated these values by 4% on average in post-stress and rest acquisitions.

Although estimations of lower normal limits were provided and good correlations between the software packages were found, it remains unadvisable to process clinical MPS acquisitions with different software packages. Despite of the linearity of the relationship between the values determined by the two packages, substantial patient specific variations in parameter estimates were also present. Additionally, there is evidence that the discrepancies between the values provided by these software packages may have been influenced by heart size. Consequently, it is extremely difficult to convert the parameter values for individual patients after transition to another software package is made.

In a recent study, Lavender et al.²⁸ found that other factors, such as filtering, may also influence the LVEF estimates. They compared QGS and 4D-MSPECT in 101 patients and also found a good correlation and clinically significant differences between the LVEF values determined by the two packages. In addition, the LVEF was overestimated using Butterworth filters at cut-off frequencies ≤ 0.8 cycles/pixel in 26 of 30 patients. It was concluded that changing the cut-off frequency by as little as 0.1 cycles/pixel can cause clinically significant differences in the LVEF values. These aspects were not part of the present study, but should definitely be taken into account in clinical practice.

Cardiac MRI is being increasingly used for functional imaging of the myocardium in clinical practice. In a recent study by Wang et al.²⁹, MRI was used as a reference method to evaluate the software-specific characteristics of QGS, 4D-MSPECT and the Emory cardiac toolbox (ECTB) in patients with dilated cardiomyopathy. EDV and ESV assessed by QGS did not differ significantly from those assessed by cardiac MRI, whereas ECTB and 4D-MSPECT overestimated EDV and ESV. In addition, all software packages overestimated the LVEF compared with MRI. These findings underline the fact that all modalities and tools available for quantitative analysis of myocardial studies will produce different results, which means that the results are not interchangeable.

Finally, in the present study, administration of adenosine resulted in a significant mean decrease in LVEF. The exact mechanism involved in this phenomenon is still unknown and has been reported before, but regarding the data presented in the tables, it seems to be related to a slight increase in ESV.³⁰ Whether this is a direct effect of adenosine or is related to other factors has to be studied. Since both QGS and 4D-MSPECT demonstrated this phenomenon, there seems to be no relationship with the software packages used in present study.

CONCLUSION

In this study we sought a common trend for the differences in parameter values obtained by 4D-MSPECT and QGS, and factors that may induce a bias in this relationship. Although the software packages showed a good correlation, 4D-MSPECT overestimated the values by on average 4% for the post-stress and rest acquisitions compared to values calculated by QGS. There were excellent linear relationships between the values determined by the two systems and between the values determined by the two systems and the phantom data. The differences between the software estimates were especially apparent in patients with normal and increased heart size, since deviations between the software estimates were greatly influenced by heart size. The discrepancy between the values obtained by the software packages was clinically relevant, and should be taken into high account when a new quantitative software system is introduced, or when multiple software systems used within the same institution.

REFERENCE LIST

- (1) Ficaro EP, Corbett JR. Advances in quantitative perfusion SPECT imaging. *J Nucl Cardiol.* 2004;11:62-70.
- (2) Germano G, Kavanagh PB, Slomka PJ, Van Kriekinge SD, Pollard G, Berman DS. Quantitation in gated perfusion SPECT imaging: the Cedars-Sinai approach. *J Nucl Cardiol.* 2007;14:433-454.
- (3) Ficaro EP, Lee BC, Kritzman JN, Corbett JR. Corridor4DM: the Michigan method for quantitative nuclear cardiology. *J Nucl Cardiol.* 2007;14:455-465.
- (4) Ficaro EP, Quaipe RA, Kritzman JN, Corbett JR. Accuracy and Reproducibility of 3D-MSPECT for Estimating Left Ventricular Ejection Fraction in Patients with Severe Perfusion Abnormalities. *Circulation* 126. 1999. Abstract
- (5) Sharir T, Germano G, Waechter PB et al. A new algorithm for the quantitation of myocardial perfusion SPECT. II: validation and diagnostic yield. *J Nucl Med.* 2000;41:720-727.
- (6) Kritzman JN, Ficaro EP, Corbett JR. Reproducibility of 3D-MSPECT for Quantitative Gated SPECT Sestamibi Perfusion Analysis. *J Nucl Med* 41[5], 166. 2000. Abstract
- (7) Lipke CS, Kuhl HP, Nowak B et al. Validation of 4D-MSPECT and QGS for quantification of left ventricular volumes and ejection fraction from gated 99mTc-MIBI SPET: comparison with cardiac magnetic resonance imaging. *Eur J Nucl Med Mol Imaging.* 2004;31:482-490.
- (8) Nakajima K, Taki J, Higuchi T et al. Gated SPET quantification of small hearts: mathematical simulation and clinical application. *Eur J Nucl Med.* 2000;27:1372-1379.
- (9) Ford PV, Chatziioannou SN, Moore WH, Dhekne RD. Overestimation of the LVEF by quantitative gated SPECT in simulated left ventricles. *J Nucl Med.* 2001;42:454-459.
- (10) Lum DP, Coel MN. Comparison of automatic quantification software for the measurement of ventricular volume and ejection fraction in gated myocardial perfusion SPECT. *Nucl Med Commun.* 2003;24:259-266.
- (11) Schaefer WM, Lipke CS, Standke D et al. Quantification of left ventricular volumes and ejection fraction from gated 99mTc-MIBI SPECT: MRI validation and comparison of the Emory Cardiac Tool Box with QGS and 4D-MSPECT. *J Nucl Med.* 2005;46:1256-1263.
- (12) Schaefer WM, Kaiser HJ, Kuehl H, Koch KC, Nowak B, Buell U. Quantification of left ventricular volumes and ejection fraction from 16- and rebinned 8-frame gated 99mTc-tetrofosmin SPECT. Comparison of 4D-MSPECT and QGS. *Nuklearmedizin.* 2007;46:22-28.
- (13) Stegger L, Lipke CS, Kies P et al. Quantification of left ventricular volumes and ejection fraction from gated 99mTc-MIBI SPECT: validation of an elastic surface model approach in comparison to cardiac magnetic resonance imaging, 4D-MSPECT and QGS. *Eur J Nucl Med Mol Imaging.* 2007;34:900-909.
- (14) Bland JM, Altman DG. Measuring agreement in method comparison studies. *Stat Methods Med Res.* 1999;8:135-160.

- (15) Bland JM, Altman DG. Applying the right statistics: analyses of measurement studies. *Ultrasound Obstet Gynecol.* 2003;22:85-93.
- (16) Nakajima K, Higuchi T, Taki J, Kawano M, Tonami N. Accuracy of ventricular volume and ejection fraction measured by gated myocardial SPECT: comparison of 4 software programs. *J Nucl Med.* 2001;42:1571-1578.
- (17) Germano G, Kavanagh PB, Waechter P et al. A new algorithm for the quantitation of myocardial perfusion SPECT. I: technical principles and reproducibility. *J Nucl Med.* 2000;41:712-719.
- (18) Germano G, Kavanagh PB, Chen J et al. Operator-less processing of myocardial perfusion SPECT studies. *J Nucl Med.* 1995;36:2127-2132.
- (19) Germano G, Kavanagh PB, Su HT et al. Automatic reorientation of three-dimensional, transaxial myocardial perfusion SPECT images. *J Nucl Med.* 1995;36:1107-1114.
- (20) Ficaro EP, Corbett JR. Technical Considerations in Quantifying Myocardial Perfusion and Function. *Nuclear Cardiology: Technical Applications.* McGraw-Hill Medical; 2008.
- (21) Faber TL, Stokely EM, Peshock RM, Corbett JR. A model-based four-dimensional left ventricular surface detector. *IEEE Trans Med Imaging.* 1991;10:321-329.
- (22) Faber TL, Akers MS, Peshock RM, Corbett JR. Three-dimensional motion and perfusion quantification in gated single-photon emission computed tomograms. *J Nucl Med.* 1991;32:2311-2317.
- (23) Kakhki VR, Sadeghi R. Gated myocardial perfusion SPECT in patients with a small heart: effect of zooming and filtering. *Clin Nucl Med.* 2007;32:404-406.
- (24) Hambye AS, Vervaeke AM, Dobbeleir AA, Galt JR, Cullom J, Garcia EV. Head-to-head comparison of uncorrected and scatter corrected, summed and end diastolic myocardial perfusion SPECT in coronary artery disease. *Nucl Med Commun.* 2004;25:347-353.
- (25) Galt JR, Cullom J, Garcia EV. Attenuation and scatter compensation in myocardial perfusion SPECT. *Semin Nucl Med.* 1999;29:204-220.
- (26) Lomsky M, Johansson L, Gjerdtsson P, Bjork J, Edenbrandt L. Normal limits for left ventricular ejection fraction and volumes determined by gated single photon emission computed tomography--a comparison between two quantification methods. *Clin Physiol Funct Imaging.* 2008;28:169-173.
- (27) Ababneh AA, Sciacca RR, Kim B, Bergmann SR. Normal limits for left ventricular ejection fraction and volumes estimated with gated myocardial perfusion imaging in patients with normal exercise test results: influence of tracer, gender, and acquisition camera. *J Nucl Cardiol.* 2000;7:661-668.
- (28) Lavender FM, Meades RT, Al-Nahas A, Nijran KS. Factors affecting the measurement of left ventricular ejection fraction in myocardial perfusion imaging. *Nucl Med Commun.* 2009;30:350-355.

- (29) Wang F, Zhang J, Fang W et al. Evaluation of left ventricular volumes and ejection fraction by gated SPECT and cardiac MRI in patient with dilated cardiomyopathy. *Eur J Nucl Med Mol Imaging*. 2009;36:1611-21.
- (30) Brinkman N, Dibbets-Schneider P, Scholte AJ, Stokkel MP. Myocardial perfusion scintigraphy with adenosine: does it impair the left ventricular ejection fraction obtained with gated SPECT? *Clin Nucl Med*. 2008;33:89-93

Chapter 3

Relevance of the injection-acquisition time interval

I. Albutaihi, B.J. van der Veen, A.J. Scholte, M.P. Stokkel,

The effects of early and late scanning on image quality
and functional parameters in myocardial perfusion imaging.

Clin Nucl Med 2010; 35(10):764-769

ABSTRACT

Background: Timing of acquisition is a factor that may influence the subdiaphragmatic activity in myocardial perfusion scintigraphy (MPS). According to the instructions of tetrofosmin, scintigraphy may already be started 15 minutes post-injection. The aim of the present study was to compare the image quality and the functional parameters between early and late scanning.

Methods: 49 consecutive patients underwent a 2-day MPS protocol in which 15 and 45 minutes after the injection of 500 MBq of Tc-99m tetrofosmin scintigraphy both at stress and rest were performed. The amount of subdiaphragmatic tracer activity was scored from 'no tracer activity' to 'severe'. Moderate and severe subdiaphragmatic tracer activity was considered relevant for the interpretation of the myocardial perfusion scan.

Results: Two-thirds of the patients (64%) showed a considerable amount of subdiaphragmatic activity on the 15 minutes rest images, whereas only 9 patients (18%) had considerable subdiaphragmatic activity on the late images. Stress imaging showed comparable results, however, subdiaphragmatic activity was generally less frequent and less prominent following stress. The value of the ejection fraction was significantly lower during early imaging comparing with late imaging. Lower ejection fraction was exclusively noticed in images with moderate and severe subdiaphragmatic tracer activity suggesting a relation with inaccurate border estimates.

Conclusions: Acquisition 15 minutes after the injection of Tc-99m tetrofosmin shows a significant and clinically relevant subdiaphragmatic activity in most myocardial perfusion scans leading to poorer image quality and to erroneous measurements of the ejection fraction. Therefore, early acquisition in MPS is not recommended in clinical practice.

Keywords: Myocardial perfusion scintigraphy ▪ Time-intervals ▪ Acquisition quality ▪ Quantitative parameters

INTRODUCTION

Myocardial perfusion scintigraphy (MPS) is considered an important non-invasive diagnostic and prognostic tool in the evaluation of ischemic heart diseases. MPS is capable of identifying abnormalities in perfusion patterns, and provides information on myocardial function.^{1,2} The quality of visual and quantitative analysis of these images is influenced by factors such as heart size, extent of perfusion defects and most importantly subdiaphragmatic activity.^{3,4}

The Technetium-99m (Tc-99m) labelled compounds sestamibi and tetrofosmin, both commonly used for MPS, initially localize in the liver and are then excreted via the hepatobiliary tract into the duodenum. From there, tracer activity will move distally in the small bowel, which may be positioned in the left upper quadrant of the abdomen, and it may reflux into the stomach, which lies immediately adjacent to the inferior wall of the left ventricle. Such subdiaphragmatic activity may create artefacts due to scatter, filtering, or tomographic image processing.^{5,6}

Tc-99m tetrofosmin, routinely used at our department, demonstrates a rapid clearance from blood, liver and lungs, and reaches the maximum myocardial uptake already after 5 minutes. Therefore, it is recommended by the manufacturer that images can be acquired as soon as 15 minutes after injection.⁷ However, European Association of Nuclear Medicine (EANM) guidelines for MPS advise acquisition 30 to 60 minutes post-injection, to enable more extensive liver clearance.⁸ Due to these mixed messages, it is accepted in the clinical practice accepted to obtain acquisitions as early as 15 minutes post-injection. Accordingly, the present study was initiated to examine the effects of the time interval between injection and acquisition on image quality and functional parameters in relation to subdiaphragmatic activity.

MATERIALS AND METHODS

Patient population

Between May and July 2009 a total of 50 patients referred for Tc-99m tetrofosmin MPS were prospectively included. For a practical purpose, each first patient on the daily schedule was selected, after giving an informed consent. Clinical data of the patients

were retrospectively included. All patients underwent a 2-day stress/rest protocol in which acquisitions were performed 15 and 45 min after injection of Tc-99m tetrofosmin.

Gated-SPECT protocol

Gated single photon emission computed tomography (SPECT) acquisitions were conducted using a 2-day protocol with post-stress acquisitions on the first and rest acquisitions on the second day. Patients underwent physical exercise on a bicycle ergometer. When contraindications to exercise were present, adenosine was used to induce stress. Patients who underwent dobutamine stress protocol were not included. Patients were instructed to stop β -blockers and calcium antagonists 48 hours and caffeine-containing products 12 hours before post-stress acquisition. The radioisotope was injected at peak exercise, or in the third minute of adenosine stress induction. Eventually, 49 consecutive patients underwent a 2-day MPS protocol in which 15 and 45 minutes after the injection of approximately 500 MBq Tc-99m tetrofosmin SPECT at post-stress and rest were performed.

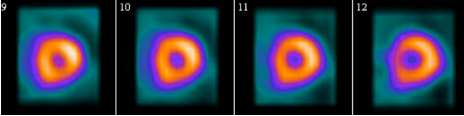
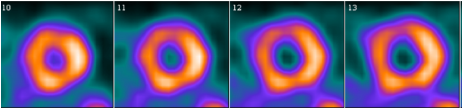
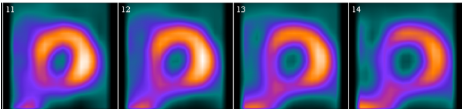
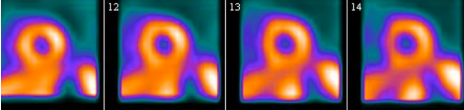
Data acquisition and analysis

Myocardial images were acquired with a triple-headed camera system (Toshiba, CGA 9300, Tokyo, Japan). A total of 20 images were acquired over a 120 degrees arc (6 degrees for 40 seconds/direction). ECG gating was performed at 16 frames per cardiac cycle, with a tolerance window of 50%. The raw SPECT data were pre-filtered with Butterworth filter (eighth order, cut-off frequency 0.26 cycles/pixel), and reconstructed using a filtered back projection algorithm. The reconstructed data were reoriented into oblique-angle tomograms parallel to the horizontal and short axis of the left ventricle.

The Corridor 4D-MSPECT software package (Version 5.2 SP 2) was used to project the data as tomographic slices in short-axis and vertical/horizontal long-axis directions. The data were visually evaluated using the automatically generated images and adjustments to the apex or basal planes were limited to a minimum. Numerical parameter values were automatically generated by the system for end diastolic volume (EDV), end systolic volume (ESV) and left ventricular ejection fraction (LVEF).

Post-stress and rest acquisitions of each patient were visually analysed by two experienced observers, who were blinded for clinical information, and additionally evaluated for subdiaphragmatic tracer activity in the liver and the intestine/stomach. All

TABLE 1. SCORING METHOD FOR SUBDIAPHRAGMATIC ACTIVITY

Definition	Example
0 No subdiaphragmatic tracer activity present in MPS data	
1 Mild subdiaphragmatic activity, but at some distance from myocardium, thus no effect on the visual interpretation	
2 Moderate subdiaphragmatic activity, visually significant effect on interpretation, especially with respect to the size of the perfusion defect	
3 Severe subdiaphragmatic activity, interpretation is severely affected. Information on defect size and distinction between reversible or persistent defects is not possible	

tomographic slices were used in combination with the polarmaps to score the tracer activity as follows; 0 = *no tracer activity*, 1 = *mild*, 2 = *moderate*, or 3 = *severe*. The higher the score, the more the images were disturbed by the subdiaphragmatic activity. The interpretation of the mentioned scoring method is shown in Table 1.

Statistical methods

All statistical analyses were performed using the statistical package SPSS v16.0. The subdiaphragmatic activity in an acquisition was determined as the maximal score ascribed to the liver or intestine. For each acquisition, the quantitative parameters EDV, ESV and LVEF were determined, and ratios (early/late) were calculated to reduce the effects of volume variation within a group of patients. The categorical scorings of the subdiaphragmatic activity cannot be considered normally distributed, so the Wilcoxon Sign Rank test and the Mann-Whitney U test were used. With these non-parametric equivalents of the paired and unpaired Student's t -test differences (early-late) in scoring were determined. The effects of acquisition moment on the quantitative parameters were analysed by (paired) Student's t -tests, since they did had a normal distribution.

TABLE 2. SCORES OF LIVER, INTESTINE/STOMACH AND SUBDIAPHRAGMATIC ACTIVITY

		<i>Early acquisition</i>		<i>Late acquisition</i>	
		Mean	Sum	Mean	Sum
Stress	Liver	0.70 ± 1.20	35	0.20 ± 0.57	10
	Intestine/stomach	0.76 ± 1.14	38	0.30 ± 0.71	15
	Subdiaphragmatic	1.04 ± 1.28	52	0.40 ± 0.78	20
Rest	Liver	0.90 ± 1.05	43	0.12 ± 0.44	6
	Intestine/stomach	1.62 ± 1.28	81	0.48 ± 0.79	24
	Subdiaphragmatic	1.94 ± 1.04	97	0.56 ± 0.84	28

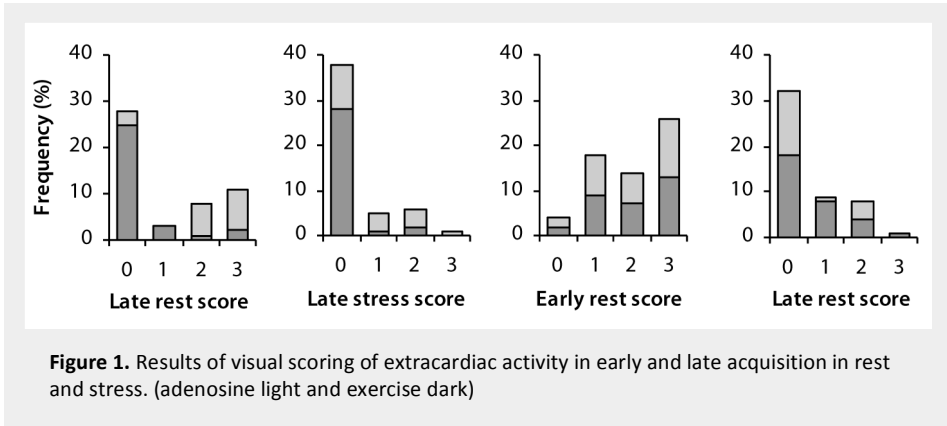
RESULTS

A total of 49 patients with each two stress and two rest scans were finally included within this study. Eventually, 18 patients were stressed with adenosine and 31 patients with bicycle exercise. One patient had to be excluded because of an incomplete dataset. Within the adenosine stressed population all 18 patients showed perfusion abnormalities (6 persisted, 5 reversible and 7 combined persisted and reversible defects). Within the exercise stressed population, 5 had normal and 26 had abnormal perfusion patterns (16 persisted, 6 reversible and 4 combined persisted and reversible defects). The mean time between the injection and early stress or early rest acquisition was 18 ± 6 and 17 ± 4 minutes ($p = 0.74$), respectively. The mean time between injection and late acquisition were 52 ± 20 and 56 ± 14 minutes ($p = 0.53$) for stress and rest acquisition, respectively.

Subdiaphragmatic activity in early and late acquisitions

The mean scores and summation of the scores for the intestine/stomach and liver over the entire population ($n = 49$) are displayed in Table 2. The subdiaphragmatic activity shown in Table 2 represents the maximal score in either the liver or the intestine. The distributions of the subdiaphragmatic activity in early and late acquisitions are displayed in Figure 1.

The Wilcoxon Sign Rank test showed no changes between the early and late acquisition in 5 patients during rest acquisition, 43 patients had higher scores during early acquisition, and 2 patients had higher scores during late acquisition. During stress, 31 patients showed no changes between the early and late acquisition, 18 patients had higher scores during early acquisition, and 1 patient had a higher score during late



acquisition. These differences between the distributions of the early and late acquisitions were considered significant ($p < 0.001$). Overall, the early acquisitions had a tendency to show more subdiaphragmatic activity comparing with the late acquisitions.

The difference in subdiaphragmatic activity between exercise and adenosine subpopulations was significant during both early stress ($p < 0.001$) and late stress ($p = 0.002$) acquisitions. This difference was not considered significant during early rest ($p = 0.785$) and late rest ($p = 0.499$) acquisitions. Overall, the amount of subdiaphragmatic activity was substantial higher in the adenosine stressed population, especially during early acquisition (Figure 1).

Effects of subdiaphragmatic activity on image interpretation

A score of moderate or severe subdiaphragmatic activity (score ≥ 2), was considered relevant, in that it had direct influence on the visual interpretation of perfusion aspect in

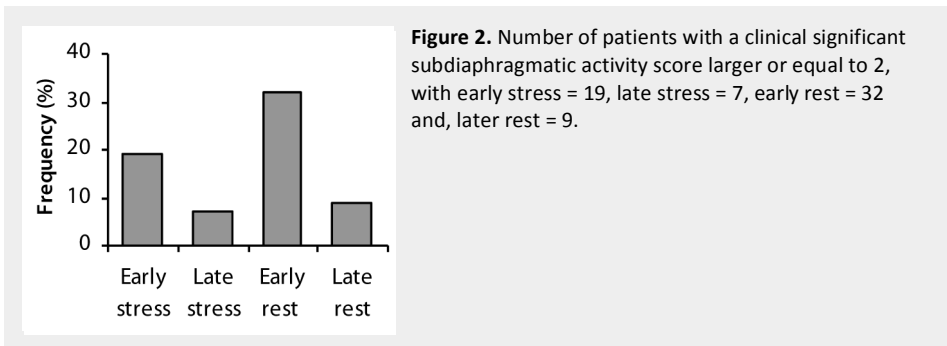


TABLE 3. VALUES FOR EDV AND LVEF

		<i>Exercise (n=31)</i>		<i>Adenosine (n=18)</i>		<i>Total (n=49)</i>	
		Mean	p-value	Mean	p-value	Mean	p-value
Stress	EDV _{early} (ml)	200.7 ± 105.5	0.021*	124.3 ± 38.7	0.082	150.6 ± 79.3	0.135
	EDV _{late} (ml)	182.0 ± 108.6		127.2 ± 37.3		145.8 ± 75.8	
	LVEF _{early} (%)	42.1 ± 17.6	0.010*	59.7 ± 12.1	0.537	53.5 ± 16.5	
	LVEF _{late} (%)	50.0 ± 19.8		59.1 ± 13.4		56.1 ± 16.5	
Rest	EDV _{early} (ml)	192.7 ± 123.7	0.093	135.6 ± 38.3	0.431	155.2 ± 84.0	0.059
	EDV _{late} (ml)	178.0 ± 105.9		134.2 ± 37.8		148.9 ± 72.9	
	LVEF _{early} (%)	47.7 ± 19.2	0.379	53.7 ± 11.3	0.015*	51.9 ± 14.9	
	LVEF _{late} (%)	50.3 ± 22.1		57.2 ± 12.4		55.1 ± 16.8	

Independent Student's t-test, with * indicating significance of <0.05

the myocardium. Figure 2 shows the number of patients that had clinical relevant scores. The Wilcoxon Signed Rank test indicated that the differences between early and late are significant in both stress ($p = 0.001$) and rest ($p < 0.001$) acquisitions. In 18 of the 50 patients this change in subdiaphragmatic activity between early and late acquisitions had a direct influence on the visual interpretation of the defect size.

In 29 patients, the amount of subdiaphragmatic activity influenced the automatic analysis of the patient data by the software system. In 15 cases the border estimates that were produced by 4D-MSPECT were visually scored as erroneous in the early stress acquisition, and in 3 cases, the borders were erroneous during the late acquisition. For the early rest acquisitions, 19 cases were provided erroneous borders, and in 4 cases, the borders were erroneous in late acquisition. The effects on the quantitative parameters were profound in all the scans with erroneous border estimates. Figure 3 illustrates the effects of erroneous automatic border estimates on the LVEF. From this, it can be concluded that late LVEF is assumed to be correct due to visual assessment of LV border tracking alone.

Effects of time interval on quantitative parameters

The quantitative parameters for the entire population and the adenosine and exercise subgroups are provide in Table 3. Significant differences in the quantitative parameters were observed between early and late acquisitions. The LVEF was lower and EDV was higher during the early acquisitions.

TABLE 4. EFFECT OF TIME-INTERVAL ON EDV AND LVEF

<i>Population with good border estimate and exercise stress (n=18)</i>		
	Mean	p-value
Stress	EDV _{early} (ml)	114.8 ± 45.6
	EDV _{late} (ml)	116.8 ± 41.7
	LVEF _{early} (%)	60.7 ± 14.1
	LVEF _{late} (%)	62.2 ± 13.6
Rest	EDV _{early} (ml)	121.8 ± 42.5
	EDV _{late} (ml)	120.7 ± 40.3
	LVEF _{early} (%)	57.0 ± 12.1
	LVEF _{late} (%)	59.9 ± 14.4

Paired Student's *t*-test, with * indicating significance of <0.05

The effect of subdiaphragmatic activity on border estimates was shown to influence the values of the functional parameters (Figure 3). In many patients, the amount of subdiaphragmatic activity was severe enough to seriously affect the automatic border detection in one or more acquisitions, especially in the inferior wall. To provide an insight in the effects of time on the quantitative parameters, only patients with accurate automatically determined borders were selected. This resulted in a dataset containing 2 adenosine and 18 exercise stressed patients. As it is not possible to perform a Student's *t*-test on 2 patients, the adenosine stress acquisitions were excluded from further analysis. The newly selected group shows no significant difference in the functional parameters between early and late acquisitions (Table 4). These results show that there is no indication to assume significant influence of time on the quantitative parameters in the exercise-stressed population.

DISCUSSION

This study shows the effect of time interval between injection of Tc-99m tetrofosmin and acquisition on the image quality of MPS. The quality of the MPS is generally inversely related to the amount and the intensity of subdiaphragmatic activity.^{5,6} In our study, there was a clear decrease in the amount of subdiaphragmatic activity during the late images in most patients (88%). This decrease was observed during stress and rest acquisitions and for both exercise and adenosine protocols. Only 2 patients (4%) had higher scores for subdiaphragmatic activity during late acquisition. In both cases, the

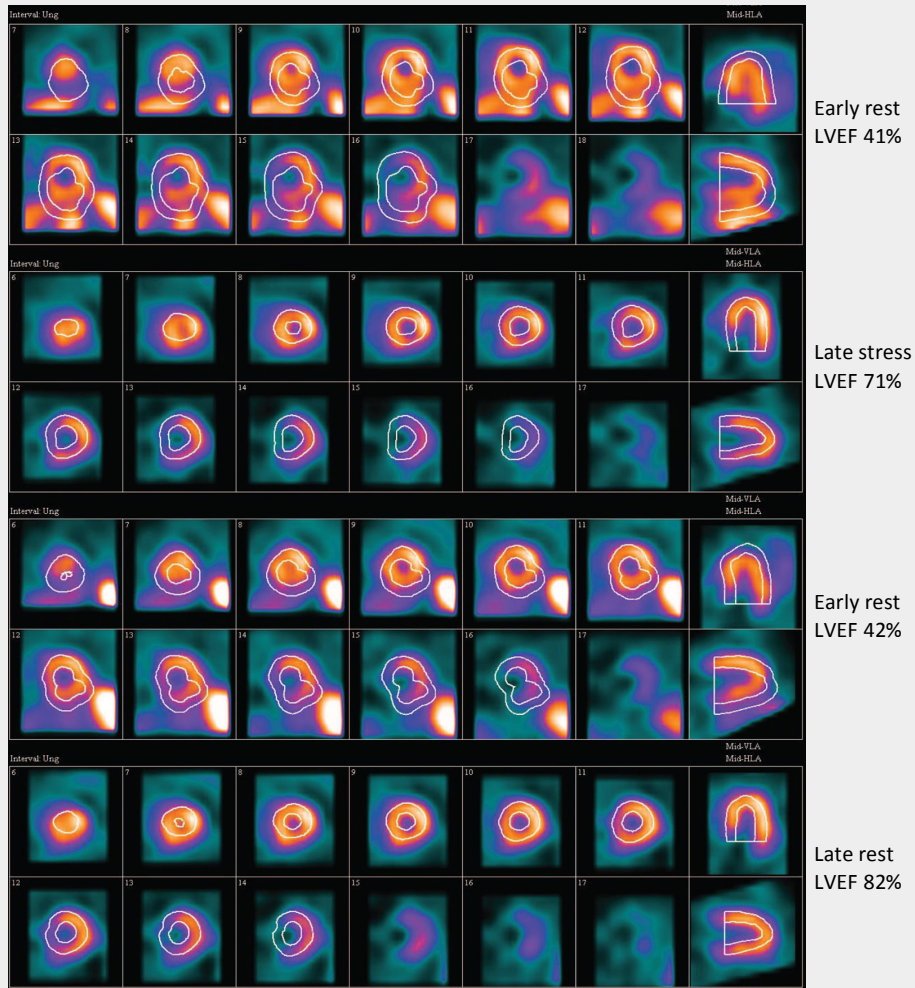


Figure 3. Patient with severe subdiaphragmatic activity during early stress and early rest acquisitions. Due to the amount of activity, and the close proximity to the myocardium, the software system is not able to provide accurate border estimates, resulting in erroneous LVEF values in these early acquisitions.

scores were smaller than two, which indicates that the activity in these cases did not interfere with the visual interpretation of these images and, therefore, can be considered irrelevant. In the present study there was a significant decrease in intensity with time in both the liver and intestine. It seems that late imaging leads to decrease in the subdiaphragmatic activity independent of the location of the tracer accumulation.

The number of scans that show moderate or severe subdiaphragmatic activity interfering with the visual interpretation of the MPS during early and late scanning is represented in Figure 2. Almost two-thirds of the patients (64%) have a considerable amount of subdiaphragmatic activity shortly following injection of the radioactivity during rest MPS. The subdiaphragmatic activity decreased in most of these patients with the time. Only 9 patients (18%) still had considerable subdiaphragmatic activity around 56 minutes following tracer injection. Stress imaging shows comparable results to that of rest imaging regarding the time-related decrease in the subdiaphragmatic activity, except for that fact that the subdiaphragmatic activity was generally less frequent and less prominent in stress imaging.

A number of earlier studies have explored methods to reduce extracardiac activity in myocardial perfusion imaging. Most articles focused on the effects of filling of the stomach, different food types, use of medication such as metoclopramide, as well as the time from injection to acquisition on the image quality.^{5,9-20} In these articles, the effect of time was studied together with one or more variables. Additionally, the effect of time on the image quality was most often studied in randomized, blind trials in more than one subgroup of patients. In our study, acquisitions were performed early following injection and repeated about 45 minutes later in all included patients. To our knowledge, this is the first study which shows the effect of time on the subdiaphragmatic activity in MPS on the same group of patients.

Most of the earlier performed studies had used the radiopharmaceutical sestamibi instead of tetrofosmin. Although both are cleared through the hepatobiliary tract and are eliminated through the duodenum, there are other essential differences in biokinetics between these two compounds, including differences in extracardiac activity.²¹ We studied the effect of time on the subdiaphragmatic activity in a MPS SPECT protocol using tetrofosmin. It seems that tetrofosmin results in a better contrast between cardiac and subdiaphragmatic structures when the acquisitions are delayed following injection of the tracer.

If acquisitions are performed late after physical or chemical stress protocol, this could theoretically affect the functional parameters that are measured with MPS. The effects of early and late scanning on the functional parameters of the entire populations are reported in Table 3. These results showed significantly lower value of LVEF in the early acquisitions comparing with late acquisitions. The acquisitions with the most profound differences in LVEF between early and late scans were closely analysed. Surprisingly,

inaccurate automatic border detection was the cause of this difference in LVEF in all cases. In these cases, the amount of extracardiac activity was severe enough to seriously affect the automatic border detection in one or more acquisitions, especially of the inferior wall and mostly in the early acquisitions (Figure 3). The data were analysed in the stress group following exclusion of the scans with inaccurate determined borders. Table 4 shows the results of the functional parameters of exclusively the acquisitions with accurate automatic border estimation. There was no significant difference in the ejection fraction between the early and late acquisition in the last selected group. These results show that there is no indication to assume significant influence of time on the quantitative parameters in MPS.

CONCLUSION

Late imaging after Tc-99m tetrofosmin leads to a decrease in subdiaphragmatic activity in most myocardial perfusion scan and consequently in a significantly better image quality. Rest/stress and exercise/adenosine perfusion studies show comparable patterns regarding the time-related decrease in the extracardiac activity. Late imaging does not have a significant effect on the functional parameters of MPS, including the ejection fraction. However, as lower values of the ejection fraction can be seen in early imaging almost exclusively due to wrong border estimation of the myocardium and image quality improves significantly over time, late acquisitions are recommended in clinical practice, this in contrast to the instructions of Tc-99m tetrofosmin.

REFERENCE LIST

- (1) Ficaro EP, Corbett JR. Advances in quantitative perfusion SPECT imaging. *J Nucl Cardiol.* 2004;11:62-70.
- (2) Hansen CL, Goldstein RA, Akinboboye OO et al. Myocardial perfusion and function: single photon emission computed tomography. *J Nucl Cardiol.* 2007;14:e39-e60.
- (3) Ficaro EP, Corbett JR. Technical Considerations in Quantifying Myocardial Perfusion and Function. *Nuclear Cardiology: Technical Applications.* McGraw-Hill Medical; 2008.
- (4) Lavender FM, Meades RT, Al-Nahhas A, Nijran KS. Factors affecting the measurement of left ventricular ejection fraction in myocardial perfusion imaging. *Nucl Med Commun.* 2009;30:350-355.
- (5) Rehm PK, Atkins FB, Ziessman HA et al. Frequency of extra-cardiac activity and its effect on 99Tcm-MIBI cardiac SPET interpretation. *Nucl Med Commun.* 1996;17:851-856.
- (6) Middleton GW, Williams JH. Interference from duodeno-gastric reflux of 99Tcm radiopharmaceuticals in SPET myocardial perfusion imaging. *Nucl Med Commun.* 1996;17:114-118.
- (7) GE health care. Myoview Kit - Preparation of Tc99m Tetrofosmin for injection. 1-2-2006. GE health care.
- (8) Hesse B, Tagil K, Cuocolo A et al. EANM/ESC procedural guidelines for myocardial perfusion imaging in nuclear cardiology. *Eur J Nucl Med Mol Imaging.* 2005;32:855-897.
- (9) Boz A, Yildiz A, Gungor F, Karayalcin B, Erkilic M. The volume effect of the stomach on intestinal activity on same-day exercise--rest Tc-99m tetrofosmin myocardial imaging. *Clin Nucl Med.* 2001;26:622-625.
- (10) Boz A, Gungor F, Karayalcin B, Yildiz A. The effects of solid food in prevention of intestinal activity in Tc-99m tetrofosmin myocardial perfusion scintigraphy. *J Nucl Cardiol.* 2003;10:161-167.
- (11) Cherng SC, Chen YH, Lee MS, Yang SP, Huang WS, Cheng CY. Acceleration of hepatobiliary excretion by lemon juice on 99mTc-tetrofosmin cardiac SPECT. *Nucl Med Commun.* 2006;27:859-864.
- (12) Hofman M, McKay J, Nandurkar D. Efficacy of milk versus water to reduce interfering infra-cardiac activity in 99mTc-sestamibi myocardial perfusion scintigraphy. *Nucl Med Commun.* 2006;27:837-842.
- (13) Hurwitz GA, Clark EM, Slomka PJ, Siddiq SK. Investigation of measures to reduce interfering abdominal activity on rest myocardial images with Tc-99m sestamibi. *Clin Nucl Med.* 1993;18:735-741.
- (14) Hurwitz GA. Increased extra-cardiac background uptake on immediate and delayed post-stress images with 99Tcm sestamibi: determinants, independence, and significance of counts in lung, abdomen and myocardium. *Nucl Med Commun.* 2000;21:887-895.

- (15) Iqbal SM, Khalil ME, Lone BA, Gorski R, Blum S, Heller EN. Simple techniques to reduce bowel activity in cardiac SPECT imaging. *Nucl Med Commun.* 2004;25:355-359.
- (16) Lyngholm AM, Pedersen BH, Petersen LJ. Randomized, single-blind, factorial design study of the interaction of food and time on intestinal activity in ^{99m}Tc-tetrofosmin stress myocardial perfusion scintigraphy. *Nucl Med Commun.* 2008;29:759-763.
- (17) Middleton GW, Williams JH. The significance of gastric activity in ²⁰¹Tl myocardial perfusion imaging. *Nucl Med Commun.* 1995;16:980.
- (18) Peace RA, Lloyd JJ. The effect of imaging time, radiopharmaceutical, full fat milk and water on interfering extra-cardiac activity in myocardial perfusion single photon emission computed tomography. *Nucl Med Commun.* 2005;26:17-24.
- (19) van Dongen AJ, van Rijk PP. Minimizing liver, bowel, and gastric activity in myocardial perfusion SPECT. *J Nucl Med.* 2000;41:1315-1317.
- (20) Weinmann P, Moretti JL. Metoclopramide has no effect on abdominal activity of sestamibi in myocardial SPET. *Nucl Med Commun.* 1999;20:623-625.
- (21) Hambye AS, Delsarte P, Vervaet AM. Influence of the different biokinetics of sestamibi and tetrofosmin on the interpretation of myocardial perfusion imaging in daily practice. *Nucl Med Commun.* 2007;28:383-390.

Chapter 4

Transient Ischemic Dilatation

B.J. van der Veen, N. Kuperij, M.P.M. Stokkel,

Transient Ischemic Dilatation ratio derived from myocardial
perfusion scintigraphy; What are we looking at?

J Nucl Cardiol 2010; 17(2):207-215

ABSTRACT

Background: An elevated transient ischemic dilatation (TID) ratio during myocardial perfusion scintigraphy (MPS) is described as a marker of severe CAD, even in acquisitions with normal perfusion. This study was initiated to explore the effects of stressor type on the TID. Additionally, the relation between the TID and other functional parameters, such as end-diastolic volume (EDV), end-systolic volume (ESV), and left ventricle ejection fraction (LVEF), heart rate (HR), and the severity of ischemia, were evaluated.

Methods: A total of 299 consecutive patients referred for a 2-day stress/rest MPS protocol were included. Patients were stressed with either adenosine ($n = 164$) or exercise ($n = 135$). MPS data were analysed with an automated software tool to determine TID, EDV, ESV, LVEF, summed stress score (SSS), and summed difference score (SDS). The SDS was used to quantify the degree of ischemia, with a $SDS \geq 3$ considered ischemic.

Results: Comparison of the adenosine and exercise stressed population revealed significant differences, especially in parameters derived from the post-stress acquisition. Within the exercise stressed population, TID was proportional with the SDS ($R^2 = 0.12$); whereas the adenosine population did not show such a relation ($R^2 = 0.001$). Difference in HR between rest and post-stress acquisitions showed high levels of linear regression with TID values of both the adenosine ($R^2 = 0.41$) and exercise ($R^2 = 0.29$) stressed population.

Conclusion: In an exercise stressed population, TID is determined by both the degree of ischemia and the heart-rate difference between the two acquisition moments. TID within the adenosine population was found to be highly proportional with the HR, rather than with the degree of ischemia.

Keywords: Myocardial perfusion imaging ▪ SPECT ▪ Coronary artery disease ▪ Myocardial ischemia ▪ Ischemic dilatation

INTRODUCTION

Myocardial perfusion imaging using gated single photon emission computer tomography (SPECT) is a validated and powerful tool for the diagnosis and evaluation of myocardial perfusion in patients with known or suspected ischemic heart diseases, such as coronary artery disease (CAD).¹⁻³ Stress/rest acquisition protocols can provide information on functional and perfusion status of the left ventricular (LV) myocardium. The gated SPECT acquisitions are analysed visually, with additional (semi-) quantitative parameters which are automatically derived by software packages. These standard software packages obtain several functional parameters, one of which is the transient ischemic dilatation (TID) ratio.

Although the TID was already described by Slutsky et al.⁴ half way the 20th century, Stolzenberg popularized the index in 1980 by describing TID in myocardial perfusion scintigraphy (MPS) as a finding in three patients.⁵ Ever since, multiple studies confirmed the diagnostic value of TID in predicting severe CAD utilizing various isotopes (Tc-99m, Tl-201), protocols (single-day, separate day and dual isotope) and imaging approaches (planar, SPECT, gated SPECT).⁶⁻⁸ An apparent increase in TID ratio is now regarded as a serious finding that may indicate extensive CAD, even when the perfusion distribution seems normal.⁹ Still, the underlying mechanisms that cause abnormal TID findings are a matter of controversy. Possible explanations include subendocardial hypo-perfusion, systolic dysfunction, and actual physical dilatation.¹⁰⁻¹²

Earlier studies indicated that, although, the TID values may depend on radiopharmaceutical (typically Tl-201 or Tc-99m), method of stress induction and the patient gender, it is relatively independent of the algorithm used to calculate this ratio.^{10,13} As the method of stress induction may influence the TID ratio, it is interesting to explore the effects of exercise and adenosine stress induction on the TID value. Thus, the aim of this study was to investigate the influence of these two stressor types on the automatically generated TID ratio in patients presenting various degrees of coronary artery disease. Additionally, the relation between TID and other automatically derived quantitative parameters, such as end-diastolic volume (EDV), end-systolic volume (ESV) and left ventricular ejection fraction (LVEF), and patient specific factors, such as heart rate (HR) and CAD severity, was evaluated.

MATERIALS AND METHODS

Patient population

Patients referred for MPS with Tc-99m tetrofosmin, between November 2008 and March 2009, were included in this retrospective study. These patients underwent either adenosine- or exercise-induced post-stress study as part of the 2-day stress/rest protocol. Relevant information was gathered for each patient with respect to risk factors for CAD, previous CAD or infarctions and medication use. All SPECT acquisitions were analysed by the Corridor 4D-MSPECT software packages (Invia Medical Imaging Solutions, Ann Arbor, Michigan, USA) to calculate the quantitative parameters.

MPS protocol

At the department of Nuclear Medicine at the Leiden University Medical Centre, MPS studies are performed with a 2-day stress/rest protocol using Tc-99m tetrofosmin. The population underwent a post-stress acquisition on the first and rest acquisition on the second day. Stress was induced either by physical exercise on a bicycle ergometer, or by intravenous infusion of adenosine ($140\mu\text{g kg}^{-1}\text{ min}^{-1}$) for 6 minutes. Patients were instructed to stop both β -blockers and calcium antagonist intake for 48 hours, and abstinence from caffeine containing products 12 hours before stress. Tc-99m tetrofosmin (approximately 500 MBq) was administered intravenously at peak exercise, or during the third minute of adenosine infusion. Post-stress and rest gated SPECT acquisitions were initiated 45 minutes after tracer administration.

Images were acquired using a triple headed SPECT camera system produced by Toshiba (CGA 9300, Tokyo, Japan) over 360 degrees (in 6 degree steps, 40 seconds/direction). Automatic ECG gating was applied on the R-R interval with 16 frames per cardiac cycle, with a tolerance window of 50%. The data were prefiltered using a Butterworth filter (eighth order, cut-off frequency 0.26 cycles/pixel), and the images were reconstructed in topographic transaxial images using filtered back projection. No attenuation or scatter correction was applied.

Automated analysis of the acquisitions were performed using the Corridor 4DM-SPECT software.¹⁴ This system automatically determines apex, base and the myocardial borders of the LV. Adjustments to the apex or basal planes by the clinicians was allowed, but were limited to an absolute minimum.

Data interpretation

During adenosine and exercise stress, the HR was recorded before stress induction at resting conditions and at the moment of maximal stress. The difference between HR at maximal stress and rest was considered the HR response. In the post-stress and rest acquisitions, the HR of the patients was also recorded. The difference in HR during post-stress acquisition and the mean HR during rest acquisition is defined as Δ HR.

Functional parameters were derived from gated (LVEF, EDV, ESV and HR) or ungated acquisitions (TID). The summed stress score (SSS) and summed rest score (SRS) were calculated based on an automatically created polar map, which is compared to the manufacturer's normal database to reduce effects of attenuation. The summed difference score (SDS) was obtained as the sum of all segmental differences between SSS and SRS, provided that the difference of a segment met the condition $SSS > SRS$. The TID is calculated as the ratio between rest and post-stress ungated LV volumes ($TID = UGV_{stress} / UGV_{rest}$). The LVEF is calculated within the post-stress and rest acquisition and is the percentage of change between the EDV and ESV.

CAD severity was assigned in correspondence with the frequently used summed difference score (SDS). This summed score is based on polar map reproductions of the myocardium that display count distributions, thus indicating abnormalities in perfusion patterns. According to Hsu et al., the SDS scoring method of 4D-MSPECT provides good resemblance with visual scoring of CAD severity.¹⁵ Abnormal SDS scores are frequently defined as a summed score ≥ 3 , which will be referred to as '*ischemic*' from now on. An abnormal TID is within previous studies used to indicate severe and extensive CAD in myocardial perfusion SPECT acquisitions. In patients undergoing exercise a TID threshold of >1.22 , and in patients undergoing adenosine a threshold of >1.36 was used to indicate severe CAD.^{10,16}

Statistical analysis

Statistical analysis was performed using the SPSS software version 16.0 (SPSS Inc. Chicago, USA). Continuous variables are expressed by mean \pm standard deviation. Differences in parameter values between the adenosine and exercise groups were assessed using Student's *t*-test analysis, and differences in medical history or medications use were assessed using χ -square analysis. Significant differences were

defined with p -values <0.05 . Pearson correlation coefficients and/or linear regression analysis were performed to determine the presence of relations between parameters.

RESULTS

A total of 303 patients underwent diagnostic MPS with a 2-day stress/rest protocol using Tc-99m tetrofosmin. Four patients had to be excluded from this study because of inadequate acquisitions due to unfinished stress/rest protocols or due to the presence of extensive extracardiac activity. Thus, 299 patients were eventually included, comprising 164 adenosine and 135 exercise stressed patients. Table 1 provides a summary of the patient's characteristics for the total population, and for the adenosine and exercise subgroups.

Adenosine versus exercise stressed populations

It can be stated that patients who are stressed with adenosine are slightly older, have a higher body mass index (BMI), are more frequently diabetic and users of β -blockers, than exercise-stressed patients. Thus, there is a clear difference in patient profile between the two populations. Overall patients undergoing bicycle exercise will have a significantly higher HR response to the stress compared to the adenosine group. The exercise group had overall lower volumes, higher LVEF values and a higher HRs during the post-stress acquisition. Especially this difference in HR response to stress and the HR during post-stress acquisition between the two groups is prominent. Within the rest acquisitions these differences are less prominent, although lower volumes, and higher LVEF values during the rest acquisition can still be found in the exercise group.

Regarding the TID, significant differences in TID values are shown between the two groups. Overall, the mean TID of the exercise-stressed patients was slightly lower (0.90 ± 0.17 beats per minute) than that of the adenosine stressed patients (1.01 ± 0.17 beats per minute). Nonetheless, the frequency of an abnormal TID is low over the entire population ($n = 8$) and does not vary significantly between the two populations when applying the stress related normal limits.

TABLE 1. PATIENT CHARACTERISTICS

	Total (n =299)	Adenosine (n = 164)	Exercise (n = 135)	p-value
Risk factors				
Age	60.3 ± 10.3	61.4 ± 10.3	59.0 ± 10.2	0.048*
BMI	27.2 ± 4.4	27.9 ± 4.8	26.5 ± 3.8	0.007*
Smoker	104 (34.8)	61 (37.2)	43 (31.9)	0.334
Hypertension	142 (47.5)	81 (49.4)	61 (45.2)	0.469
Hypercholesteremia	97 (32.4)	59 (36.0)	38 (28.1)	0.150
Diabetic	63 (21.1)	43 (26.2)	20 (14.8)	0.016*
Family history	110 (36.8)	57 (34.8)	53 (39.3)	0.422
History of CAD or infarction	148 (49.5)	75 (45.7)	73 (54.1)	0.151
Medication use				
ACE inhibitor	107 (35.8)	53 (32.3)	54 (40.0)	0.168
Beta-blocker	180 (60.2)	94 (57.3)	86 (63.7)	0.262
Calcium Antagonist	37 (12.4)	32 (19.5)	5 (3.7)	<0.001*
Ischemic	55 (18.4)	35 (21.3)	20 (14.8)	0.148
MPS parameters				
HR response (bpm)	38.6 ± 32.0	16.2 ± 12.5	65.7 ± 27.1	<0.001*
SSS	6.1 ± 9.1	6.9 ± 9.6	5.1 ± 8.3	0.077
SDS	1.3 ± 2.3	1.5 ± 2.4	1.1 ± 2.1	0.185
HR rest (bpm)	68.0 ± 13.4	69.1 ± 14.0	66.7 ± 12.5	0.129
EDV rest (mL)	142.0 ± 73.9	151.5 ± 87.8	130.5 ± 50.3	0.010*
ESV rest (mL)	68.7 ± 67.4	78.0 ± 81.3	57.4 ± 42.7	0.005*
LVEF rest (%)	58.2 ± 15.6	56.6 ± 17.3	60.0 ± 13.2	0.063
HR stress (bpm)	77.8 ± 16.2	73.6 ± 15.0	82.8 ± 16.2	<0.001*
EDV stress (mL)	139.4 ± 76.9	152.9 ± 90.1	122.9 ± 52.9	<0.001*
ESV stress (mL)	66.3 ± 70.2	78.7 ± 84.2	51.2 ± 43.8	<0.001*
LVEF stress (%)	59.8 ± 16.3	57.1 ± 17.6	63.0 ± 13.8	0.001*
ΔHR (HR stress – HR rest)	9.7 ± 14.6	4.6 ± 11.7	16.1 ± 15.2	<0.001*
TID ratio	0.96 ± 0.18	1.01 ± 0.17	0.90 ± 0.17	<0.001*
Abnormal TID	8 (2.7)	4 (2.4)	4 (3.0)	0.589

Chi-square or independent Student's t-test, with * indicating significance of <0.05. Frequencies are indicated in number (percentage)

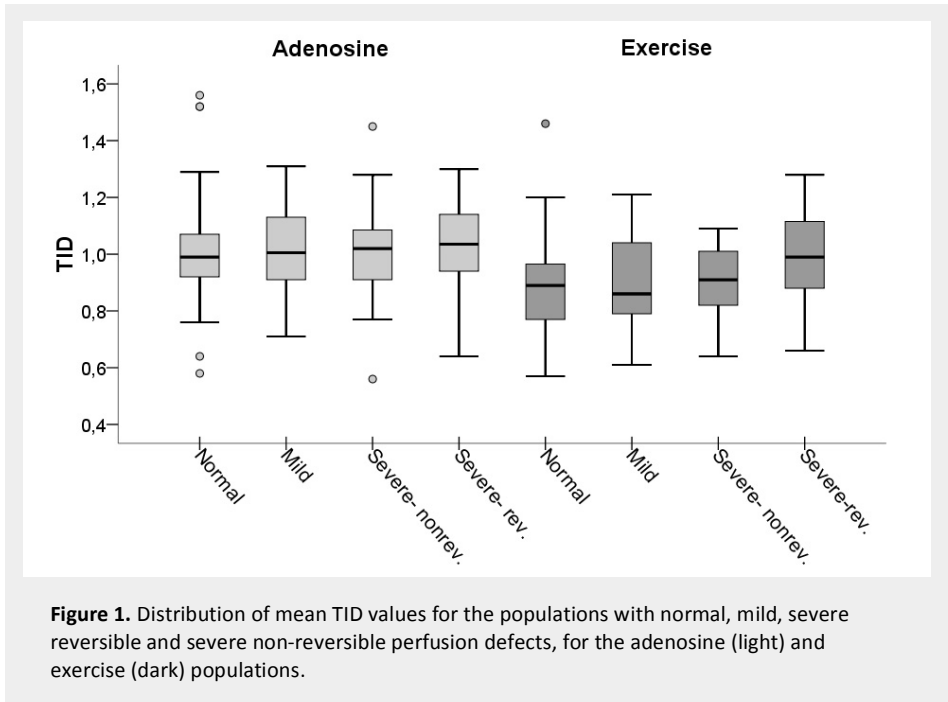
TABLE 2. THE EFFECTS OF VARIOUS MEDICAL FACTORS ON TID VALUES

	Mean TID value				Mean TID value		
	Adenosine	Exercise	p-value		Adenosine	Exercise	p-value
Gender				Family history			
Male	1.01±0.15	0.90±0.15	<0.001*	Negative	1.02±0.15	0.90±0.16	<0.001*
Female	1.01±0.20	0.93±0.18	0.052	Positive	1.01±0.19	0.91±0.16	0.005*
p-value	0.886	0.257		p-value	0.659	0.812	
Smoker				CAD or infarction			
Negative	1.02±0.16	0.90±0.17	<0.001*	Negative	1.03±0.18	0.89±0.17	<0.001*
Positive	1.00±0.18	0.93±0.15	0.032*	Positive	1.00±0.15	0.92±0.16	0.003*
p-value	0.528	0.243		p-value	0.223	0.323	
Alcohol use				ACE inhibitor			
Negative	1.01±0.17	0.90±0.16	<0.001*	Negative	1.02±0.17	0.89±0.15	<0.001*
Positive	1.05±0.17	0.95±0.21	0.260	Positive	1.00±0.17	0.92±0.17	0.026*
p-value	0.401	0.399		p-value	0.418	0.304	
Hypertension				β-blocker			
Negative	0.99±0.17	0.91±0.19	0.007*	Negative	1.02±0.17	0.94±0.15	0.012*
Positive	1.04±0.16	0.90±0.13	<0.001*	Positive	1.01±0.16	0.88±0.16	<0.001*
p-value	0.085	0.556		p-value	0.541	0.034*	
Hypercholesterolemia				Calcium Antagonist			
Negative	1.01±0.17	0.89±0.16	<0.001*	Negative	1.00±0.16	0.91±0.16	<0.001*
Positive	1.01±0.17	0.94±0.18	0.031*	Positive	1.05±0.17	0.89±0.17	0.054
p-value	0.964	0.168		p-value	0.130	0.856	
Diabetic				Ischemic			
Negative	1.02±0.17	0.90±0.17	<0.001*	SDS ≥ 3	1.01±0.16	1.00±0.17	0.803
Positive	1.00±0.17	0.91±0.15	0.062*	SDS < 3	1.01±0.17	0.89±0.16	<0.001*
p-value	0.524	0.781		p-value	0.942	0.005*	

Independent Student's *t*-test, with * indicating significance of <0.05

Effect of medical factors on TID

In Table 1, an uneven distribution of medical factors within the two stressor groups is shown, which could affect the TID values within the two populations. To study the effects of this uneven distribution within the two groups on the derived TID ratio, the two populations were subdivided based on the presence or absence of these factors. The

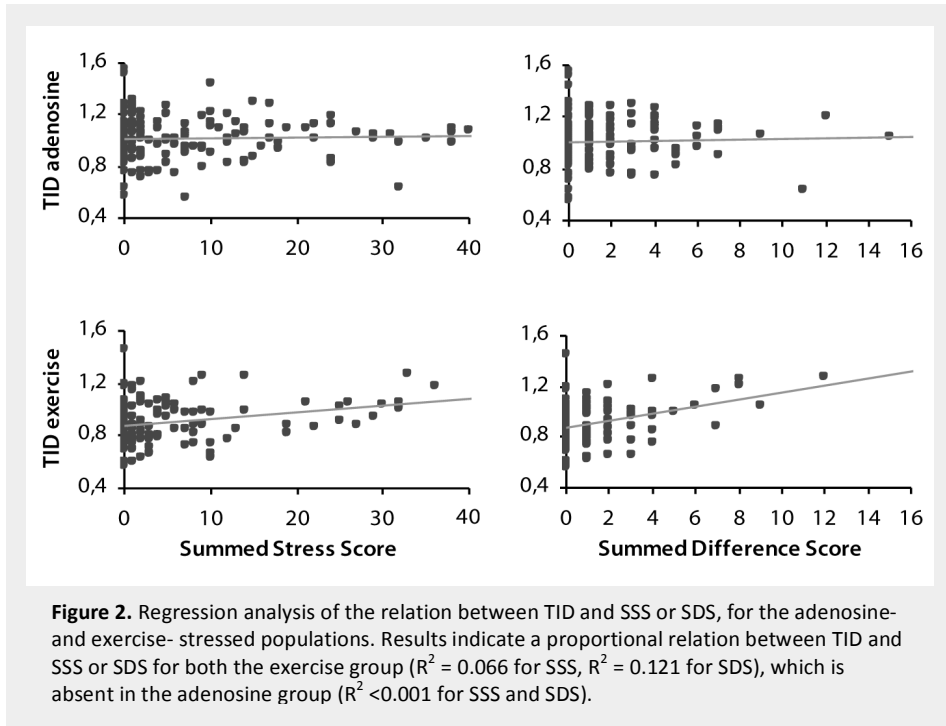


mean TID value for each of these groups is calculated and independent Student's *t*-tests were performed to determine the significance of the differences. The results (Table 2) indicate that only the factors 'ischemic' and ' β -blocker' induce significant differences in TID. All other factors did not show significant effects on the TID. The differences between the adenosine and exercise stressed populations remained present for all factors.

Relation between TID and degree of ischemia

Based on the threshold of $SDS \geq 3$, 18.4% ($n = 55$) of the total population was considered ischemic. Evaluation of the relationship between the TID and the SDS score over the entire population showed a significant correlation (PCC 0.175, $p = 0.003$). Additionally, the relation between the TID and the categorized 'ischemic or non-ischemic' was determined, which also yielded a significant correlation (PCC 0.118, $p = 0.043$).

To further evaluate the effects of ischemia and perfusion abnormalities on the TID the population was divided into the groups normal (SSS = 0), mild defects (SSS <3), severe defects with ischemia (SSS ≥ 3 & SDS ≥ 3) and severe defects without ischemia (SSS ≥ 3 &



SDS <3). Since the type of exercise was also included, a total of 8 groups were generated (Figure 1); normal adenosine ($n = 53$, TID 1.01 ± 0.19), mild adenosine ($n = 34$, TID 1.02 ± 0.16), severe-nonreversible adenosine ($n = 40$, TID 1.00 ± 0.16), severe-reversible adenosine ($n = 36$, TID 1.02 ± 0.16), normal exercise ($n = 55$, TID 0.88 ± 0.17), mild exercise ($n = 30$, TID 0.90 ± 0.16), severe-nonreversible exercise ($n = 29$, TID 0.90 ± 0.13) and severe-reversible exercise ($n = 55$, TID 1.00 ± 0.17). Nonsignificant mean differences were shown between the mean TID values of the different adenosine groups. Within the exercise stressed groups, significant differences were found between the normal versus severe-reversible ($p = 0.008$), mild versus severe-reversible ($p = 0.031$), severe-nonreversible versus severe-reversible ($p = 0.033$) groups. Nonetheless, variance within the groups is relatively high, and the groups show overlay in the TID domains. The regression between SSS or SDS and the TID is visualized in Figure 2. This figure indicates the proportional relation between SDS and TID for the exercise group, and the lack of such a relation for the adenosine group.

TABLE 3. THE CORRELATION BETWEEN TID AND OTHER FUNCTIONAL MPS PARAMETERS

	<i>All patients (n =299)</i>		<i>Adenosine (n = 164)</i>		<i>Exercise (n = 135)</i>	
	PCC	p-value	PCC	p-value	PCC	p-value
SSS	0.148	0.011*	0.029	0.711	0.256	0.003*
SDS	0.175	0.003*	0.044	0.575	0.349	<0.001*
LVEF rest (%)	-0.106	0.067	-0.025	0.754	-0.166	0.054
LVEF stress (%)	-0.216	<0.001*	-0.093	0.237	-0.300	<0.001*
HR response	-0.237	<0.001*	0.031	0.697	-0.010	0.905
HR stress (bpm)	-0.352	<0.001*	-0.221	0.004*	-0.375	<0.001*
HR rest (bpm)	0.210	<0.001*	0.263	0.001*	0.098	0.258
Δ HR (bpm)	-0.632	<0.001*	-0.637	<0.001*	-0.540	<0.001*

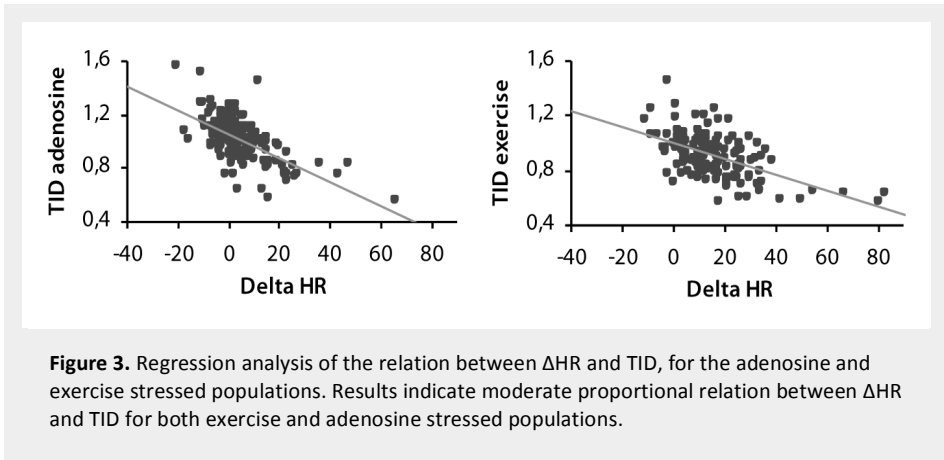
Pearson Correlation Coefficients (PCC), with * indicating significance of <0.05

Relation between TID and functional MPS parameters

The other functional parameters showed significant correlations with the TID, which is overall more evident in the post-stress parameters, than in the rest parameters (Table 3). Within the adenosine stressed group no significant correlations are observed between the TID and the rest or post-stress parameters, except for the HR measured during the acquisitions and the Δ HR. The exercise group, on the other hand, produces significant correlations between the TID and all other MPS parameters, except for the HR during rest acquisition and the rest LVEF.

Effects of HR variability

In the process of studying the relation between MPS parameters and TID, the relation between TID and the HR revealed surprising information. The HR response to exercise did not have significant correlations with the TID in the adenosine and exercise subgroups. The mean HR measured during the rest and post-stress acquisitions seem to have a high correlation with the TID ratio. In both populations, the HR during rest acquisition is proportional and the HR during post-stress acquisition is inversely proportional to the TID (Table 3). The correlation between TID and Δ HR is even better and significant ($p < 0.001$) in both the adenosine and exercise group. The Δ HR in the exercise group is nonetheless more prominent (16.1 ± 15.2 beats per minute) than in the adenosine stressed population (4.6 ± 11.7 beats per minute).



The regression between the Δ HR and the TID for these groups is visualized for both stressor groups in Figure 3. This figure visualizes the eminent relation between Δ HR and TID for both the adenosine ($R^2 = 0.406$) and exercise ($R^2 = 0.292$) stressed group, which may indicate the dependence of TID on the HR during acquisition.

Evaluating the relation between the Δ HR and the SDS indicates a poor non-significant correlation (PCC -0.098 , $p = 0.089$) for the total population, and even worse correlations for the adenosine (PCC -0.68 , $p = 0.386$) and exercise group (PCC -0.097 , $p = 0.265$). Still, the correlation between Δ HR and TID for the subgroups is -0.637 ($p < 0.001$) and -0.540 ($p < 0.001$), respectively. Still, the correlation between Δ HR and TID for the subgroups is respectively -0.637 ($p < 0.001$) and -0.540 ($p < 0.001$).

DISCUSSION

In the present study, the effects of stress induction on the TID were analysed in a population of 299 patients that were referred for MPS. Additionally, the relation between the TID and other functional parameters, and the effects of various medical factors on TID, were also evaluated. This study therefore provides a complete overview of influences of a variety of factors on the TID.

TID is described within literature as a useful marker for the detection of severe CAD. Abnormal TID ratios may even indicate severe CAD if tracer distributions throughout the myocardium do not show heterogeneities. Abidov et al.¹⁰ described the usefulness of the TID ratio within adenosine stressed patients in detecting severe CAD during a dual-

isotope MPS protocol. Nonetheless, there are also studies indicating that TID should be analysed with caution, because factors that may influence TID, and the underlying pathophysiology, are not yet fully understood.

The results of the study indicate significant differences in TID values between the adenosine and exercise stressed populations, which are especially profound in the non-ischemic part of the population. Within the adenosine population non-significant differences were found comparing the ischemic and non-ischemic patients; whereas TID values for non-ischemic patients are significantly lower than those for ischemic patient in the exercise stressed population. Additionally, large variations are present in the ischemic and non-ischemic groups, for both adenosine and exercise stressed populations. Regression analysis between TID and SDS or SSS for both groups revealed a proportional relation in the exercise population, however this relation is absent in the adenosine group. From these results it can be concluded that TID is a phenomenon that is mainly useful in the exercise stressed population.

Heart rate dependence

Several case reports of erroneous cavity estimations and their relation to HR are presented within literature.¹⁷⁻²⁰ Transient arrhythmias, both tachy- and brady-arrhythmias, during the acquisition can produce falsely elevated or reduced TID measurements. Elevated HR during post-stress acquisition can be due to continued effects of exercise or pharmacological stress, or due to temporarily withdrawal of negative chronotropic medication. Additionally, there is the natural occurring day-to-day variation within HR, which depends on complex physiological principles. Thus, any scanning protocol is bound to suffer from a difference in HR between the two acquisition moments.

The study of Leslie et al. reported the influence of HR variation on the TID ratio.²¹ They found an overall difference in HR of 6 ± 9 beats per minute between the stress and rest acquisition. Although this Δ HR is somewhat lower than that in this study (adenosine 4.6 ± 11.7 beats per minute, exercise 16.1 ± 15.2 beats per minute), they also found a lower Δ HR for the pharmacological stressed population, than for exercise stressed population. This study also indicated an inversely proportional relation between the Δ HR and TID for the overall population, but did not distinguish between adenosine and exercise stressed patients.

Though the exact mechanism behind the effects of HR during acquisition and TID are not yet fully understood, a possible explanation can be hypothesized. A difference in HR

will directly influence the perfusion distribution within the myocardium due to the embedded nature of the coronary vasculature within the myocardial muscle. During diastole the myocardial forces are relatively small, thus vascular compression decreases, resulting in the overall increase of blood flow to the intra-myocardial vasculature. During systole, on the other hand, the increased muscle contraction reduces flow within the intra-cardiac circulation, especially in the subendocardial regions.²² This complex mechanism ensures that at slower HRs the diastolic phase is prolonged, creating optimal perfusion of the sub-endocardium. At faster HRs diastole is shortened and perfusion to the sub-endocardium is limited. Due to this relation tracer distribution, and thus also count distribution, is reduced in the sub-endocardium at higher HRs. Since TID is calculated based upon differences in volumes that are derived from the count distributions, decreased subendocardial perfusion during post-stress acquisition can induce the impression of increased TID.

A second approach, in which HR can influence TID measurements, is explained by the nature of the ungated volume on which TID measurements are based. Ungated implies that the image is a summation of acquisitions of the entire cardiac cycle. An increase in HR will ensure a smaller contribution of diastolic images to the entire summed volume, because the heart will remain a shorter period of the time in diastole. These images are referred to as 'systolic pattern', and tend to display a LV cavity that is smaller with contracted walls. A reduced HR will produce the opposite, a 'diastolic pattern', with an enlarged LV cavity and dilated walls. Both patterns are normal observations, but may influence the TID measurements without the presence of actual physical dilatation.

Adenosine versus exercise stress

Adenosine stress induction relies on different basic principles than exercise stress induction, so there are also differences in the functional measurements to be expected. Although vasodilators will mainly induce coronary hyperaemia, they also reduce sinoatrial and atrioventricular node activity, atrial contractility, ventricular automaticity, and influence the actions of catecholamine's (nor-epinephrine). The hemodynamic response to adenosine infusion is a moderate increase of HR and systolic pressure, and minor decrease in diastolic pressure. In the presence of ischemic heart diseases, the increase in coronary blood flow is inversely proportional to the severity of the stenosis. Affected arteries are already dilated at baseline level, thus infusion of adenosine will cause limited additional dilatation. Heterogeneities in dilatation, and consequently in

blood flow, will induce a heterogenic tracer uptake throughout the myocardium resulting in perfusion defects. Only in severe stenotic arteries, the '*steal effect*' can occur, resulting in a truly ischemic reaction of the myocardium.^{23,24}

During exercise, on the other hand, the increase in peripheral oxygen demand results in a necessity to increase cardiac output, this results in an increasing HR, contractility and ventricular work of the heart. This initiates in turn a series of mechanisms to meet the increased oxygen demand of the myocytes.²⁵ In affected coronary arteries many of these mechanisms fail, which in combination with the increased oxygen demand, initiates truly ischemic reactions.

Based on these differences in physiological reactions during adenosine and exercise stress induction, the degree of the ischemia resulting from both methods is different. Additionally, there is a difference in HR response and HR during stress acquisition between both methods. These factors could possibly explain the differences in some MPS parameters and the TID values that were found between the two groups. With adenosine infusion, only a limited amount of patients with heterogeneities in perfusion distribution will actually experience ischemia. Therefore, patients with high SSS do not necessarily experience true ischemia and will not have increased TID values.

The meaning of abnormal TID

Several pathophysiological and physiological mechanisms may be accountable for TID findings during a MPS acquisition. Initially it was described as an enlargement of the LV cavity during stress due to extensive ischemia that is prolonging the return of ventricular function and size.¹² Nowadays TID is more frequently described as a combination of this true physical dilatation, and apparent dilation caused by non-visualization of the sub-endocardium. Which factor dominates during exercise or adenosine stress is not yet identified in literature. This study, however, supports the theory that dilatation within the adenosine population is mainly based on display derived factors, rather than on true dilatation. Within the exercise group there was a relation between TID and extensiveness of CAD, however the HR during acquisition also affected the TID within this groups to a large extent. Because TID is influenced by HR in both populations it is advised to use the TID as a complementary parameter and never as a single indicator of extensive and severe CAD.

Study limitations

The main limitation of this study is its retrospective nature, which accounts for the unequal distribution of medical factors within the groups and which may induce a population bias. As mentioned before, the assumption is made that the unequal distribution of factors between the two subgroups does not influence the TID. However, the use of β -blockers may affect the TID, as is indicated in Table 2. Abstinance of β -blocker medication is only asked during the post-stress acquisition. This abstinance of medication can cause an increased HR during post-stress acquisition. Because medication is started immediately after stress acquisition, the HR will be lowered during rest acquisition, thus influencing TID.

CONCLUSION

TID is described as indicator of severe CAD, which correlates with the degree of ischemia. The results of this study contradict the current concept of TID, and indicate no correlation between TID and degree of ischemia for the adenosine-stressed patients. In exercise-stressed patients there was a slight proportional relation between TID and the degree of ischemia. In both populations, the difference in HR during the acquisition was inversely proportional with the TID. Other medical factors did not affect the TID values. Given the strong relation with the HR, it is advisable to use the TID as a complementary parameter that is to be evaluated in combination with other perfusion and functional parameters, and never as a single indicator of extensive CAD.

REFERENCE LIST

- (1) Abidov A, Germano G, Hachamovitch R, Berman DS. Gated SPECT in assessment of regional and global left ventricular function: major tool of modern nuclear imaging. *J Nucl Cardiol.* 2006;13:261-279.
- (2) Gimelli A, Rossi G, Landi P et al. Stress/Rest Myocardial Perfusion Abnormalities by Gated SPECT: Still the Best Predictor of Cardiac Events in Stable Ischemic Heart Disease. *J Nucl Med.* 2009;50:546-553.
- (3) Hansen CL, Goldstein RA, Akinboboye OO et al. Myocardial perfusion and function: single photon emission computed tomography. *J Nucl Cardiol.* 2007;14:e39-e60.
- (4) Slutsky R, Karliner J, Ricci D et al. Response of left ventricular volume to exercise in man assessed by radionuclide equilibrium angiography. *Circulation.* 1979;60:565-571.
- (5) Stolzenberg J. Dilatation of left ventricular cavity on stress thallium scan as an indicator of ischemic disease. *Clin Nucl Med.* 1980;5:289-291.
- (6) Mazzanti M, Germano G, Kiat H et al. Identification of severe and extensive coronary artery disease by automatic measurement of transient ischemic dilation of the left ventricle in dual-isotope myocardial perfusion SPECT. *J Am Coll Cardiol.* 1996;27:1612-1620.
- (7) McClellan JR, Travin MI, Herman SD et al. Prognostic importance of scintigraphic left ventricular cavity dilation during intravenous dipyridamole technetium-99m sestamibi myocardial tomographic imaging in predicting coronary events. *Am J Cardiol.* 1997;79:600-605.
- (8) Duarte PS, Smanio PE, Oliveira CA, Martins LR, Mastrocolla LE, Pereira JC. Clinical significance of transient left ventricular dilation assessed during myocardial Tc-99m sestamibi scintigraphy. *Arq Bras Cardiol.* 2003;81:474-482.
- (9) Abidov A, Bax JJ, Hayes SW et al. Transient ischemic dilation ratio of the left ventricle is a significant predictor of future cardiac events in patients with otherwise normal myocardial perfusion SPECT. *J Am Coll Cardiol.* 2003;42:1818-1825.
- (10) Abidov A, Bax JJ, Hayes SW et al. Integration of automatically measured transient ischemic dilation ratio into interpretation of adenosine stress myocardial perfusion SPECT for detection of severe and extensive CAD. *J Nucl Med.* 2004;45:1999-2007.
- (11) Bestetti A, Di LC, Alessi A, Triulzi A, Tagliabue L, Tarolo GL. Poststress end-systolic left ventricular dilation: a marker of endocardial post-ischemic stunning. *Nucl Med Commun.* 2001;22:685-693.
- (12) Weiss AT, Berman DS, Lew AS et al. Transient ischemic dilation of the left ventricle on stress thallium-201 scintigraphy: a marker of severe and extensive coronary artery disease. *J Am Coll Cardiol.* 1987;9:752-759.

- (13) Rivero A, Santana C, Folks RD et al. Attenuation correction reveals gender-related differences in the normal values of transient ischemic dilation index in rest-exercise stress sestamibi myocardial perfusion imaging. *J Nucl Cardiol.* 2006;13:338-344.
- (14) Ficaro EP, Lee BC, Kritzman JN, Corbett JR. Corridor4DM: the Michigan method for quantitative nuclear cardiology. *J Nucl Cardiol.* 2007;14:455-465.
- (15) Hsu CC, Chen YW, Hao CL et al. Comparison of automated 4D-MSPECT and visual analysis for evaluating myocardial perfusion in coronary artery disease. *Kaohsiung J Med Sci.* 2008;24:445-452.
- (16) Abidov A, Germano G, Berman DS. Transient ischemic dilation ratio: a universal high-risk diagnostic marker in myocardial perfusion imaging. *J Nucl Cardiol.* 2007;14:497-500.
- (17) Kirkpatrick ID, Leslie WD. Erroneous Left ventricular cavity size measurements on myocardial perfusion SPECT resulting from transient arrhythmias. *Clin Nucl Med.* 2005;30:783-786.
- (18) Choong KK, Russell PA. Transient left ventricular dilatation in the absence of epicardial disease on angiography. *Clin Nucl Med.* 2004;29:348-351.
- (19) Hardebeck CJ. Transient ischemic dilation. *J Am Coll Cardiol.* 2004;44:211-212.
- (20) Robinson VJ, Corley JH, Marks DS et al. Causes of transient dilatation of the left ventricle during myocardial perfusion imaging. *AJR Am J Roentgenol.* 2000;174:1349-1352.
- (21) Leslie WD, Levin DP, Demeter SJ. Variation in HR influences the assessment of transient ischemic dilation in myocardial perfusion scintigraphy. *BMC Nucl Med.* 2007;7:1.
- (22) Spaan J, Kolyva C, van den WJ et al. Coronary structure and perfusion in health and disease. *Philos Transact A Math Phys Eng Sci.* 2008;366:3137-3153.
- (23) Iskandrian AE, Heo J. Myocardial perfusion imaging during adenosine-induced coronary hyperemia. *Am J Cardiol.* 1997;79:20-24.
- (24) McGuinness ME, Talbert RL. Pharmacologic stress testing: experience with dipyridamole, adenosine, and dobutamine. *Am J Hosp Pharm.* 1994;51:328-346.
- (25) Duncker DJ, Bache RJ. Regulation of coronary blood flow during exercise. *Physiol Rev.* 2008;88:1009-1086.

Chapter 5

Ventricular dyssynchrony

B.J. van der Veen, I. Al Younis, N. Ajmone-Marsan, J.J. Westenberg,
J.J. Bax, M.P. Stokkel, A. de Roos,

Ventricular dyssynchrony assessed by gated myocardial perfusion
SPECT using a geometrical approach: a feasibility study.

Eur J Nucl Med Mol Imaging 2011; 39(3):421-429

ABSTRACT

Background: Left ventricular dyssynchrony may predict response to cardiac resynchronization therapy and may well predict adverse cardiac events. Recently, a geometrical approach for dyssynchrony analysis of myocardial perfusion scintigraphy (MPS) was introduced. In this study the feasibility of this geometric method to detect dyssynchrony was assessed in a population with a normal MPS and in patients with documented ventricular dyssynchrony.

Methods: For the normal population 80 patients (40 male, 40 female) with normal perfusion (summed stress score ≤ 2 and summed rest score ≤ 2 ,) and function (LVEF 55-80%) on MPS were selected; 24 heart failure patients with proven dyssynchrony on MRI were selected for comparison. All patients underwent a two-day stress/rest MPS protocol. Perfusion, function and dyssynchrony parameters were obtained by the Corridor4DM software package (Version 6.1).

Results: For the normal population time to peak motion was 42.8 ± 5.1 % RR-cycle, SD of peak motion was 3.5 ± 1.4 % RR-cycle and bandwidth was 18.2 ± 6.0 % RR-cycle. No significant gender-related differences or differences between rest and post-stress acquisition were found for the dyssynchrony parameters. Discrepancies between the normal and abnormal population were most profound for the mean wall motion ($p < 0.001$), SD of peak motion ($p < 0.001$) and bandwidth ($p < 0.001$).

Conclusion: It is feasible to quantify ventricular dyssynchrony in MPS using the geometric approach as implemented by Corridor4DM.

Keywords: Ventricular dyssynchrony • Gated SPECT • Myocardial perfusion imaging • Nuclear imaging

INTRODUCTION

In recent years mechanical ventricular dyssynchrony has become an important clinical parameter, as it may indicate the effectiveness of cardiac resynchronization therapy (CRT) in heart failure patients.¹⁻⁵ Additionally, several studies have demonstrated that ventricular dyssynchrony can be used as an independent predictor for adverse cardiac events.^{6,7}

Ventricular dyssynchrony can be quantified by several imaging modalities, such as echocardiography, magnetic resonance imaging (MRI) and nuclear imaging techniques.⁸⁻¹¹ In spite of the large base of evidence and the widespread availability of echocardiography, it is also highly user-dependent. Radionuclide ventriculography has been used to study inter- and intraventricular dyssynchrony and has proven to be a reproducible and precise technique.⁵ Still, this nuclear technique does only provide functional information on the contractility. MRI and nuclear perfusion imaging are not only reproducible but also incorporate pathophysiological information on left ventricular function and the location of myocardial scarring. These factors were found to be additive to the dyssynchrony analysis in the prediction of CRT response.^{12, 13} Even so, MRI has some important disadvantages such as limited availability, complicated image analysis and incompatibility with cardiac devices.^{10, 11} Nuclear imaging techniques, and gated SPECT myocardial perfusion imaging (MPS) in particular, are generally used in daily clinical practice and have the ability to quantify cardiac perfusion in relation to regional cardiac function.

With the introduction of automated algorithms by Emory Cardiac Toolbox (ECTb)¹⁴ gated MPS has become a valid tool for dyssynchrony analysis. This count-based algorithm, which determines myocardial contraction based on the time-activity relation, is already applied in several MPS-dyssynchrony studies.^{3, 15-21} More recently, Corridor4DM also implemented an automated tool which uses geometric algorithms, rather than count-based methods, to quantify ventricular dyssynchrony. This method of automated dyssynchrony detection has not previously been evaluated in clinical patients. Therefore, the aim of this study was to assess the feasibility of this geometric dyssynchrony method in clinical patients with a normal MPS. Subsequently, the results of this normal population were compared to patient-data with proven ventricular dyssynchrony to assess the discriminatory value of the geometrical method.

MATERIALS AND METHODS

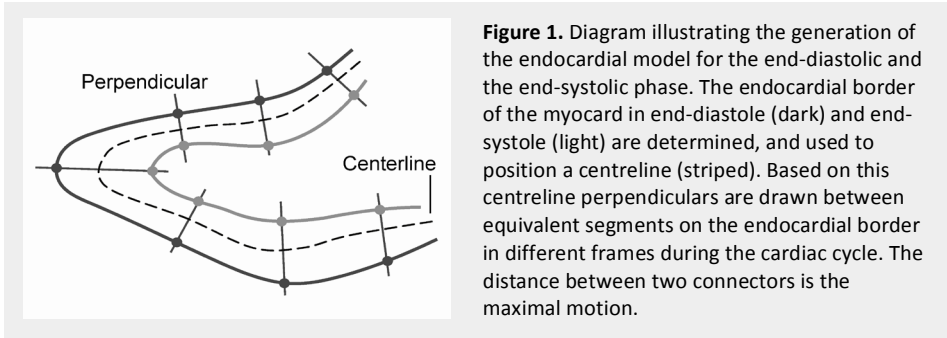
Patient Selection

For this retrospective study patients with a normal MPS were selected. The MPS acquisition was considered normal when no significant perfusion defects were present (summed stress score ≤ 2 and summed rest score ≤ 2 , visually confirmed by an expert reviewer) and left ventricular ejection fraction is 55% to 80%.^{22,30} In all acquisitions image quality had to be optimal, which implies that there was no patient movement, triggering problems or subdiaphragmatic tracer uptake overlapping the myocardial wall. Patients with arrhythmias on electrocardiogram (ECG) or implantable cardiac devices were also excluded. Equally sized groups were created for the post-stress MPS (male-physical stress; male-adenosine stress; female-physical stress; female-adenosine stress), so it was also possible to assess the impact of stress-induction on the dyssynchrony parameters. All MPS studies were part of standard clinical care and the retrospective nature of the study exempted the need for an IRB waiver.

For comparison, patients with congestive heart failure and proven cardiac dyssynchrony on MRI (septal-to-lateral delay >30 ms, methods described in ²²) were included. All heart failure patients had a New York Heart Association scale II-IV under optimal cardiac medication. The MRI acquisition protocols, image processing techniques and the results have previously been reported by Marsan et al.²²

Data acquisition

Patients underwent a two-day stress/rest MPS protocol, with post-stress acquisition on the first day. Stress was induced by physical exercise limited by symptoms, or when contraindications to exercise were present, by intravenous infusion of adenosine ($140\mu\text{g kg}^{-1} \text{ min}^{-1}$) for 6 minutes. At peak exercise, or in the third minute of adenosine infusion, an average dose of 500MBq Tc-99m Tetrofosmin was injected. Post-stress and rest images were made approximately 45 minutes after tracer administration. Projections were acquired using a double-head gamma camera equipped with a low energy high resolution collimator over 180 degrees (6 degrees per step, 40 seconds per projection). ECG-gating was applied at 16 frames per cardiac cycle, with a tolerance window of 50%. The data were pre-filtered with a low-pass Butterworth filter (8th order, cut-off frequency 0.26 cycles/pixel) and reconstructed using filtered back projection to yield



short-axis images. No attenuation or scatter correction was applied. Acquisitions were post-processed with the Corridor4DM software package (Version 6.1, Invia Medical Imaging Solutions, Ann Arbor, Michigan, USA).²³

Contraction analysis

Initial localization of the endocardial and epicardial borders by Corridor4DM is performed based on gradient operators and predefined information on shape, location and continuity of the ventricular wall. Using a cylindrical-spherical sampling configuration, intensity profiles are created between the endocardial and epicardial boundaries.^{24,25} More refined surface estimates are determined by a set of one- and two-dimensional weighted splines. A Gaussian-function is applied to the intensity profiles contained by these new surface estimates to locate peak myocardial activity. The Full Width Half Maximum of the Gaussian-function is utilized to estimate the thickness of the myocardial wall, which is scaled to an average thickness of 10mm in end-diastole.^{24,25} In all other frames the thickness is scaled with preservation of mass.^{24,25} The endocardial and epicardial borders are used to calculate the time-volume curve.

Polarmaps are constructed by radial sampling of 460 sectors within the myocardial volume (bounded by the cardiac borders) at each gating interval. The perfusion maps are based on the maximal count value within each sector. Wall thickening, which is based on these perfusion maps, is defined as the difference between the maximum count value occurring within a sector during the cardiac cycle and the count value at end-diastole.²⁵ Wall motion analysis is based on an adapted implementation of the centreline technique.^{26,27} A midline is positioned between the endocardial surface at end-diastole and end-systole (see figure 1). Perpendicular to this midline, normal vectors are placed

TABLE 1. PARAMETERS (REST) OF THE NORMAL POPULATION

	Male (n = 40)		Female (n = 40)		p-value
	Range	Mean ± SD	Range	Mean ± SD	
EDV (ml)	72 – 163	108.1 ± 22.4	48 – 134	85.9 ± 18.3	<0.001*
ESV (ml)	17 – 52	32.3 ± 9.2	12 – 70	25.5 ± 9.9	0.001*
LVEF (%)	63 – 80	70.5 ± 4.3	60 – 80	70.2 ± 9.5	0.952
Motion (mm)	7.2 – 12.6	9.7 ± 1.3	7.3 – 12.1	9.2 ± 1.2	0.101
Thickening (% counts)	49 – 103	66.4 ± 11.9	38 – 100	64.1 ± 13.6	0.436
TtPM (% RR cycle)	33 – 53	43.2 ± 4.7	31 – 54	42.1 ± 5.4	0.226
SD (% RR cycle)	1.2 – 7.5	3.3 ± 1.5	1.3 – 7.2	3.6 ± 1.4	0.876
Bandwidth (% RR cycle)	9 – 33	17.7 ± 5.4	9 – 40	18.7 ± 7.1	0.484

Independent Student's *t*-test, with * indicating significance of <0.05. EDV, end diastolic volume; ESV, end systolic volume; LVEF, left ventricular ejection fraction; TtPM, time to peak motion; SD, standard deviation of time to peak motion

connecting corresponding sectors in the end-diastolic and end-systolic frame. Maximal motion of a sector is defined as the absolute length of a vector between the end-systolic and end-diastolic positions of that segment, and is depicted in millimetres. The time to peak motion is used to describe the timing of ventricular contraction patterns. The moment of peak motion in a sector is defined as the percentage of the cardiac cycle at which the motion-vector is maximal (% RR-cycle).

In this study left ventricular ejection fraction (LVEF), end-diastolic volume (EDV), end-systolic volume (ESV), mean wall motion and mean wall thickening are used to describe global cardiac function. The myocardial contraction is described by the time to peak motion, standard deviation (SD) of time to peak motion and the bandwidth. These parameters have been shown to identify ventricular dyssynchrony in other studies.¹⁴

Statistical analysis

Continuous variables are expressed as mean ± standard deviation (SD), and categorical data are expressed as frequencies and/or percentages. In the normal population distinction was made between parameters acquired at rest, after physical stress or after adenosine stress. Possible differences in the dyssynchrony indices between rest and post-stress MPS in the normal population were evaluated with Paired Student *t*-tests. The distribution of the MPS parameters in the normal population and in the population with

TABLE 2. COMPARISON OF REST AND POST-STRESS PARAMETERS

	Adenosine MPS (n = 40)			Exercise MPS (n = 40)		
	Rest	Post-stress	p-value	Rest	Post-stress	p-value
EDV (ml)	97.9 ± 25.7	99.8 ± 25.2	0.263	95.9 ± 20.8	92.2 ± 22.3	0.005*
ESV (ml)	29.2 ± 9.4	29.9 ± 12.6	0.488	27.6 ± 8.5	23.8 ± 9.8	<0.001*
LVEF (%)	70.3 ± 4.4	71.0 ± 6.4	0.409	71.4 ± 4.4	75.1 ± 6.8	<0.001*
Motion (mm)	9.5 ± 1.2	9.4 ± 1.1	0.940	9.5 ± 1.3	10.2 ± 1.3	0.002*
Thickening (% counts)	64.7 ± 13.5	63.3 ± 13.6	0.569	65.8 ± 12.1	68.3 ± 12.0	0.210
TtPM (% RR cycle)	43.3 ± 4.8	44.1 ± 4.2	0.330	42.4 ± 5.5	44.2 ± 4.8	0.070
SD (% RR cycle)	3.7 ± 1.4	4.2 ± 1.3	0.083	3.5 ± 1.5	3.8 ± 1.4	0.162
BW (% RR cycle)	19.0 ± 6.7	18.5 ± 4.7	0.602	17.5 ± 6.0	18.4 ± 5.7	0.352
Heart rate (bpm)	72.3 ± 13.3	74.9 ± 12.3	0.104	67.9 ± 12.2	77.4 ± 12.4	<0.001*

Paired Student's *t*-test, with * indicating significance of <0.05. EDV, end diastolic volume; ESV, end systolic volume; LVEF, left ventricular ejection fraction; TtPM, time to peak motion; SD, standard deviation of time to peak motion; BW, bandwidth

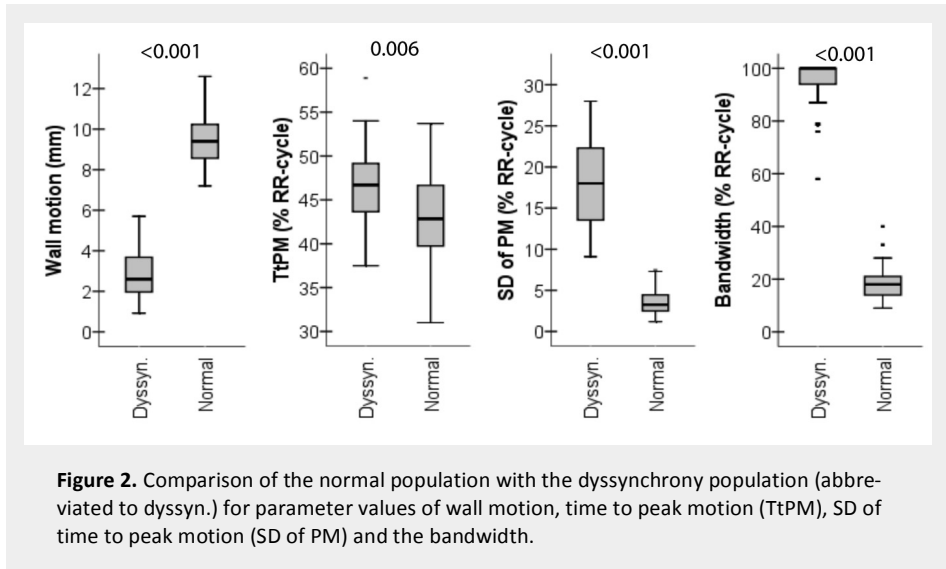
proven dyssynchrony was compared with Independent Student's *t*-tests. Statistical significance was defined as <0.05, two-sided *p*-values were used for all tests.

RESULTS

Normal population

The normal population consisted of 80 patients (20 male-physical stress; 20 male-adenosine stress; 20 female-physical stress; 20 female-adenosine stress; mean age 56.4 ± 10.5 years). The main indications for MPS were pre-operative screening (*n* = 22, 27.5%), chest pain (*n* = 24, 30%), increased risk profile for coronary artery disease (*n* = 15, 18.8%), abnormal ECG on stress test (*n* = 11, 18.8%), evaluation of suspected ischemia (*n* = 6, 7.5%), or evaluation of abnormality found on other imaging modality (*n* = 2, 2.5%). The global rest-MPS and dyssynchrony indices of the normal population are shown in Table 1. Significant gender-related differences were found for EDV and ESV, as could be expected. For all other parameters, including the dyssynchrony indices, no gender-related differences were found in the normal population.

Segmental wall motion was heterogeneous throughout the myocardium in the normal population. Maximal amplitudes were observed in the anterior (11.1 ± 1.7 mm) and



lateral (10.0 ± 2.0 mm) segments, whereas the septal had the lowest amplitude (7.7 ± 1.6 mm) compared to the other segments. Such a heterogeneous distribution was not observed for the segmental quantification of the time to peak motion.

Rest versus post-stress MPS

As part of the two-day stress/rest protocol patients underwent a post-stress MPS with either adenosine or exercise induced stress. Comparing the rest MPS indices of the exercise and adenosine subgroups showed no differences (p -values range from 0.180 to 0.836) between these populations, suggesting that any differences that is to be found post-stress may be allocated to the stress induction. The evaluation of the post-stress and rest MPS parameters for the adenosine and exercise stressed subgroups is shown in Table 2. Significant differences were found for the volumetric parameters between rest and post-stress acquisitions in the exercise subgroup. The mean wall motion was also slightly higher (10.2 ± 1.3 mm, $p = 0.002$) compared to rest (wall motion 9.5 ± 1.3 mm). No profound differences were found between rest and post-stress for the dyssynchrony indices in this subgroup. In the adenosine MPS subgroup no significant differences were found between parameters obtained post-adenosine and at rest.

TABLE 3. MPS RESULTS OF NORMAL AND HEART FAILURE POPULATIONS

	Normal (n = 80)	Heart failure (n = 24)	p-value
EDV (ml)	96.9 ± 23.3	283.6 ± 106.7	<0.001*
ESV (ml)	28.4 ± 9.0	207.2 ± 104.3	<0.001*
LVEF (%)	70.8 ± 4.4	30.1 ± 10.9	<0.001*
Motion (mm)	9.5 ± 1.2	2.9 ± 1.3	<0.001*
Thickening (% counts)	65.4 ± 12.7	24.2 ± 8.0	<0.001*
Peak motion (% RR cycle)	42.8 ± 5.1	46.5 ± 5.0	0.006*
SD (% RR cycle)	3.5 ± 1.4	18.0 ± 5.2	<0.001*
BW (% RR cycle)	18.2 ± 6.0	92.2 ± 11.1	<0.001*
Heart rate (bpm)	70.1 ± 12.9	67.6 ± 12.1	0.414

Independent Student's *t*-test, with * indicating significance of <0.05. EDV = end diastolic volume, ESV = end systolic volume, LVEF = left ventricular ejection fraction, SD = standard deviation of time to peak motion; BW, bandwidth

Differences between normal and dyssynchrony population

The included heart failure patients ($n = 24$, age 63.1 ± 9 years, 18 male, 92% ischemic cardiomyopathy) had proven dyssynchrony on MRI (mean SL-delay 73.7 ± 74.1 ms).²² In general, these patients had a depressed left ventricular function (rest LVEF $28.6 \pm 9.5\%$) and abnormal perfusion patterns (SRS 25.2 ± 11.7) on MPS. Wall motion (2.7 ± 1.1 mm) and wall thickening ($23.5 \pm 7.7\%$) also indicated a depressed cardiac function.

The comparison of this abnormal population with the previous cohort of patients with normal MPS is shown in Figure 2 and Table 3. For all dyssynchrony indices significant differences are found between the distributions of the two populations. These differences are most profound for the SD of time to peak motion ($p < 0.001$) and the bandwidth ($p < 0.001$). Figure 3 and 4 show examples of a normal and abnormal patient, demonstrating the differences in these populations.

DISCUSSION

The results of the current study indicate that it is feasible to detect ventricular dyssynchrony using a geometrical method. In the population with normal MPS, there is low variance for time to peak motion (42.8 ± 5.1 % RR-cycle), SD (3.5 ± 1.4 % RR-cycle) and bandwidth (18.2 ± 6.0 % RR-cycle). No gender-related differences were found for

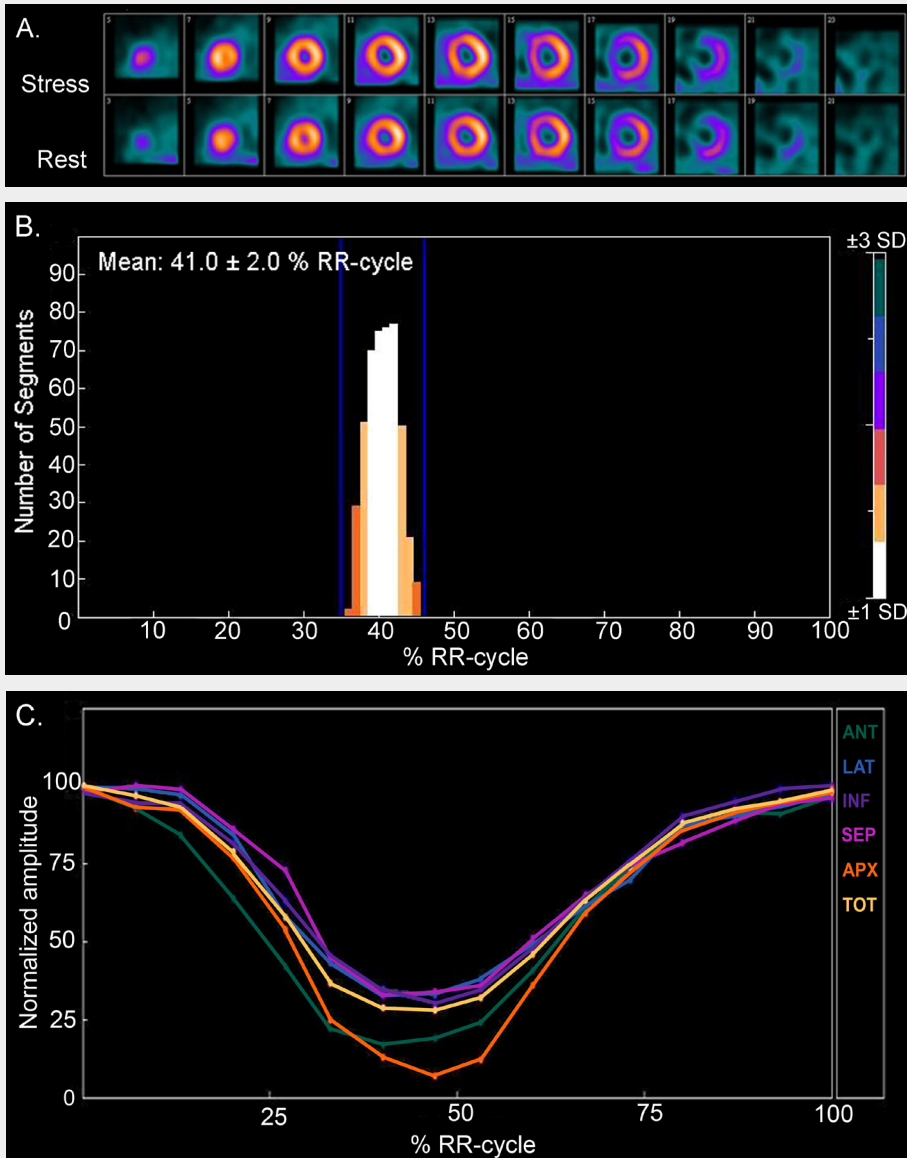


Figure 3. Patient referred for pre-operative screening. **A.** A normal MPS acquisition with no apparent regions of ischemia (EDV 140; LVEF 64%; WM 9.3mm). **B.** Normal, narrow contractility histogram. The dark blue vertical lines indicate the bandwidth and colour coding demonstrate the deviation from the mean in standard deviations (TtPM 42.8 ± 2.1 % RR-cycle; BW 9% RR-cycle). **C.** Normal contraction pattern in which all regions contract at the same time. The contraction is normalized to motion at end-diastole.

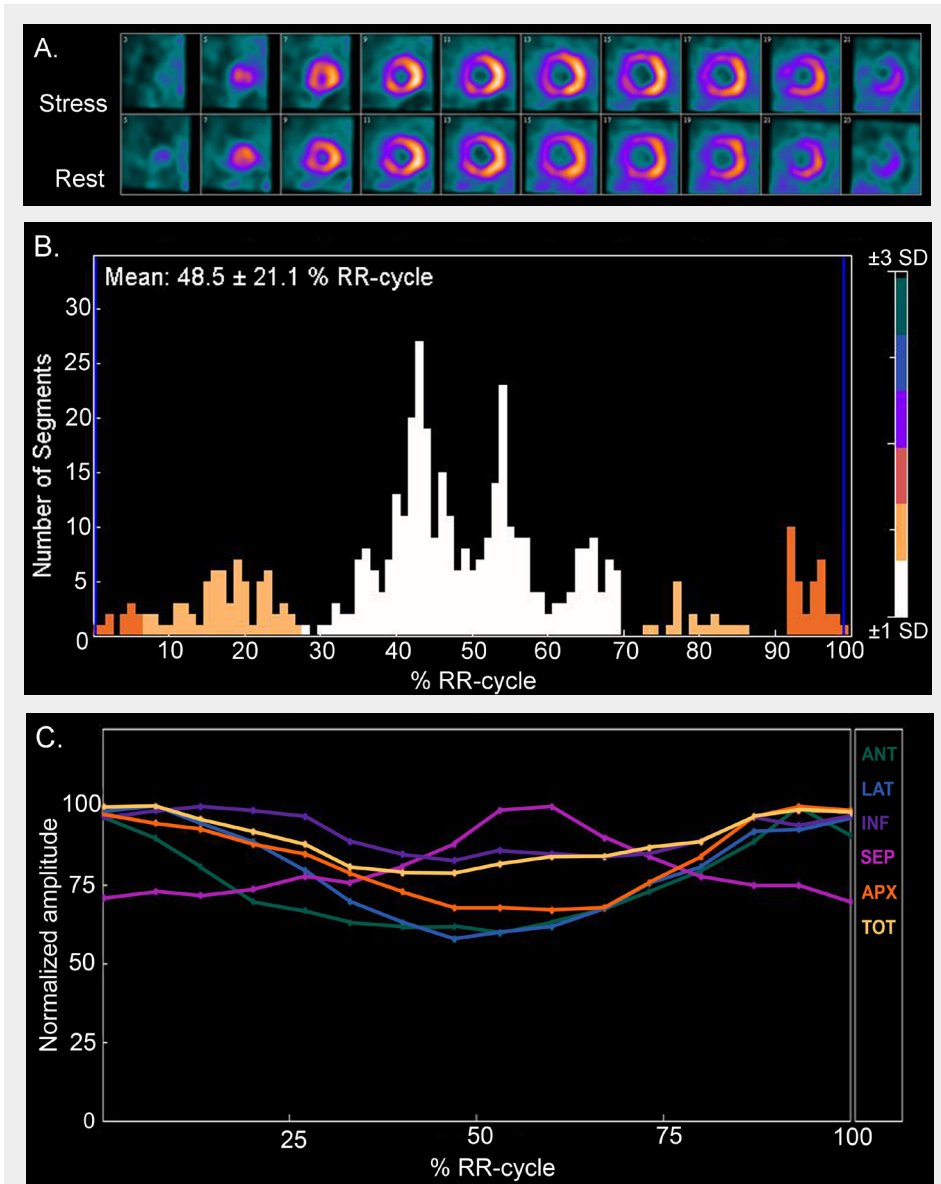


Figure 4. Patient with dilated cardiomyopathy and left bundle branch block (LBBB). **A.** Dilated myocardium with reduced tracer uptake in anterior, septal and apical regions (EDV 327; LVEF 30%; WM 1.7mm). **B.** The wide and highly distributed histogram is indicative for cardiac dyssynchrony (TtPM 48.5 ± 21.1 % RR-cycle; BW 100% RR-cycle). **C.** Curves clearly demonstrate dyssynchrony of the septal region, as is typical in LBBB, and a reduced contraction of the inferior region.

these indices. Additionally, the method of stress induction had no clinically relevant effect on the determination of dyssynchrony in the population with normal MPS. This independence of dyssynchrony to exercise is also described by Kühne et al.²⁸ for echocardiography and by Aljaroudi et al.¹⁵ for MPS in normal populations. Comparison of the normal MPS with the heart failure patients showed profound differences especially for the SD of time to peak motion ($p < 0.001$) and the bandwidth ($p < 0.001$). All these observations suggest that the geometrical approach is a reliable method to diagnose dyssynchrony in either rest or post-stress MPS.

Automated assessment of dyssynchrony

The addition of a dyssynchrony toolbox to the arsenal of nuclear cardiology has potential clinical utility. A number of recent studies describe the long term prognostic value of dyssynchrony analysis. In general dyssynchrony indices may provide better identification of CRT response or major cardiac events compared to other commonly used predictors such as LVEF and QRS duration.^{2,3,5,6} Although the present study primarily focuses on the geometrical approach, other feasible automated methods to determine ventricular dyssynchrony in MPS have been proposed most of which are count-based.

Chen et al. performed count-based phase analysis on MPS acquisitions of 90 patients with a <5% likelihood of coronary artery disease (modification of the Emory Cardiac toolbox).¹⁴ In general, methods that apply Fourier analysis will provide information regarding the phase of contraction in degrees, which can be easily converted to percentage of RR-cycle. The method provides a peak phase of 137.4 ± 14.6 degrees (38.2 ± 4.1 % RR-cycle), a phase SD of 13.0 ± 5.2 degrees (3.6 ± 1.4 % RR-cycle) and a bandwidth of 34.7 ± 10.7 degrees (9.7 ± 3.0 % RR-cycle) for the normal population. Comparable with the results of our study, no gender-related differences were found. Subsequent studies show that this method produces repeatable dyssynchrony indices (coefficient of variation is 8.7% for bandwidth and 8.8% for SD of peak contraction), and can distinguish normal from asynchronous contraction in clinical populations.^{18, 21}

Kriekinge et al. evaluated their count-based phase-analysis algorithm (modification of the Cedars-Sinai Quantitative Gated SPECT software) in 68 normal patients and 72 patients with LBBB, all with a normal MPS and low pre-test likelihood for CAD.²⁹ In the normal population significant gender-related differences were found for the global dyssynchrony indices (SD and bandwidth), these gender-related differences were not

observed in the LBBB population. Comparison of the normal and LBBB populations showed significant differences in global dyssynchrony parameters, again indicating that this is also a feasible method to evaluate cardiac contraction in MPS.

It is well known that there are discrepancies between commercial software packages with respect to the algorithms for left ventricular segmentation and estimation of the myocardial count distribution.³⁰⁻³¹ Main differences are found for the techniques to locate ventricular borders, the valve-plane motion constraints and the methods applied to model wall thickening. All these factors will also play a role in the determination of dyssynchrony indices from MPS acquisitions. Consequently, the determination of dyssynchrony indices may also show algorithm-specific normal values.

Pros and cons of a geometrical approach

The ability to evaluate cardiac contraction depends on the capability of the software to detect endocardial and epicardial borders accurately.²⁶ Estimations of myocardial count distributions are not determined by perfusion alone, but also by factors such as extra-cardiac activity, attenuation, scatter, filtering and image reconstruction. Automated software packages can provide estimations of cardiac borders despite the presence of large perfusion defects due to predefined assumptions on continuity of the ventricular wall and the ability to detect very low count densities. Though border detection is very robust, it has an important drawback; the inability to recognize large left ventricular aneurysms. Generally, aneurysms do not convey with the assumption of ventricular continuity. Conflicts with this continuity assumption can also arise when extra-cardiac activity is projected over the ventricular wall. In these cases the geometrical approaches may be sensitive to errors, and could provide incorrect parameter values. Still, the evaluation of regional cardiac perfusion is also considered to be unreliable in acquisitions with severe extra-cardiac activity. Accordingly, count-based methods to determine dyssynchrony indices may also prove erroneous in these cases.

A second factor that is known to affect perfusion and functional assessment of MPS is the quality of ECG-gating. Studies of Nichols et al. indicated that inadequate ECG-gating especially affected the wall thickening values. The volumetric indices on the other hand were not influenced by these gating errors.³²⁻³³ These results suggest that the border estimates are relatively insensitive to variations in count distributions throughout the cardiac cycle. Thus, it is plausible that geometric methods to determine dyssynchrony are also less sensitive to gating-errors compared to count-based methods. Nonetheless,

the presence of inadequate ECG-gating should always be recognized and subsequent errors in perfusion or functional estimates should be described.

Both geometrical and count-based techniques to calculate dyssynchrony from MPS will estimate the translational contraction patterns of the ventricle (i.e. the inward movement of the wall towards the heart-axis). Systolic rotation and torque are also important aspects of a normal cardiac contraction pattern, but are difficult to determine using nuclear techniques. Still, these factors may play a role in characterizing the pathology of ventricular dyssynchrony.³⁴ Nichols et al. proposed a method to detect cardiac torsion in MPS data.³⁵ In short axis images, the right ventricular attachment can be seen as a slight reduction of counts in the left ventricular wall generally at the 7 o'clock and 11 o'clock positions. These right ventricular insertion points were used as reference during the cardiac cycle to detect torsion. They used this data to improve the perfusion images by correcting for the rotational motion. Still, this method is not widely used, and implementation can be hampered by the limited resolution of MPS.

Limitations

The aim of this study was to evaluate the feasibility of a geometrical approach for the detection of ventricular dyssynchrony in MPS. For this specific problem it is sufficient to differentiate between a normal and an abnormal population, as was done in this study. Still, one has to bear in mind that a technique does not need to be really sensitive to make a distinction between the two populations included in the present study. Although, the current study indicates that it is feasible to detect dyssynchrony using the geometrical approach, more extensive validation using this technique has to be done. Also, the additive value of the geometrical approach in specific patient cases, rather than a group comparison, needs to be determined. It will also be interesting to eventually perform a direct comparison between the count-based and geometrical assessment, as these are the two main methods to assess dyssynchrony in MPS acquisitions.

The normal population used in our study consisted of 80 patients with a normal perfusion pattern, no ventricular dysfunction and optimal image quality. Although this population was sufficient to evaluate the feasibility, the population is not optimal for determining normal ranges or cut-off values. First of all, these patients were selected from a single centre, so there was no variation in acquisition settings. Furthermore, the dependence of this geometrical approach on factors such as heart rate, scatter, extra-cardiac activity and image reconstruction needs to be established.

CONCLUSION

The results of the current study indicate that the geometrical approach is a feasible method for evaluating ventricular dyssynchrony in MPS acquisitions. Nonetheless, more research has to be performed to identify factors that influence the calculation of dyssynchrony indices, to evaluate the diagnostic or prognostic value of the dyssynchrony analysis and to establish normal ranges.

REFERENCE LIST

- (1) Bax JJ, Marwick TH, Molhoek SG et al. Left ventricular dyssynchrony predicts benefit of cardiac resynchronization therapy in patients with end-stage heart failure before pacemaker implantation. *Am J Cardiol* 2003;92:1238-40.
- (2) Van Bommel RJ, Bax JJ, Abraham WT et al. Characteristics of heart failure patients associated with good and poor response to cardiac resynchronization therapy: a PROSPECT (Predictors of Response to CRT) sub-analysis. *Eur Heart J* 2009;30:2470-7.
- (3) Boogers MM, Van Krieking SD, Henneman MM et al. Quantitative gated SPECT-derived phase analysis on gated myocardial perfusion SPECT detects left ventricular dyssynchrony and predicts response to cardiac resynchronization therapy. *J Nucl Med* 2009;50:718-25.
- (4) White JA, Yee R, Yuan X et al. Delayed enhancement magnetic resonance imaging predicts response to cardiac resynchronization therapy in patients with intraventricular dyssynchrony. *J Am Coll Cardiol* 2006;48:1953-60.
- (5) Dauphin R, Nonin E, Bontemps L et al. Quantification of ventricular resynchronization reserve by radionuclide phase analysis in heart failure patients: a prospective long-term study. *Circ Cardiovasc Imaging* 2011;4:114-21.
- (6) Pazhenkottil AP, Buechel RR, Husmann L et al. Long-term prognostic value of left ventricular dyssynchrony assessment by phase analysis from myocardial perfusion imaging. *Heart* 2011;97:33-7.
- (7) Aljaroudi WA, Hage FG, Hermann D et al. Relation of left-ventricular dyssynchrony by phase analysis of gated SPECT images and cardiovascular events in patients with implantable cardiac defibrillators. *J Nucl Cardiol* 2010;17:398-404.
- (8) Yu CM, Bax JJ, Gorcsan J, III. Critical appraisal of methods to assess mechanical dyssynchrony. *Curr Opin Cardiol* 2009;24:18-28.
- (9) Trimble MA, Borges-Neto S, Velazquez EJ et al. Emerging role of myocardial perfusion imaging to evaluate patients for cardiac resynchronization therapy. *Am J Cardiol* 2008;102:211-7.
- (10) Abraham T, Kass D, Tonti G et al. Imaging cardiac resynchronization therapy. *JACC Cardiovasc Imaging* 2009;2:486-97.
- (11) Oyenuga OA, Onishi T, Gorcsan J, III. A practical approach to imaging dyssynchrony for cardiac resynchronization therapy. *Heart Fail Rev* 2011;16:397-410.
- (12) Bilchick KC, Dimaano V, Wu KC et al. Cardiac magnetic resonance assessment of dyssynchrony and myocardial scar predicts function class improvement following cardiac resynchronization therapy. *JACC Cardiovasc Imaging* 2008;1:561-8.
- (13) Adelstein EC, Tanaka H, Soman P et al. Impact of scar burden by single-photon emission computed tomography myocardial perfusion imaging on patient outcomes following cardiac resynchronization therapy. *Eur Heart J* 2011;32:93-103.

- (14) Chen J, Garcia EV, Folks RD et al. Onset of left ventricular mechanical contraction as determined by phase analysis of ECG-gated myocardial perfusion SPECT imaging: development of a diagnostic tool for assessment of cardiac mechanical dyssynchrony. *J Nucl Cardiol* 2005;12:687-95.
- (15) Aljaroudi W, Koneru J, Heo J, Iskandrian AE. Impact of ischemia on left ventricular dyssynchrony by phase analysis of gated single photon emission computed tomography myocardial perfusion imaging. *J Nucl Cardiol* 2011;18:36-42.
- (16) Cooke CD, Garcia EV, Cullom SJ, Faber TL, Pettigrew RI. Determining the accuracy of calculating systolic wall thickening using a fast Fourier transform approximation: a simulation study based on canine and patient data. *J Nucl Med* 1994;35:1185-92.
- (17) Henneman MM, van der Wall EE, Ypenburg C et al. Nuclear imaging in cardiac resynchronization therapy. *J Nucl Med* 2007;48:2001-10.
- (18) Lin X, Xu H, Zhao X et al. Repeatability of left ventricular dyssynchrony and function parameters in serial gated myocardial perfusion SPECT studies. *J Nucl Cardiol* 2010;17:811-6.
- (19) Trimble MA, Borges-Neto S, Smallheiser S et al. Evaluation of left ventricular mechanical dyssynchrony as determined by phase analysis of ECG-gated SPECT myocardial perfusion imaging in patients with left ventricular dysfunction and conduction disturbances. *J Nucl Cardiol* 2007;14:298-307.
- (20) Trimble MA, Borges-Neto S, Honeycutt EF et al. Evaluation of mechanical dyssynchrony and myocardial perfusion using phase analysis of gated SPECT imaging in patients with left ventricular dysfunction. *J Nucl Cardiol* 2008;15:663-70.
- (21) Chen J, Garcia EV, Lerakis S et al. Left ventricular mechanical dyssynchrony as assessed by phase analysis of ECG-gated SPECT myocardial perfusion imaging. *Echocardiography* 2008;25:1186-94.
- (22) Marsan NA, Westenberg JJ, Tops LF et al. Comparison between tissue Doppler imaging and velocity-encoded magnetic resonance imaging for measurement of myocardial velocities, assessment of left ventricular dyssynchrony, and estimation of left ventricular filling pressures in patients with ischemic cardiomyopathy. *Am J Cardiol* 2008 15;102:1366-72.
- (23) Ficaro EP, Lee BC, Kritzman JN, Corbett JR. Corridor4DM: the Michigan method for quantitative nuclear cardiology. *J Nucl Cardiol* 2007;14:455-65.
- (24) Faber TL, Stokely EM, Peshock RM, Corbett JR. A model-based four-dimensional left ventricular surface detector. *IEEE Trans Med Imaging*;10:321-9.
- (25) Invia Solutions. Program Algorithms. 2011. Internet Communication
- (26) Sheehan FH, Bolson EL, Dodge HT, Mathey DG, Schofer J, Woo HW. Advantages and applications of the centerline method for characterizing regional ventricular function. *Circulation* 1986;74:293-305.

- (27) Faber TL, Akers MS, Peshock RM, Corbett JR. Three-dimensional motion and perfusion quantification in gated single-photon emission computed tomograms. *J Nucl Med* 1991;32:2311-7.
- (28) Kuhne M, Blank R, Schaer B, Ammann P, Osswald S, Sticherling C. Effects of physical exercise on cardiac dyssynchrony in patients with impaired left ventricular function. *Europace* 2011;13:839-44 .
- (29) Van Kriekinghe SD, Nishina H, Ohba M, Berman DS, Germano G. Automatic global and regional phase analysis from gated myocardial perfusion SPECT imaging: application to the characterization of ventricular contraction in patients with left bundle branch block. *J Nucl Med* 2008;49:1790-7.
- (30) Lin GS, Hines HH, Grant G, Taylor K, Ryals C. Automated quantification of myocardial ischemia and wall motion defects by use of cardiac SPECT polar mapping and 4-dimensional surface rendering. *J Nucl Med Technol* 2006;34:3-17.
- (31) van der Veen BJ, Scholte AJ, Dibbets-Schneider P, Stokkel MP. The consequences of a new software package for the quantification of gated-SPECT myocardial perfusion studies. *Eur J Nucl Med Mol Imaging* 2010;37:1736-44.
- (32) Nichols K, Dorbala S, Depuey EG, Yao SS, Sharma A, Rozanski A. Influence of arrhythmias on gated SPECT myocardial perfusion and function quantification. *J Nucl Med* 1999;40:924-34.
- (33) Nichols K, Yao SS, Kamran M, Faber TL. Clinical impact of arrhythmias on gated SPECT cardiac myocardial perfusion and function assessment. 2001;8:19-30.
- (34) Bertini M, Sengupta PP, Nucifora G et al. Role of left ventricular twist mechanics in the assessment of cardiac dyssynchrony in heart failure. *JACC Cardiovasc Imaging* 2009;2:1425-35.
- (35) Nichols K, Kamran M, Cooke CD et al. Feasibility of detecting cardiac torsion in myocardial perfusion gated SPECT data. *J Nucl Cardiol* 2002;9:500-7.

Part 2

Myocardial Innervation Scintigraphy

Chapter 6

Quantitative parameters of planar I-123 MIBG studies

BJ van der Veen, AJ Scholte, MPM Stokkel,

Mathematical methods to determine quantitative parameters of
myocardial I-123 MIBG studies: a review of the literature.

Nucl Med Comm 2010; 31(7);617-623

ABSTRACT

Iodine-123 meta-iodobenzylguanidine (I-123 MIBG) scintigraphy is used to visualize and quantify the sympathetic nerve activity (SNA). Although it is used since 1980 to identify myocardial innervation, it is not yet considered a routine sympathetic imaging agent in this respect. The lack of large multicentre studies and the presence of variations in the protocols that are used for planar I-123 MIBG acquisition confines the comparability of study results and application of normal values. Therefore, the aim of this study was to assess the variations in mathematical methods that are currently used to quantify the Heart-to-Mediastinum ratio (HM) and washout rate (WOR). Additionally normal values were evaluated in concordance with these methods.

A systematic literature search yielded 169 unique articles, of which 30 contained a complete description of the acquisition protocol for planar I-123 MIBG acquisition, image analysis and quantification of the parameters. The results indicate not only large variations in mathematical methods, but also in various aspects of the protocols that are used during acquisition. In many articles method specific normal values were used, however these values were generally generated from small, single centre studies. Current study stresses the need to produce guidelines to achieve a standardized method for I-123 MIBG acquisition, image analysis and methods to quantify parameters.

Keywords: I-123 meta-iodobenzylguanidine ▪ Myocardial innervation ▪ Quantitative analysis ▪ Systematic review

INTRODUCTION

Heterogeneities within the efferent sympathetic innervation pattern of the heart can occur in several diseases, such as coronary artery disease, hypertension, diabetes mellitus and chronic heart failure. With the use of I-123 meta-iodobenzylguanidine (I-123 MIBG) scintigraphy the sympathetic nerve activity (SNA) can be visualized and quantified. I-123 MIBG resembles the neurotransmitter nor-epinephrine (NE) with respect to the molecular structures, synaptic re-uptake and storage mechanisms. However, unlike NE, I-123 MIBG does not participate in the signalling processes or in the enzymatic degradation pathways, but it is stored within vesicles of the efferent sympathetic nerve endings, and released by exocytose during nerve excitement. Therefore, initial uptake of I-123 MIBG will provide information on the reuptake mechanisms of NE, and over time the clearance of I-123 MIBG will provide information about the integrity and activity of the neurons.¹

In addition to visual evaluation of myocardial I-123 MIBG images, there are also techniques to determine the global uptake and the degree of I-123 MIBG turnover of the myocardial neurons. The parameters introduced to measure these two factors are, respectively, the heart-to-mediastinum ratio (HM ratio) and the washout rate (WOR). The HM ratio determines the uptake of I-123 MIBG at set moments in time by relating the myocardial uptake against the uptake within the blood volume. The WOR, on the other hand, compares the uptake levels within the myocardium over time and is related to the MIBG clearance.

Although I-123 MIBG scintigraphy is a technique that is used since 1980, it has not yet been considered a routine sympathetic imaging agent. Studies with I-123 MIBG are mainly limited to Europe, Japan and some special centres in the US.^{2,3} A systematic review of Verberne et al.⁴ evaluated the relationship between (semi-)quantitative parameters and the prognosis in chronic heart failure. In their discussion, a couple of crucial limitations are mentioned with respect to I-123 MIBG studies that are also noted in other articles, including;⁵⁻⁷

- The presence of large variations in acquisition protocols, mainly because to differences in collimator choice, use of decay correction or not, and the different time intervals used between early and delayed acquisition
- Substantial variations in methods used to determine the quantitative parameters
- The lack of large scale studies that establish evidence for the use of I-123 MIBG

In addition to these factors, the absence of patient characteristics, such as gender, age, medication use, disease status, in manuscripts also limits the comparability of study results. Altogether, it remains troublesome to apply results concerning (ab-)normal values for quantitative parameters found within literature in the clinical setting.

The aim of this study was to assess the mathematical methods that are used to determine HM ratio and WOR and to evaluate the normal values that are used in concordance with these methods. To illustrate the discrepancies that arise from use of different mathematical methods, each of the methods was used on two different populations to determine the mean HM ratios and WORs.

MATERIALS AND METHODS

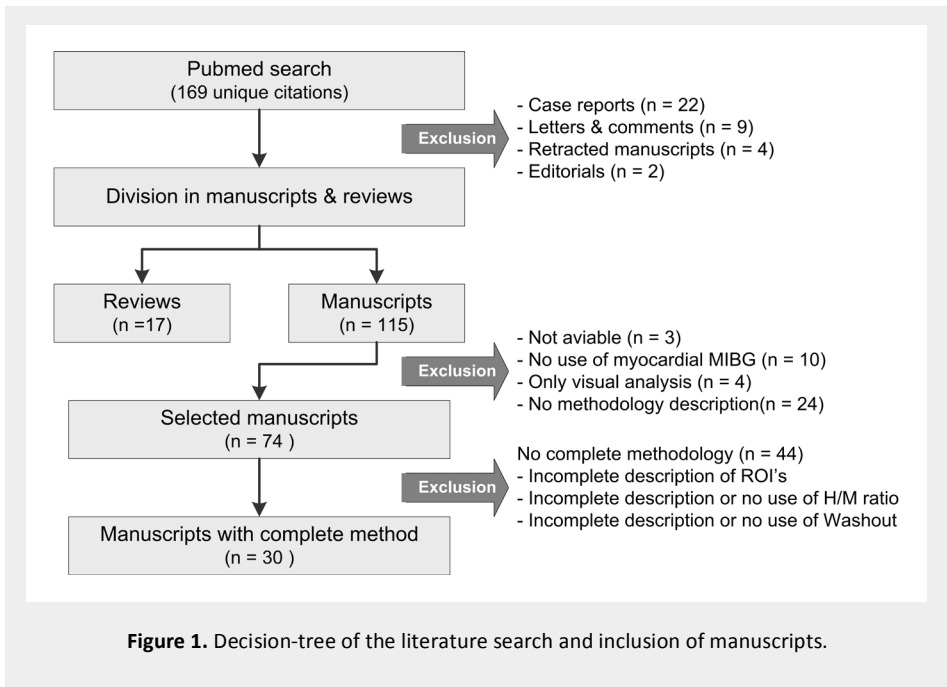
Search query

To provide a complete overview of mathematical techniques that are used to calculate I-123 MIBG parameters a literature study was performed. In August 2009 the search was performed within the Pubmed database to accumulate papers fulfilling the following criteria;

- Match the query ("3-iodobenzylguanidine"[MeSH Terms] OR "3-iodobenzylguanidine" [All Fields] OR "MIBG" [All Fields] OR "meta-iodobenzylguanidine" [All Fields]) AND (("Heart" [MeSH Terms] OR "Heart" [All Fields]) OR ("Myocardium" [MeSH Terms] OR "Myocardium" [All Fields]))
- Published between 2006/01/01 and 2009/08/01
- Restrictions; language = English, population = Human

Inclusion of articles

This systematic search yielded 169 unique manuscripts. Only articles containing information on methods to determine the I-123 MIBG parameters from a planar scintigram were useful for this study; thus, case reports, letters, comments, editorials and retracted articles were excluded (total $n = 37$). The remaining reviews ($n = 17$) and manuscripts ($n = 115$) were screened for the presence of actual performed I-123 MIBG scintigraphic procedures during the study, as some studies just refer to the technique rather than actually performing I-123 MIBG acquisitions. All studies were screened for



the presence of a quantitative method description that provided insight into the techniques used to determine the ROIs, HM ratio and WOR. Some studies performed only a visual analysis ($n = 4$), or did not include a description of the quantitative methods that were used ($n = 24$), these studies were excluded. The remainder of the manuscripts ($n = 74$) contained information on I-123 MIBG quantification. Nonetheless, some manuscripts did not contain a complete description of the methods or did not use both the HM ratio and the WOR. The final constrain for inclusion was the presence of a detailed description on the quantitative techniques used to calculate both HM ratio and WOR. When reviews included information on mathematical methods the primary source was used. This primary source had to fulfil all demands that were set upon the articles. (Figure 1)

Applying mathematical methods on clinical data

To clarify the effects of the variations on HM ratios and WOR, the most common methods were applied on two clinical datasets. The selected data contained acquisitions of 15 patients with diabetes mellitus and a normal myocardial perfusion study, and of 15

patients with implantable cardiac device (ICD) and an abnormal myocardial perfusion. A normal myocardial perfusion study was characterized by a homogenous physiological distribution of tracer activity and an ejection fraction >55%. Studies with persisted perfusion defects and an ejection fraction <50% were considered abnormal.

RESULTS

The initial Pubmed search revealed 169 unique publications, of which 30 manuscripts fulfilled all criteria. Table 1 (placed at the end of this chapter) provides an overview of these articles including the topic, population, study protocol, reference populations and a summary of the conclusion. Most manuscripts contain information on the use of MIBG in various cardiac diseases; however, the use of I-123 MIBG in dementia, Alzheimer's disease and Parkinson's disease was also frequently mentioned. Four manuscripts were generated by the same author, and referred to each other.⁸⁻¹¹

Protocol variations

The amount of activity used ranged from 111 to 370 MBq. Early acquisitions were most frequently performed after 15 minutes ($n = 22$), but manuscripts also describe intervals of 10 ($n = 1$), 20 ($n = 5$) and 30 minutes ($n = 2$). Late acquisitions were performed after 3 ($n = 10$), 3.5 ($n = 2$) and 4 ($n = 18$) hours post-injection. In almost all studies low energy collimators were used; however, in two studies medium energy collimators were used. Four articles did not mention the collimator used in the study. ROI determination was in all studies based on manual techniques that include drawing or placing a predetermined shape over the heart and mediastinum. There was no consensus on the shape, size and positioning of the ROIs for the heart and the mediastinum. In all the studies the mean counts per pixel were used for calculation of the HM ratio and WOR.

Mathematical determination of HM ratio

There are two principles described within the literature to calculate the HM ratio;

$$1. \quad HM_{early} = \frac{eH/A_H}{eM/A_M} \quad HM_{delayed} = \frac{dH/A_H}{dM/A_M}$$

$$2. \quad HM_{early} = \frac{eH}{eM} \qquad HM_{delayed} = \frac{dH}{dM}$$

In the first method H and M are described by mean counts in, respectively, the heart and mediastinum ROIs. The A_H and A_M are considered the number of pixels within each of these ROIs, so that the HM ratio is described as the difference in mean counts per pixel. In the second method the H and M are already described by the mean counts per pixel; so the two methods share total agreement.

Mathematical determination of WOR

There is little consensus on the determination of WOR within the literature. In the 30 manuscripts included in this study, seven different methods were described. The H and M are provided in mean counts per pixel and T is the half time of I-123 decay, unless stated otherwise.

$$1. \quad WOR = \frac{(eH - eM) - (dH - dM)}{(eH - eM)} \times 100\%$$

$$2. \quad WOR = \frac{(eH / eM) - (dH / dM)}{(eH / eM)} \times 100\%$$

$$3. \quad WOR = \frac{(eH - dH)}{eH} \times 100\%$$

$$4. \quad WOR = \frac{(eH' - dH')}{eH \times t} \times 100\%$$

$eH' = eH - (A_H / A_M) \times eM$
 $dH' = [dH - (A_H / A_M) \times dM] \times 2^{t/T}$
 $t =$ time between early and delayed images, H and M in count rates, WOR in %/min

$$5. \quad WOR = \frac{(eHCD - dHCD)}{eHCD} \times 100\%$$

HCD = heart count density

$$6. \quad WOR = \frac{\left(\frac{eH}{0.5^{et/T}} - \frac{eM}{0.5^{et/T}} \right) - \left(\frac{dH}{0.5^{dt/T}} - \frac{dM}{0.5^{dt/T}} \right)}{\left(\frac{eH}{0.5^{et/T}} - \frac{eM}{0.5^{et/T}} \right)} \times 100\%$$

$$7. \quad WOR = \frac{\left(\frac{eH}{et} - \frac{eM}{et} \right) - \left(\frac{dH}{dt} - \frac{dM}{dt} \right)}{\left(\frac{eH}{et} - \frac{eM}{et} \right)} \times 100\%$$

$et =$ time to early image, $dt =$ time to delayed image)

Some manuscripts mention that the counts are corrected for decay but the methods are rarely described in combination with the appropriate formulas. Radioactive decay is based on exponential decay, which is described by;

$$N_t = N_0 e^{-\lambda t} = N_0 \frac{1}{2}^{t/T}$$

Counts in the early and delayed acquisition can therefore be corrected for decay by dividing them by the decay coefficient. When the early scan is assumed to occur at $t = 0$ only the delayed scan is corrected with $t = t_{\text{delayed}} - t_{\text{early}}$. All the methods mentioned before can eventually be deduced to one of the three following methods;

	<i>Non-decay corrected</i>	<i>Decay corrected</i>
1.	$WOR = \frac{(eH - eM) - (dH - dM)}{(eH - eM)} \times 100\%$	$WOR = \frac{\left(\frac{eH}{0.5^{e t / T}} - \frac{eM}{0.5^{e t / T}} \right) - \left(\frac{dH}{0.5^{d t / T}} - \frac{dM}{0.5^{d t / T}} \right)}{\left(\frac{eH}{0.5^{e t / T}} - \frac{eM}{0.5^{e t / T}} \right)} \times 100\%$
2.	$WOR = \frac{(eH - dH)}{eH} \times 100\%$	$WOR = \frac{\left(\frac{eH}{0.5^{e t / T}} \right) - \left(\frac{dH}{0.5^{d t / T}} \right)}{\left(\frac{eH}{0.5^{e t / T}} \right)} \times 100\%$
3.	$WOR = \frac{(eH / eM) - (dH / dM)}{(eH / eM)} \times 100\%$	

The use of normal values

In a number of articles patients were compared to normal values used within the clinical setting^{8,11-20}, whereas other articles determine their normal values based on populations that are included during the study.^{9,21-23} Nonetheless most normal ranges or cut-off values are based on information of small populations of normal, healthy volunteers. An overview of the normal ranges and cut off values arranged by mathematical methods is provided in Table 2.

The mathematical methods for the HM ratio were similar in most articles; therefore, the normal values should also be comparable throughout the different articles. Most articles with healthy volunteers describe normal ranges for eHM >1.9 and for dHM >1.8. Normal values for the WOR are much harder to find and compare, since the variation in mathematical methods is high. The normal ranges and cut off values mentioned in Table 2

TABLE 2. VARIATION IN NORMAL VALUES

Ref.	N	eHM	dHM	WOR				
				Method 1 Non DC	Method 1 DC	Method 2 Non DC	Method 2 DC	Method 3
<i>Normal ranges (mean ± 2SD) and cut off values in literature</i>								
²⁴	20				> 27			
²⁵	10	1.9 - 2.8	1.8 - 2.7		> 27			
²⁰	10	< 1.93	< 1.81			> 22.7		
²⁶	8		1.56 ± 0.2					
<i>Results of studies with normal volunteers (mean ± 2SD)</i>								
⁹	10	2.44 ± 0.5	2.44 ± 0.5	25.0 ± 5.0				
²¹	6	2.17 ± 0.8	2.59 ± 1.1		0.22±0.2*			
²³	7	1.21 ± 0.6	1.38 ± 0.6			21.0±16.0		
²⁰	10	2.07 ± 0.4	2.18 ± 0.5			15.1±14.8		
²²	10	2.60 ± 0.6	2.50 ± 0.6				25.0±24.0	
²⁷	18	2.93 ± 0.8	2.85 ± 0.8					2.1±1.92

N, number of included individuals in each study; DC, decay correction; * WOR provided in %/min

indicate that the normal values are method depended. However, because of the lack of studies per method, and the limited number of individuals included in each study, there are no specific normal ranges assigned to each method.

Effects of variations in mathematical methods

The population of diabetic patients had a mean early heart uptake (eH) of 46.4 ± 13.6 , and a delayed heart uptake of (dH) 36.0 ± 11.3 . The ICD patients had a mean early heart uptake of 40.1 ± 4.9 , and a delayed heart uptake of 27.9 ± 4.8 . Both groups had an early mediastinal uptake (eM) of approximately 25 and a delayed mediastinal uptake (dM) of approximately 19. (Counts were corrected for decay)

Within the total population (diabetic patients and ICD patients) there are clear significant differences between all methods described to calculate the WOR (Table 3). However, if only the DB population is analysed the differences between method 1 and 2 with decay correction, and between method 1 and 2 without decay correction, are not significant anymore. Within the ICD population the significant differences between all methods remain. These results indicate that if H and M have values that meet the

TABLE 3. EFFECTS OF VARIATIONS IN QUANTIFICATION METHOD

	eHM	dHM	WOR				
			Method 1 Non DC	Method 1 DC	Method 2 Non DC	Method 2 DC	Method 3
Total	1.7±0.24	1.6±0.30	45.6±14.8	39.7±7.4	33.7±17.9	26.6±8.7	5.0±9.1
DB	1.8±0.18	1.8±0.27	36.5±13.1	36.5±7.1	22.8±15.8	22.7±8.4	-0.3±9.0
ICD	1.6±0.24	1.4±0.19	54.8±10.4	43.0±6.3	44.8±12.4	30.4±7.3	10.4±5.3

DB Diabetes Mellitus; DC decay correction; ICD Implantable cardiac device

condition $eHM \approx dHM$, the differences between method 1 and 2 become very small. In these instances the WOR derived from method 3 will approximate zero. Nonetheless, the relation $eHM \approx dHM$ is only applicable in certain cases, thus in general the discrepancies that arise from the use of different mathematical principles are clinically relevant.

DISCUSSION

With regard to manuscripts on I-123 MIBG scintigraphy in nuclear cardiology no previous systematic reviews were found in Pubmed, Embase or the Cochrane library that summarize mathematical methods that can be used to quantify different parameters in SPECT. The only available systematically performed literature study on this subject is the paper of Verberne et al ⁴. However, this study focused on the prognostic value of I-123 MIBG in chronic heart failure, thus excluding papers with other clinical topics which may comprise different methods for determining the parameters. Therefore, the main goal of this literature study was to assess the mathematical methods that are currently used, and to find the normal ranges that have to be applied for each of the methods. The results indicate not only large variations in mathematical principles, but also in various aspects of the protocols that are used during acquisition.

Collimator use

All the included manuscripts (n=30) had a detailed description, or referred to a detailed description of the methods that were used. These studies, except for two, used a low-energy collimator to image the 159-keV photons of ¹²³I. In addition to these low energy photons, medium energy photons (>400-keV) are also emitted, which cause scatter in the low energy acquisition range when they penetrate the septa. Although the use of

medium energy collimators reduces scatter and improves accuracy, the spatial resolution can reduce due to the lower yield of medium energy photons (~2.2%). However, studies indicate better results with respect to variability and accuracy of myocardial parameter estimates in both planar and SPECT acquisitions with medium-energy collimators.^{28,29} Nonetheless, most centres probably use the low-energy collimators since they are compatible with the multi-head systems that are used in the clinical practice. As collimator choice will influence the (semi-)quantitative estimates it is important to mention the collimator type and the type of scatter correction that is used.

Time interval between injection and acquisition

A second important factor that could affect the estimates is the time between early and late acquisitions, because the clearance of I-123 MIBG from the synaptic region is time depended. Once transported into the cell, I-123 MIBG is stored in vesicles and released by exocytose during nerve excitement. Similar to NE, I-123 MIBG will partly diffuse to the bloodstream, or be transported into the myocytes by the NE-transporters, once it is released into the synaptic cleft. These two mechanisms ensure that, over time, I-123 MIBG concentrations within the synaptic region will reduce. This clearance of NE and I-123 MIBG appears to follow first-order kinetics in the first 24 hours after injection.³⁰ Thus the amount of I-123 MIBG at a given moment in time (t) can be described by a turnover rate (k) and an initial cardiac uptake (A_0);

$$A(t) = A_0 e^{-t \frac{\ln 2}{T_{1/2}}} = A_0 e^{-tk}$$

It has to be noted that all included studies are based on the assumption that the clearance of I-123 MIBG follows zero order kinetics (linear relation). If the WOR is calculated based on the ratio between two acquisition moments, the reduction will relate to the time between the measurements. So a relatively early 'late acquisition' will yield higher WORs, then a 'late acquisition' made at a later moment in time. There are no clear findings on the impact of variable time intervals on the WOR; however, it is advisable to use fixed time intervals within the I-123 MIBG protocol to minimize variations.

Region of interest

The determination of the mediastinal and myocardial ROIs was manually set in all studies; however shape, size and positioning of these ROIs differed throughout the

articles. Although most studies use a square or rectangular ROI for the mediastinum, there was no consensus on the size and positioning. As the mediastinal ROI is used to correct for the I-123 MIBG activity within the blood pool and background, it should not contain organs that will accumulate I-123 MIBG. So it is advised to use a ROI with a fixed size, which correlates to matrix dimensions, that is placed on the mediastinal midline between the lung apex, and below the thyroid gland. The placement of the myocardial ROI was more consistent; however, shape and size differed in the studies. Within a large multi centre study ($n = 290$) Agostini et al.³¹ used a manually drawn ellipse heart ROI that contained both ventricles, and the atria if these were present. In addition a square, fixed size mediastinal ROI was used to calculate the early and delayed HM ratios. These ROIs were placed by an experienced technologist, and evaluated by at least two blinded readers. In 91% of the cases the readers accepted the placing of the ROIs and the resulting parameter estimates. Another study by Somsen et al.³² confirmed the low inter-observer and within-subject variations that are associated with using myocardial ROIs that contain the left ventricular cavity. This study also indicated that HM ratios are influenced by the type of myocardial ROIs; therefore, it was advised to use a standardized shape, for example an ellipse, which includes the myocardium and the left ventricular cavity.

Variations in mathematical principles

Within this study only limited variation was shown between the methods used to determine HM ratios. Some studies included decay correction to the data, whereas other studies used uncorrected values. All studies used the number of counts per pixel to determine the values for H and M . The use of mean counts per pixel and ratios between heart and mediastinal uptake both reduce the effects of ROI specification and are therefore recommended.

The variation in the methods used to determine WOR could be deduced to the use of decay correction or not, and the use of a ratio or a difference. If ratios (H/M) are used, like in method 3, decay correction will have no effect on the data. In the methods that use differences, like methods 1 and 2, the application of decay correction will have a direct effect on the parameter estimates. Thus, it is important to provide a detailed description of the methods that are used during a study and the use of decay correction during the study.

The results of this study indicate that significant differences between parameter values arise when using different mathematical methods. The effects of the different methods were especially profound for the WOR and can be considered clinically relevant. Within literature no studies were found that compare the use of different methods, or provide information on the effects of the methods on the clinical interpretation of parameter values. Thus, it is unclear which of the methods will provide the most accurate and reproducible estimates.

Applying normal values

A decrease in I-123 MIBG uptake has been described earlier in primary cardiomyopathies, including dysautonomias and heart transplantation, and secondary cardiomyopathies including CAD, infarction and cardiomyopathies.¹ To stratify patients into low-risk and high-risk groups, normal ranges and cut-off values are frequently used. Normal ranges should ideally be based on large datasets containing normal, healthy individuals which originate from multicentre trials. However, the normal ranges that were found in this study for both the HM ratio and the WOR did not concur with these requirements. All normal ranges were based on single centre studies with small numbers of relatively young healthy volunteers ($n = 6-20$). These selection procedures for the generation of normal values could induce discrepancies, if these ranges are applied in other settings, or on other patient populations.

Earlier studies have indicated that it is important to take the physiological fluctuations of I-123 MIBG distribution with respect to age and gender into account when evaluating planar and SPECT acquisitions.^{26,33-35} Sakata et al.³³ showed in a study including 315 patients that there were gender- and age-related differences in regional uptake throughout the myocardium. Within the population of less than 50 years, both genders had relative similar uptake distributions; however, the population of 50 years and older showed specific age and gender related differences. Men within this population showed uptake decrease in the inferior wall, whereas women had a characteristic decrease in the lateral wall. The WORs were, overall, higher in men than in women aged under 50 years for all segments within the myocardium. With advancing age these rates only mildly increased in men, but showed a very prominent increase in women. Similar results were also shown by Tsuchimochi et al. in a smaller population.³⁵ Both studies indicate that these heterogeneities are more profound on SPECT acquisitions, and are possible negligible within planar acquisitions. Nonetheless, Estorch et al. showed an age

related uptake of I-123 MIBG in 39 normal individuals (16-75 years).²⁶ Especially within the group of patients less than 60 years, there was a clear decrease in HM ratio compared to the other age groups. Therefore, the need for age dependent normal values has to be considered.

CONCLUSION

Within this study great diversity was found in the methods that are used to determine the I-123 MIBG parameters in planar images. The results that are obtained with these methods differ significantly in most patient populations. Furthermore, the acquisition protocols varied substantially between all included manuscripts, indicating the presence of great variation in protocols used throughout the clinical settings. The use of different protocols and mathematical methods prohibits the exchangeability and comparability of patient data and normal values throughout various clinics. This study therefore accentuates the need to produce guidelines to achieve a standardized method for I-123 acquisition and evaluation.

TABLE 1. OVERVIEW OF THE INCLUDED MANUSCRIPTS

Author	Topic	Population	Dose	Time	Collim	ROI delineation	HM	WOR	Ref. population	Conclusions
Nanjo et al. ¹²	DCM in patients with SBD	53 patients with DCM (32 SBD -; 21 SBD +)	111 MBq	15 min 4 h	LEGP	Manually drawn ROI on mediastinum and heart. Mean counts per ROI. C	1	4	Comparison of SBD – and +. Cut-off values used are dHM 2.2; WR 22% (no ref.)	DCM patients with SBD have elevated SNA compared to those without SBD, and I-123 MIBG can be used to detect increased SNA.
Lorincz et al. ²¹	Adrenergic innervation in patients with VVS	15 patients diagnosed with VVS and >3 episodes in last year, and 6 healthy individuals	250-370 MBq	15 min 3 h	-	Manually placed square ROI on mediastinum and heart. Count rates per ROI. A	2	5 ³⁶	Direct comparison with healthy volunteers. (mean eHM 2.17 ± 0.41; dHM 2.59 ± 0.54; WOR 0.22 ± 0.17)	In patients with VVS global I-123 MIBG deficit occurred frequently and all patients had regional adrenergic nerve function deficits.
Tamaki et al. ¹³	Predictive value of I-123 MIBG in SCD	106 patients with stable CHF (18 SCD +; 88 SCD-)	111 MBq	20 min 3.5h	LEHR parallel hole	Manually drawn ROI over LV and 7x7-pixel ROI on mediastinum. Mean counts per pixel. A 24	1	8 ²⁴	Comparison of SCD – and + patients. Cut-off WOR >27% 24	Cardiac I-123 MIBG WOR is a powerful predictor of SCD in patients with mild-to-moderate CHF, independently of LVEF.
Toyama et al. ³⁷	Effectiveness of HOT in patients with CHF	20 patients with CHF (10 HOT+; 10 HOT-)	111 MBq	15 min 4h	-	Manually drawn ROI on heart and square ROI on mediastinum. Mean counts per pixel.	1	4 ^{38,39}	Comparison of HOT – and HOR + patients.	HOT improves exercise capacity, cardiac function, and SNA in patients with CHF and central sleep apnoea.
Sakata et al. ³³	Physiological changes in cardiac sympathetic innervation	153 patients referred for cardiac catheterization with near normal coronary arteries	111 MBq	15 min 3h	LEHR parallel hole	Manually placed square ROIs on peak count density in heart and mediastinum. Mean counts per pixel. A	1 (only dHM)	3 ⁴⁰	Population divided over 10-year age groups.	Early and delayed HM ratios had significant age- and gender-related decreases and washout rate had a significant age-related increase in normal subjects.
Spinelli et al. ⁴¹	SCS in patients with CSX	11 patients with CSX who had to undergo SCS implantation	185 MBq	15 min 3h	LEGP parallel hole	Manually drawn ROI on heart and square ROI mediastinum. Mean counts per pixel. C 42,43	1	4 ^{42,43}	Comparison of SCS-ON and SCS-OFF in same patient and with 10 control patients from earlier study. (mean HM 2.19 ± 0.3) 42	Abnormal cardiac SNA in CSX patients. SCS was unable to result in significant improvement of cardiac I-123 MIBG uptake abnormalities.
Shibata et al. ⁴⁶	Sympathetic and parasympathetic dysfunction in PD	79 patients with PD (40 receiving medication)	111 MBq	15 min 3h	LEHR parallel hole	Manually placed oval ROI on heart and square ROI mediastinum. Mean counts per pixel. A	1	3	Population divided in Hoehn-Yahr stages of disease severity	Parasympathetic dysfunction presents concurrent with sympathetic denervation as revealed by I-123 MIBG in PD.

Author	Topic	Population	Dose	Time	Collim	ROI delineation	HM	WOR	Ref. population	Conclusions	
Tsutamoto et al. ¹⁴	Prognostic role of the trans-cardiac gradient of NE in patients with CHF	356 symptomatic CHF patients undergoing catheterization	Method similar to Tsutamoto et al. ¹⁶							Comparison of groups within population. Normal values are d HM 2.6±0.24; WR 28±3.1% ⁴⁴	Trans-cardiac increase in NE is an independent and useful prognostic predictor for evaluating the prognosis of CHF patients.
Tateno et al. ¹⁵	Diagnosis of DLB	25 patients with DLB	111 MBq	20 min 3h	LEHR parallel hole	Method similar to Yoshita et al. ^{20,45}			Cut-off values are eHM 1.93; dHM 1.81; WR 22.7% 20	Combining SPECT and I-123 MIBG could increase the accuracy of clinical diagnosis of DLB.	
Estorch et al. ⁴⁷	Ability of I-123 MIBG for early identification of DLB	65 patients with clinical criteria of probable DLB	370 MBq	15 min 4h	LEGP parallel hole	Manually drawn ROI on mediastinum and heart. Mean counts per pixel. A	1	3	Patients with DLB, Alzheimer and other neurodegenerative diseases. Cut-off value HM>1.56 age 60+ ²⁶	I-123 MIBG imaging allows early identification of DLB from other neurodegenerative diseases with cognitive impairment.	
Cha et al. ²²	Effect of CRT on nervous function in HF	16 patients with advanced HF and 10 age-and-gender matched controls	370 MBq	15 min 4h	ME	Manually drawn ROI excluding cavity and 20x20-pixel ROI on mediastinum. Mean counts per pixel. A ³²	1	6	Comparison between control and patient group. (mean eHM 2.6 ± 0.3; dHM 2.5 ± 0.3; WOR 25 ± 12)	Improvements in cardiac symptoms and LV function after CRT, accompanied by rebalanced cardiac autonomic control.	
Tsutamoto et al. ¹⁶	Effect of perindopril in patients with chronic HF	45 stable CHF patients on conventional therapy	111 MBq	15 min 3h	LE	Manually placed ROI heart and mediastinum. Mean counts per pixel. B	1	4 ⁴⁴	Comparison of enalapril (n=24) and perindopril (n=21) patients. Normal values are dHM 2.6±0.24; WOR 28±3.1 ⁴⁴	These findings suggest that for treatment of CHF, perindopril is superior to enalapril with respect of cardiac SNA.	
Diakakis et al. ²⁷	Myocardial innervation in patients with IGT	22 patients with IGT and 18 healthy volunteers	185 MBq	10 min 4h	LEGP	7x7-pixel ROI placed over heart and mediastinum. Mean counts per pixel.	1	7	Comparison of IGT group with volunteers (mean eHM 2.93 ± 0.4; dHM 2.85± 0.4; WOR 2.1±0.96)	Patients with IGT show reduced I-123 MIBG uptake with segmental pattern, which was related to the elevated pro-inflammatory cytokine levels.	
Nagamatsu et al. ⁴⁸	Prognostic value of I-123 MIBG in patients with heart diseases	565 patients undergoing I-123 MIBG	111 MBq	15 min 4h	LEHR	Manually drawn ROI on heart and square ROI on mediastinum. A	2	5 ³⁶	The relation between cardiac events and MIBG indices were determined without comparing groups	I-123 MIBG indices were associated with HF, SCD, and cardiac events, and were useful to provide prognosis in DCM, HCM, and IHD for diseases.	
Lorberboym et al. ²³	MIBG evaluation in MS	10 patients with MS and 7 age-and-gender matched controls	185 MBq	15 min 3h	LEHR	Manually drawn ROI heart and rectangular ROI mediastinum. Mean counts per pixel. A	1	3	Comparison of control and patient group (mean eHM 1.21 ± 0.3; dHM 1.38 ± 0.3; WOR 21 ± 8)	I-123 MIBG provides a direct evaluation of sympathetic dysfunction in MS and is a sensitive autonomic dysfunction test in patients with MS.	

Author	Topic	Population	Dose	Time	Collim	ROI delineation	HM	WOR	Ref. population	Conclusions
Buri et al. ¹⁷	Sympathetic activity after CRT	16 patients with standard indication for CRT	185 MBq	15 min 4h	-	Manually drawn ROI heart and rectangular ROI mediastinum. Mean counts per pixel are determined. A	1 ²⁵	8 ^{19,24,49}	Comparison of responders and non-responders to CRT. Normal values are eHM 1.9-2.8; dHM 1.8-2.7; WOR >27% 25	CRT induces a reduction in cardiac SNA in responders that relates to improvements in LVEF, whereas non-responders do not show significant changes.
Nishioka et al. ⁵⁰	Cardiac innervation pre- and post-CRT	30 patients with CHF, referred for CRT implantation	-	15 min 3h	LEGP	Manually drawn ROI on LV and mediastinum. Mean counts per pixel. A	1 (only dHM)	9	Comparison of responders improving to functional class I or II (n=21) and non-responders remaining in FC III or IV (n=9)	Improvement in SNA correlated with a CRT response, lower I-123 MIBG uptake before therapy was associated with CRT non-response.
Kasama et al. ⁸	Prognostic value of serial I-123 MIBG in stabilized CHF	208 patients with first episode of HF	Method similar to Kasama et al. 11						Comparison of cardiac death with non-cardiac death. (56 cardiac death; 152 no death)	ΔWOR from serial I-123 MIBG images can be useful for predicting cardiac death and SCD in stabilized patients with CHF.
Tsukamoto et al. ⁵¹	β-Adrenergic receptor density in non-ischemic CMP	16 patients with non-ischemic CMP and 8 age matched controls	111 MBq	15 min 4h	LEGP	Manually drawn ROI on LV and 9x9-pixel ROI on mediastinum. Mean counts per pixel. B	1	3	Comparison between control and patient group. (no notation of mean values)	The degree of β-receptor down regulation corresponded to the increase in WOR and a decrease in dHM ratio.
Verberne et al. ⁵²	Non-carrier vs. carrier added MIBG for evaluation of SNA	19 volunteers with low likelihood for CAD	185 MBq	15 min 4h	ME	Manually drawn ROI on heart and rectangular ROI 100 pixels on mediastinum. Mean counts per pixel. A	1	7	Comparison of CA and NCA scans in same patient	NCA MIBG yields higher relative uptake and a higher retention. For assessment of cardiac sympathetic activity, NCA MIBG is preferred over CA MIBG.
Furuhashi et al. ¹⁸	Influence of renal function on I-123 MIBG uptake	135 patients with previous history of HF	111 MBq	15 min 4h	LEHR parallel hole	Manually drawn ROI LV and 20x20-pixel ROI over mediastinum. Mean counts per pixel. B	1	4	Comparison based on GFR. Normal values are dHM 220 ± 30%; WOR 27 ± 5.8% (no ref.)	A delayed HM is a powerful predictor of cardiac death if the GFR is 60 ml/min/1.73 m ² or more.
Kioka et al. ¹⁹	I-123 MIBG as predictor for SCD in patients with CHF	97 patients with CHF with LVEF <40% (14 SCD +; 83 SCD -)	111 MBq	20 min 3.5h	LEHR parallel hole	Manually drawn ROI LV and 7x7-pixel ROI over mediastinum. Mean counts per pixel. A 24,49	1	8 ^{24,49}	Comparison of SCD – and + patients. Cut-off value WOR>27% 24,49	Cardiac I-123 MIBG imaging would be useful for predicting SCD in patients with CHF.
Kasama et al. ⁹	Remodelling in DCM during carvedilol	30 patients with DCM and 10 controls	Method similar to Kasama et al. 11						Comparison of before and after treatment and with controls (mean HM 2.44 ± 0.26; WOR 25 ± 5)	I-123 MIBG values improved in the DCM patients. There was a correlation between the changes of I-123 MIBG and echographic findings.

Author	Topic	Population	Dose	Time	Collim	ROI delineation	HM	WOR	Ref. population	Conclusions
Gould et al. ⁵³	Adrenergic function post biventricular pacing for HF	10 patients with pacing	200 MBq	15 min; 4h	-	Manually drawn ROI on myocardium; 8x8-pixel ROI on mediastinum. Mean counts per pixel. A 32,54	1	3 ^{32,54}	Comparison between inactivation of pacing or active pacing	In patients with stable HF, biventricular pacing is associated with long-term improvements in SNA, as reflected by improvements in I-123 MIBG uptake.
Arimoto et al. ⁵⁵	Sympathetic denervation in early HF	104 patients with HF	111 MBq	30 min; 4h	LEHR	Manually drawn ROI LV and 20x20-pixel ROI over mediastinum. Mean counts per pixel. C 56	1	4	Comparison of cardiac event – (n=79) and cardiac event + (n=25) patients	Determination of heart-type fatty acid binding protein adds prognostic information to dHM, and this combination may improve accuracy of prognoses in HF.
Yoshita et al. ²⁰	Differential diagnosis DLB and Alzheimer	79 patients (42 Alzheimer, 37 DLB) and 10 controls	111 MBq	20 min; 3h	LEHR parallel hole	Manually drawn ROI heart and rectangular ROI mediastinum. Mean counts per pixel. A 58,59	1	3 ^{58,59}	Comparison of all groups and with controls (mean eHM 2.07 ± 0.21; dHM 2.18 ± 0.26; WOR 15.1 ± 7.4)	DLB results in cardiac sympathetic denervation; I-123 MIBG is a sensitive tool for discriminating DLB from Alzheimer even in patients without parkinsonism.
Kasama et al. ¹⁰	Long-term nicorandil therapy in patients with AMI	52 patients with AMI	Method similar to Kasama et al. ¹¹						Comparison nicorandil (n=20) and placebo (n=20)	Long-term nicorandil therapy can be more beneficial for SNA and LV remodelling than short-term therapy in patients with acute infarction.
Kasama et al. ¹¹	Effects torasemide in patients with CHF	48 patients with first episode of non-ischemic HF	111 MBq	15 min; 4h	LEGP parallel hole	Oval ROI on heart and rectangular 7x7-pixel ROI on mediastinum. Mean counts per pixel. B 60-63	1 ⁶⁴	4	Comparison of torasemide (n=20) and furosemide (n=20) treatment. Normal values are dHM 2.0-2.8; WOR 22-32% (no ref.)	Torasemide treatment can enhance cardiac SNA and left ventricular remodelling in patients with CHF.
Pessoa et al. ⁵⁷	I-123 MIBG in patients with Takotsubo CMP	5 female patients	259 MBq	30 min; 4h	LEHR	Manually drawn circular ROI over myocardium and mediastinum. Mean counts per pixel. B	1	3	Mutual comparison off all patients. Cut-off values are HM 1.8; WOR >10% 1	Ampulla CMP is associated with a cardiac sympathetic innervation deficit characterized by reduced I-123 MIBG uptake.
Sugiura et al. ⁶⁵	Relationship between I-123 MIBG and status of diastolic HF	34 patients with diastolic HF	111 MBq	20 min; 4h	LEGP	Manually drawn ROI heart and mediastinum. Mean counts per pixel. A	1	4	The relations between cardiac events and I-123 MIBG indices were determined without comparing groups	In diastolic HF, cardiac SNA increases proportionally to severity of the disease.

Quantification formulas used in literature; (see text for further information)

1. $\frac{eH}{eM} \frac{dH}{dM}$
2. $\frac{eH/A_H}{eM/A_M} \frac{dH/A_H}{dM/A_M}$
3. $\frac{(eH-dH)}{eH} \times 100\%$
4. $\frac{(eH-eM)-(dH-dM)}{(eH-eM)} \times 100\%$
5. $eH' = eH - (A_H/A_M) \times eM$
 $dH' = [dH - (A_H/A_M) \times dM] \times 2^{t/\tau}$
 $\frac{(dH'-eH')}{(eH' \times t)} \times 100\%$
6. $\frac{(eHCD-dHCD)}{eHCD} \times 100\%$
7. $\frac{(eH/eM)-(dH/dM)}{(eH/eM)} \times 100\%$
8. $\left(\frac{eH}{0.5^{eH/\tau}} - \frac{eM}{0.5^{eM/\tau}} \right) - \left(\frac{dH}{0.5^{dH/\tau}} - \frac{dM}{0.5^{dM/\tau}} \right) \times 100\%$
 $\left(\frac{eH}{0.5^{eH/\tau}} - \frac{eM}{0.5^{eM/\tau}} \right)$
9. $\frac{(eH/eT - eM/eT) - (dH/dT - dM/dT)}{(eH/eT - eM/eT)} \times 100\%$

A = Counts are corrected for decay; **B** = no decay correction applied; **C** = No description of application of decay correction in the article

Abbreviations used in the table;

AMI, acute myocardial infarction; CA, carrier added; CHF, chronic heart failure; Collim, collimator, CRT, cardiac resynchronization therapy; CSA, cardiac sympathetic activity; CSX, cardiac syndrome X; DCM, dilated cardiomyopathy; DLB, dementia with Lewy bodies; FC, functional class; GFR, glomerular filtration rate; HCM, hypertrophic cardiomyopathy; HF, heart failure; HHD, hypertensive heart disease; HM, heart-to-mediastinum; HOT, home oxygen therapy; IGT, impaired glucose tolerance; IHD, ischemic heart diseases; LE, low energy; LEGP, low energy general purpose; LEHR, low energy high resolution; LV, left ventricle; LVEF, left ventricular ejection fraction; ME, medium energy; MIBG, meta-iodobenzylguanidine; MS, multiple sclerosis; NCA, non-carrier added; NE, norepinephrine; PD, Parkinson disease; PVD, pressure-load valvular disease; ROI, region of interest; CRT, cardiac resynchronization therapy; SBD, sleep-breathing disorder; SCD, sudden cardiac death; SCS, Spinal cord stimulation; SNA, sympathetic nerves activity; VTF, ventricular tachycardia or fibrillation; VVD, volume-load valvular disease; VVS, vasovagal syncope

REFERENCE LIST

- (1) Carrio I. Cardiac neurotransmission imaging. *J Nucl Med.* 2001;42:1062-1076.
- (2) Eisenhofer G, Pacak K, Goldstein DS, Chen C, Shulkin B. 123I-MIBG scintigraphy of catecholamine systems: impediments to applications in clinical medicine. *Eur J Nucl Med.* 2000;27:611-612.
- (3) Hattori N, Schwaiger M. Metaiodobenzylguanidine scintigraphy of the heart: what have we learnt clinically? *Eur J Nucl Med.* 2000;27:1-6.
- (4) Verberne HJ, Brewster LM, Somsen GA, van Eck-Smit BL. Prognostic value of myocardial 123I-metaiodobenzylguanidine (MIBG) parameters in patients with heart failure: a systematic review. *Eur Heart J.* 2008;29:1147-1159.
- (5) Agostini D, Carrio I, Verberne HJ. How to use myocardial 123I-MIBG scintigraphy in chronic heart failure. *Eur J Nucl Med Mol Imaging.* 2009;36:555-559.
- (6) Verberne HJ, Habraken JB, van Eck-Smit BL, Agostini D, Jacobson AF. Variations in 123I-metaiodobenzylguanidine (MIBG) late heart mediastinal ratios in chronic heart failure: a need for standardisation and validation. *Eur J Nucl Med Mol Imaging.* 2008;35:547-553.
- (7) Yamashina S, Yamazaki J. Neuronal imaging using SPECT. *Eur J Nucl Med Mol Imaging.* 2007;34:939-950.
- (8) Kasama S, Toyama T, Sumino H et al. Prognostic value of serial cardiac 123I-MIBG imaging in patients with stabilized chronic heart failure and reduced left ventricular ejection fraction. *J Nucl Med.* 2008;49:907-914.
- (9) Kasama S, Toyama T, Hatori T et al. Evaluation of cardiac sympathetic nerve activity and left ventricular remodelling in patients with dilated cardiomyopathy on the treatment containing carvedilol. *Eur Heart J.* 2007;28:989-995.
- (10) Kasama S, Toyama T, Hatori T et al. Effects of intravenous atrial natriuretic peptide on cardiac sympathetic nerve activity and left ventricular remodeling in patients with first anterior acute myocardial infarction. *J Am Coll Cardiol.* 2007;49:667-674.
- (11) Kasama S, Toyama T, Hatori T et al. Effects of torasemide on cardiac sympathetic nerve activity and left ventricular remodelling in patients with congestive heart failure. *Heart.* 2006;92:1434-1440.
- (12) Nanjo S, Yamashiro Y, Fujimoto S et al. Evaluation of sympathetic activity by 123I-metaiodobenzylguanidine myocardial scintigraphy in dilated cardiomyopathy patients with sleep breathing disorder. *Circ J.* 2009;73:686-690.
- (13) Tamaki S, Yamada T, Okuyama Y et al. Cardiac iodine-123 metaiodobenzylguanidine imaging predicts sudden cardiac death independently of left ventricular ejection fraction in patients with chronic heart failure and left ventricular systolic dysfunction: results from a comparative study with signal-averaged electrocardiogram, heart rate variability, and QT dispersion. *J Am Coll Cardiol.* 2009;53:426-435.

- (14) Tsutamoto T, Nishiyama K, Sakai H et al. Transcardiac increase in norepinephrine and prognosis in patients with chronic heart failure. *Eur J Heart Fail.* 2008;10:1208-1214.
- (15) Tateno M, Kobayashi S, Shirasaka T et al. Comparison of the usefulness of brain perfusion SPECT and MIBG myocardial scintigraphy for the diagnosis of dementia with Lewy bodies. *Dement Geriatr Cogn Disord.* 2008;26:453-457.
- (16) Tsutamoto T, Tanaka T, Sakai H et al. Beneficial effect of perindopril on cardiac sympathetic nerve activity and brain natriuretic peptide in patients with chronic heart failure: comparison with enalapril. *Circ J.* 2008;72:740-746.
- (17) Burri H, Sunthorn H, Somsen A et al. Improvement in cardiac sympathetic nerve activity in responders to resynchronization therapy. *Europace.* 2008;10:374-378.
- (18) Furuhashi T, Moroi M. Importance of renal function on prognostic value of cardiac iodine-123 metaiodobenzylguanidine scintigraphy. *Ann Nucl Med.* 2007;21:57-63.
- (19) Kioka H, Yamada T, Mine T et al. Prediction of sudden death in patients with mild-to-moderate chronic heart failure by using cardiac iodine-123 metaiodobenzylguanidine imaging. *Heart.* 2007;93:1213-1218.
- (20) Yoshita M, Taki J, Yokoyama K et al. Value of 123I-MIBG radioactivity in the differential diagnosis of DLB from AD. *Neurology.* 2006;66:1850-1854.
- (21) Lorincz I, Garai I, Varga E et al. Myocardial adrenergic innervation in patients with vasovagal syncope measured with 123I-MIBG uptake. *Nucl Med Commun.* 2009;30:134-139.
- (22) Cha YM, Oh J, Miyazaki C et al. Cardiac resynchronization therapy upregulates cardiac autonomic control. *J Cardiovasc Electrophysiol.* 2008;19:1045-1052.
- (23) Lorberboym M, Lampl Y, Nikolov G, Sadeh M, Gilad R. I-123 MIBG cardiac scintigraphy and autonomic test evaluation in multiple sclerosis patients. *J Neurol.* 2008;255:211-216.
- (24) Ogita H, Shimonagata T, Fukunami M et al. Prognostic significance of cardiac (123)I metaiodobenzyl-guanidine imaging for mortality and morbidity in patients with chronic heart failure: a prospective study. *Heart.* 2001;86:656-660.
- (25) Ohshima S, Isobe S, Izawa H et al. Cardiac sympathetic dysfunction correlates with abnormal myocardial contractile reserve in dilated cardiomyopathy patients. *J Am Coll Cardiol.* 2005;46:2061-2068.
- (26) Estorch M, Carrio I, Berna L, Lopez-Pousa J, Torres G. Myocardial iodine-labeled metaiodobenzyl-guanidine 123 uptake relates to age. *J Nucl Cardiol.* 1995;2:126-132.
- (27) Diakakis GF, Parthenakis FI, Patrianakos AP et al. Myocardial sympathetic innervation in patients with impaired glucose tolerance: relationship to subclinical inflammation. *Cardiovasc Pathol.* 2008;17:172-177.
- (28) Inoue Y, Suzuki A, Shirouzu I et al. Effect of collimator choice on quantitative assessment of cardiac iodine 123 MIBG uptake. *J Nucl Cardiol.* 2003;10:623-632.
- (29) Verberne HJ, Feenstra C, de Jong WM, Somsen GA, van Eck-Smit BL, Busemann SE. Influence of collimator choice and simulated clinical conditions on 123I-MIBG heart/mediastinum ratios: a phantom study. *Eur J Nucl Med Mol Imaging.* 2005;32:1100-1107.

- (30) Glowniak JV. Cardiac studies with metaiodobenzylguanidine: a critique of methods and interpretation of results. *J Nucl Med.* 1995;36:2133-2137.
- (31) Agostini D, Verberne HJ, Burchert W et al. I-123-mIBG myocardial imaging for assessment of risk for a major cardiac event in heart failure patients: insights from a retrospective European multicenter study. *Eur J Nucl Med Mol Imaging.* 2008;35:535-546.
- (32) Somsen GA, Verberne HJ, Fleury E, Righetti A. Normal values and within-subject variability of cardiac I-123 MIBG scintigraphy in healthy individuals: implications for clinical studies. *J Nucl Cardiol.* 2004;11:126-133.
- (33) Sakata K, Iida K, Mochizuki N, Ito M, Nakaya Y. Physiological changes in human cardiac sympathetic innervation and activity assessed by (123)I-metaiodobenzylguanidine (MIBG) imaging. *Circ J.* 2009;73:310-315.
- (34) Kiyono Y, Kanegawa N, Kawashima H et al. Age-related changes of myocardial norepinephrine transporter density in rats: implications for differential cardiac accumulation of MIBG in aging. *Nucl Med Biol.* 2002;29:679-684.
- (35) Tsuchimochi S, Tamaki N, Tadamura E et al. Age and gender differences in normal myocardial adrenergic neuronal function evaluated by iodine-123-MIBG imaging. *J Nucl Med.* 1995;36:969-974.
- (36) Momose M, Kobayashi H, Iguchi N et al. Comparison of parameters of 123I-MIBG scintigraphy for predicting prognosis in patients with dilated cardiomyopathy. *Nucl Med Commun.* 1999;20:529-535.
- (37) Toyama T, Seki R, Kasama S et al. Effectiveness of nocturnal home oxygen therapy to improve exercise capacity, cardiac function and cardiac sympathetic nerve activity in patients with chronic heart failure and central sleep apnea. *Circ J.* 2009;73:299-304.
- (38) Toyama T, Aihara Y, Iwasaki T et al. Cardiac sympathetic activity estimated by 123I-MIBG myocardial imaging in patients with dilated cardiomyopathy after beta-blocker or angiotensin-converting enzyme inhibitor therapy. *J Nucl Med.* 1999;40:217-223.
- (39) Takeishi Y, Atsumi H, Fujiwara S, Takahashi K, Tomoike H. ACE inhibition reduces cardiac iodine-123-MIBG release in heart failure. *J Nucl Med.* 1997;38:1085-1089.
- (40) Sakata K, Shirotani M, Yoshida H, Kurata C. Comparison of effects of enalapril and nitrendipine on cardiac sympathetic nervous system in essential hypertension. *J Am Coll Cardiol.* 1998;32:438-443.
- (41) Spinelli A, Lanza GA, Calcagni ML et al. Effect of spinal cord stimulation on cardiac adrenergic nerve function in patients with cardiac syndrome X. *J Nucl Cardiol.* 2008;15:804-810.
- (42) Lanza GA, Giordano A, Pristipino C et al. Abnormal cardiac adrenergic nerve function in patients with syndrome X detected by [123I]metaiodobenzylguanidine myocardial scintigraphy. *Circulation.* 1997;96:821-826.

- (43) Giordano A, Calcagni ML, Rufini V et al. Use of [123I]MIBG to assess cardiac adrenergic innervation: experience in hypertensive cardiopathy and left ventricular aneurysms. *Q J Nucl Med.* 1995;39:44-48.
- (44) Matsui T, Tsutamoto T, Maeda K, Kusukawa J, Kinoshita M. Prognostic value of repeated 123I-metaiodobenzylguanidine imaging in patients with dilated cardiomyopathy with congestive heart failure before and after optimized treatments--comparison with neurohumoral factors. *Circ J.* 2002;66:537-543.
- (45) Hanyu H, Shimizu S, Hirao K et al. The role of 123I-metaiodobenzylguanidine myocardial scintigraphy in the diagnosis of Lewy body disease in patients with dementia in a memory clinic. *Dement Geriatr Cogn Disord.* 2006;22:379-384.
- (46) Shibata M, Morita Y, Shimizu T, Takahashi K, Suzuki N. Cardiac parasympathetic dysfunction concurrent with cardiac sympathetic denervation in Parkinson's disease. *J Neurol Sci.* 2009;276:79-83.
- (47) Estorch M, Camacho V, Paredes P et al. Cardiac (123)I-metaiodobenzylguanidine imaging allows early identification of dementia with Lewy bodies during life. *Eur J Nucl Med Mol Imaging.* 2008;35:1636-1641.
- (48) Nagamatsu H, Momose M, Kobayashi H, Kusakabe K, Kasanuki H. Prognostic value of 123I-metaiodobenzyl-guanidine in patients with various heart diseases. *Ann Nucl Med.* 2007;21:513-520.
- (49) Yamada T, Shimonagata T, Fukunami M et al. Comparison of the prognostic value of cardiac iodine-123 metaiodobenzylguanidine imaging and heart rate variability in patients with chronic heart failure: a prospective study. *J Am Coll Cardiol.* 2003;41:231-238.
- (50) Nishioka SA, Martinelli FM, Brandao SC et al. Cardiac sympathetic activity pre and post resynchronization therapy evaluated by 123I-MIBG myocardial scintigraphy. *J Nucl Cardiol.* 2007;14:852-859.
- (51) Tsukamoto T, Morita K, Naya M et al. Decreased myocardial beta-adrenergic receptor density in relation to increased sympathetic tone in patients with nonischemic cardiomyopathy. *J Nucl Med.* 2007;48:1777-1782.
- (52) Verberne HJ, Sokole EB, Van Moerkerken AF et al. Clinical performance and radiation dosimetry of no-carrier-added vs carrier-added 123I-metaiodobenzylguanidine (MIBG) for the assessment of cardiac sympathetic nerve activity. *Eur J Nucl Med Mol Imaging.* 2008;35:798-807.
- (53) Gould PA, Kong G, Kalf V et al. Improvement in cardiac adrenergic function post biventricular pacing for heart failure. *Europace.* 2007;9:751-756.
- (54) Merlet P, Benvenuti C, Moyses D et al. Prognostic value of MIBG imaging in idiopathic dilated cardiomyopathy. *J Nucl Med.* 1999;40:917-923.
- (55) Arimoto T, Takeishi Y, Niizeki T et al. Cardiac sympathetic denervation and ongoing myocardial damage for prognosis in early stages of heart failure. *J Card Fail.* 2007;13:34-41.

- (56) Imamura Y, Fukuyama T, Mochizuki T, Miyagawa M, Watanabe K. Prognostic value of iodine-123-metaiodobenzylguanidine imaging and cardiac natriuretic peptide levels in patients with left ventricular dysfunction resulting from cardiomyopathy. *Jpn Circ J.* 2001;65:155-160.
- (57) Pessoa PM, Xavier SS, Lima SL et al. Assessment of takotsubo (ampulla) cardiomyopathy using iodine-123 metaiodobenzylguanidine scintigraphy. *Acta Radiol.* 2006;47:1029-1035.
- (58) Yoshita M. Differentiation of idiopathic Parkinson's disease from striatonigral degeneration and progressive supranuclear palsy using iodine-123 meta-iodobenzylguanidine myocardial scintigraphy. *J Neurol Sci.* 1998;155:60-67.
- (59) Yoshita M, Hayashi M, Hirai S. Decreased myocardial accumulation of 123I-meta-iodobenzyl guanidine in Parkinson's disease. *Nucl Med Commun.* 1998;19:137-142.
- (60) Kasama S, Toyama T, Kumakura H et al. Effect of spironolactone on cardiac sympathetic nerve activity and left ventricular remodeling in patients with dilated cardiomyopathy. *J Am Coll Cardiol.* 2003;41:574-581.
- (61) Kasama S, Toyama T, Kumakura H et al. Spironolactone improves cardiac sympathetic nerve activity and symptoms in patients with congestive heart failure. *J Nucl Med.* 2002;43:1279-1285.
- (62) Kasama S, Toyama T, Hoshizaki H et al. Dobutamine gated blood pool scintigraphy predicts the improvement of cardiac sympathetic nerve activity, cardiac function, and symptoms after treatment in patients with dilated cardiomyopathy. *Chest.* 2002;122:542-548.
- (63) Kasama S, Toyama T, Kumakura H et al. Addition of valsartan to an angiotensin-converting enzyme inhibitor improves cardiac sympathetic nerve activity and left ventricular function in patients with congestive heart failure. *J Nucl Med.* 2003;44:884-890.
- (64) Merlet P, Valette H, Dubois-Rande JL et al. Prognostic value of cardiac metaiodobenzylguanidine imaging in patients with heart failure. *J Nucl Med.* 1992;33:471-477.
- (65) Sugiura M, Yamamoto K, Takeda Y et al. The relationship between variables of 123-I-metaiodobenzylguanidine cardiac imaging and clinical status of the patients with diastolic heart failure. *Int J Cardiol.* 2006;113:223-228.

Chapter 7

Volumetric quantification of I-123 MIBG SPECT

B.J. van der Veen, I. Al Younis, A. de Roos, M.P. Stokkel,

Assessment of global cardiac I-123 MIBG uptake and washout
using volumetric quantification of SPECT acquisitions.

Accepted in **J Nucl Cardiol**

ABSTRACT

Background: Assessment of cardiac innervation using single photon emission computer tomography (SPECT) is less established than planar imaging, but may be more suitable for quantification. Therefore, a volumetric quantification of I-123 MIBG SPECT acquisitions was performed. Reproducibility, the effects of extra cardiac I-123 MIBG uptake and the relation with conventional planar indices were evaluated.

Methods: 54 patients referred for planar and SPECT I-123 MIBG acquisitions were included. Ellipsoidal or box shaped volumes of interest (VOIs) were placed on the left ventricle, cardiac lumen, mediastinum, lung and liver. SPECT segmentation was performed twice in all patients. Indices were determined based on the heart-to-mediastinum (HM), myocardial wall-to-mediastinum (MM) and myocardial wall-to-lumen (ML) regions. HM ratios and washout rates (WORs) were also determined based on anterior planar images.

Results: Cardiac count densities were highly reproducible (CV 1.5-5.4, ICC 0.96-0.99) and inter-rater variability was low (CV 1.8-6.8, ICC 0.94-0.99). Mediastinal uptake was an important explanatory variable of uptake in the entire heart (*early* R^2 0.36; *delayed* R^2 =0.43) and myocardial wall (*early* R^2 = 0.28; *delayed* R^2 = 0.37). Lung washout was an explanatory variable of organ washout of the heart (*heart* R^2 = 0.38; *myocardial wall* R^2 = 0.33). In general, SPECT indices showed moderate to good correlations with the planar uptake (PCC 0.497-0.851).

Conclusion: By applying a volumetric segmentation method we were able to segment the heart in all patients. SPECT I-123 MIBG quantification was found to be highly reproducible and had a moderate to good correlation with the planar indices.

Keywords: I-123 meta-iodobenzylguanidine ▪ Myocardial innervation ▪ SPECT ▪ Quantitative analysis

INTRODUCTION

Innervation imaging with radioiodinated meta-iodobenzylguanidine (I-123 MIBG) is the most widely used imaging technique to evaluate sympathetic nerve activity in cardiac diseases. The resemblance of MIBG to norepinephrine with respect to the molecular structure, synaptic uptake and intracellular storage makes it a suitable tracer to study sympathetic nervous activity.¹⁻⁴ In general, the in-vivo visualization of cardiac innervation is evaluated on planar anterior images, which are acquired early and 3 to 5 hours after tracer injection. For quantification, myocardial and mediastinal regions of interest (ROIs) are drawn on anterior planar images, of which mediastinal ROI is thought to represent the non-specific I-123 MIBG uptake in soft tissue.⁵ Information on the distribution of neurons and function of the (re-)uptake-1 pathway is provided by the heart-to-mediastinum (HM) ratio, while the washout rate (WOR) provides information on the sympathetic drive. Both indices are commonly applied in I-123 MIBG imaging, and the inter- and intraobserver variability of the HM ratio are considered low.^{6,7}

Though planar imaging is widely used, quantification based on these acquisitions has important limitations. Precise quantification of myocardial counts is often complicated due to superimposition of adjacent organs onto the cardiac region. Furthermore, planar images do not contain three-dimensional information, making it difficult to assess regional innervation abnormalities.^{8,9} Single photon emission computer tomography (SPECT) is known to overcome these problems. Still, the quantification of global cardiac innervation using SPECT is less established than planar I-123 MIBG imaging.

At present, SPECT imaging is considered informative in diseases like ischemic heart disease, ventricular arrhythmias and diabetes mellitus, where the cardiac innervation is affected in a heterogeneous manner.⁹ Consequently, this technique is increasingly used to assess the regional I-123 MIBG uptake.^{6,8,10-13} Using SPECT, it is possible to distinguish between myocardial wall, left ventricular lumen and surrounding organs. The ability to precisely localize these organs may suggest that SPECT acquisitions are also more suitable for the quantification of global innervation. To explore this hypothesis we applied a simple volumetric quantification method on cardiac I-123 MIBG SPECT acquisitions. Global uptake in the heart, myocardial wall, ventricular lumen and surrounding organs were determined in clinical patient groups. Based on this data we studied reproducibility of SPECT segmentation, the effect of extra cardiac I-123 MIBG uptake and the relation between SPECT or the conventional planar indices.

TABLE 1. POPULATION CHARACTERISTICS

	ICD (n=28)	NDD (n=11)	RCT (n=15)	p-value †
Age (years)	70 ± 6.1	64 ± 12.9	50 ± 10.0	<0.001
Gender (% male)	20 (71%)	10 (91%)	0	<0.001
Relevant medical history				
Autonomic dysfunction	0	9 (81%)	0	<0.001
Hypokinesia /rigidity	0	5 (45%)	1 (7%)	<0.001
Diabetes Mellitus	3 (11%)	2 (18%)	1 (7%)	0.650
Hypertension	12 (43%)	0	2 (13%)	0.010
Proven CAD	13 (46%)	1 (9%)	0	<0.001
Infarction	17 (61%)	0	0	<0.001
Heart failure	28 (100%)	0	0	<0.001
Ventricular arrhythmia	18 (64%)	0	1 (7%)	<0.001
(biventricular) ICD	6 (21%)	0	0	<0.001
Radio/chemotherapy	0	0	15 (100%)	<0.001

† Chi-square or ANOVA tests of the difference in distribution of various factors. CAD, coronary artery disease; ICD Implantable cardiac device.

MATERIALS AND METHODS

Patient population

The included population consisted of patients referred for I-123 MIBG acquisition prior to placement of a (biventricular) cardiac device (ICD) (group ICD, $n = 28$), to distinguish between neurodegenerative diseases (group NDD, $n = 11$), or after radiotherapy-chemotherapy (group RCT, $n = 15$). Since these groups all contain clinical patients, none of them can be considered a normal reference population. Still, the selection of these three populations ensures the inclusion of patients with a low cardiac I-123 MIBG uptake and a relatively normal I-123 MIBG uptake. All patients were referred for both planar and SPECT acquisitions in the period from November 2008 to March 2011 as part of their clinical work-up. Characteristics of the patient populations are provided in Table 1.

I-123 MIBG acquisition protocol

Patients were instructed to abstain from medication that could influence I-123 MIBG distribution (mainly antihypertensive drugs and tricyclic-antidepressants).⁵ Prior to I-123

MIBG administration patients underwent thyroid blocking by NaI droplets or KI capsules to prevent thyroid uptake of free radioiodine. An average dose of 185 MBq I-123 MIBG was slowly infused in 2 to 3 minutes. Anterior planar and SPECT images were obtained approximately 15 minutes (early) and 4 hours (delayed) after the injection. Anterior planar images were acquired using a dual-detector gamma camera (Toshiba, CGA 7200, Tokyo, Japan) equipped with a low energy high resolution collimator (energy range up to 170keV). Images were collected for 10 minutes with a 20% energy window centred on the 159 keV photo peak. The SPECT images were acquired with similar camera settings over 180 degrees from right anterior oblique to left posterior oblique. Projections were made every 4 degrees at 35 seconds per angle using a 128 x 128 matrix (zoom factor 1.5). SPECT data was reconstructed by ordered subset expectation maximization with 2 iterations and 10 subsets using a Gaussian post-processing filter (FWHM = 15mm). No other filter or attenuation correction was applied.

Planar image analysis

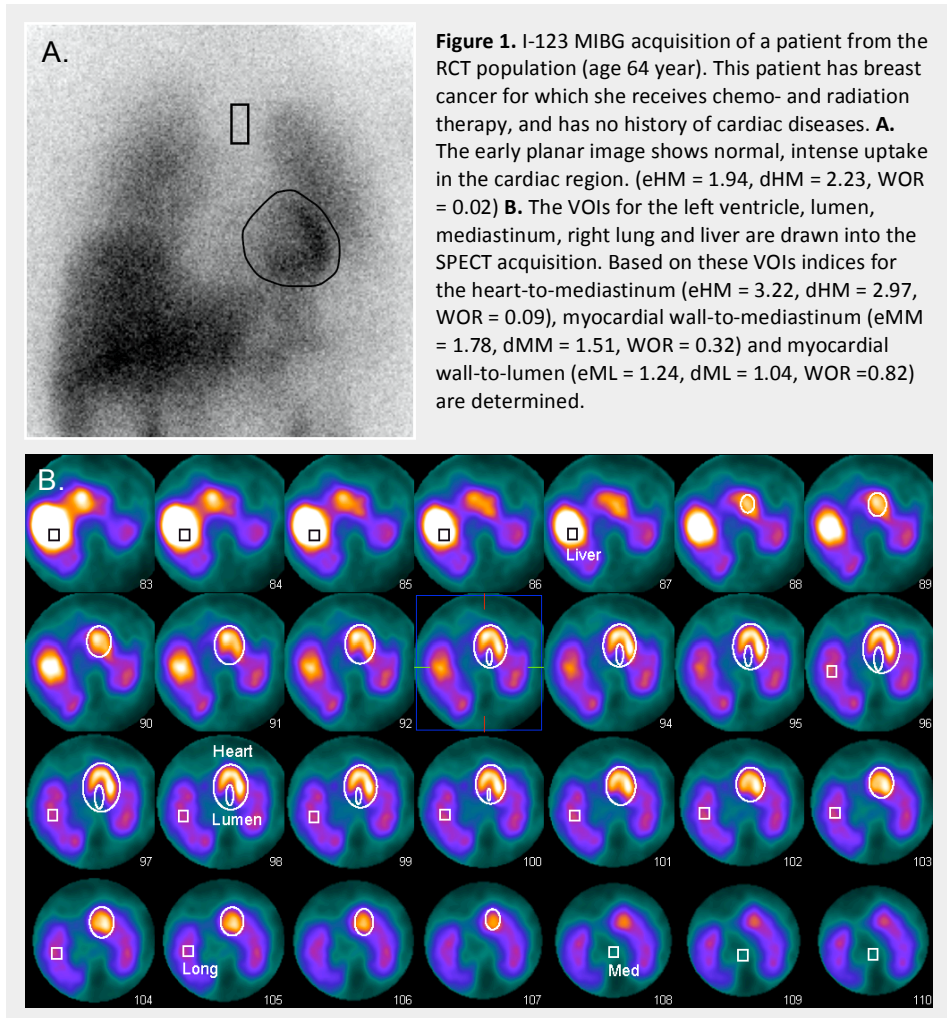
On the early and late images ROIs were defined by an experienced nuclear medicine technologist. The heart ROI was manually drawn to follow the external contours of the heart, thus including the myocardium and the left ventricular lumen. The apices of the lung and the mid-mediastinal line were used as anatomical landmarks for placement of a rectangular mediastinal ROI. The mean counts per pixel were determined in the early (e) and delayed (d) acquisitions for each ROI and corrected for decay. The early and delayed HM ratios were calculated as follows;

$$HM_{early} = \frac{eH}{eM} \qquad HM_{delayed} = \frac{dH}{dM}$$

According to the proposal for cardiac I-123 MIBG guidelines⁵, WOR is defined as;

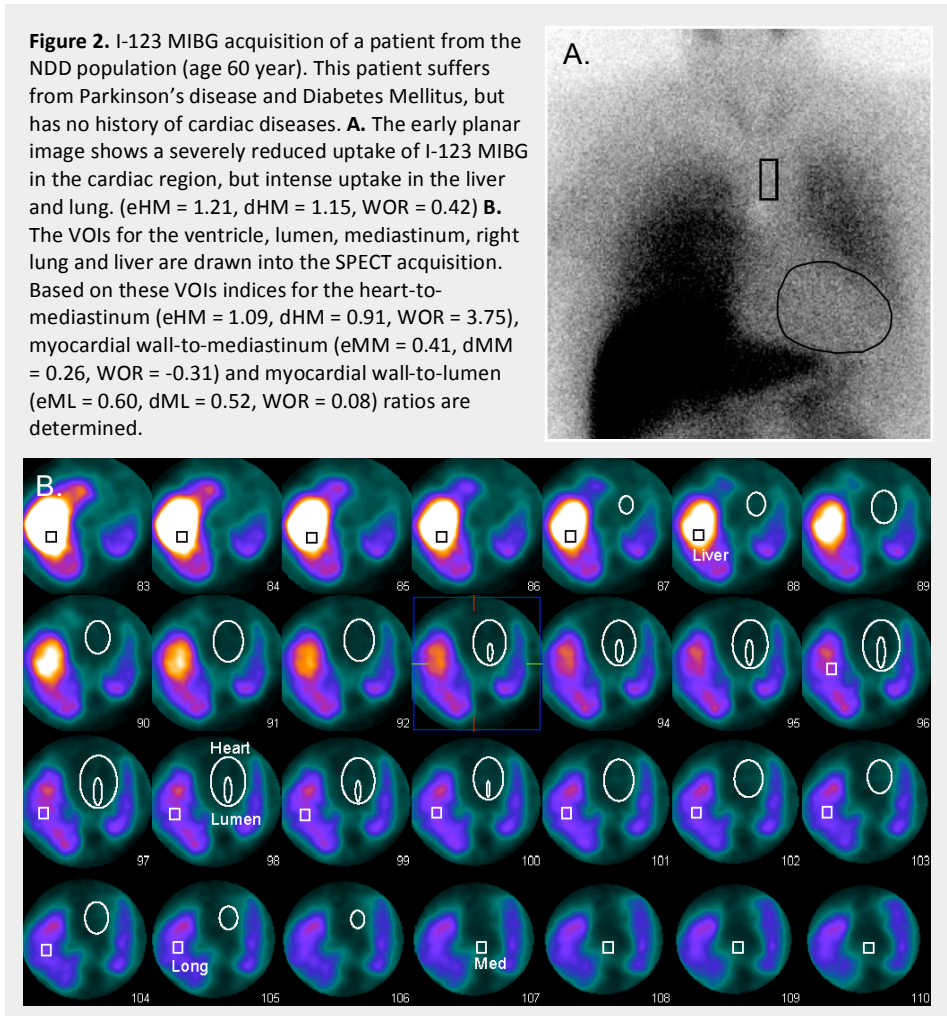
$$WOR = \frac{(eH - eM) - \left(\frac{dH}{0.5^{time/T}} - \frac{dM}{0.5^{time/T}} \right)}{(eH - eM)}$$

With, $time$ indicating the difference between the early and delayed acquisition, and T describing the physical decay of I-123. The factor $0.5^{time/T}$ in the denominator of the delayed part of this formula is used to account for the I-123 decay between the early and delayed acquisition.



SPECT image analysis

SPECT image analysis was performed on a Syngo-MI workstation (Siemens Medical Solutions, USA). In a mid-ventricular short axis (SA) view an ellipsoid was placed to contain the entire heart. In the horizontal-long axis (HLA) and vertical-long axis (VLA) views the placement of this ellipsoid was evaluated and adjusted when needed to enclose the base and apex. A second ellipsoid was positioned to contain the left ventricular lumen. (Figure 1 and Figure 2) Based on this information, three-dimensional volumes of interest (VOIs) are automatically created for the heart and lumen. The



activity in the myocardial wall was defined as 'left ventricular counts minus lumen counts'. A box shaped mediastinal VOI was placed conform the planar methodology. Uptake ratios and WOR were determined by applying the aforementioned formulas to three VOI combinations; heart-to-mediastinum, myocardial wall-to-mediastinum and myocardial wall-to-lumen regions. These values were compared to the planar indices to determine the discriminatory value of the SPECT indices in the patient populations.

The quantitative values determined on planar images are prone to count changes in the adjacent organs. To study the effects of I-123 MIBG uptake in adjacent organs in SPECT quantification, box-shaped VOIs were placed in centre of the liver and right lung. All

box-shaped VOIs were between 10-15 cm³. For each VOI the size, uptake and washout were determined. The organ-specific washout was defined as;

$$\text{washout} = \frac{e_{\text{Organ}} - \frac{d_{\text{Organ}}}{0.5^{\text{time}/T}}}{e_{\text{Organ}}}$$

Reliability is an important aspect when manual segmentation is performed to assess SPECT data. Therefore, all acquisitions were segmented twice by the same experienced observer to evaluate the test-retest variability. The second segmentation was performed two weeks after the first segmentation to reduce observer bias. The manual SPECT based segmentation was also performed by a second experienced observer to allow assessment of the inter-observer variability.

Statistical analysis

Statistical analyses were executed using the SPSS v16.0 software (SPSS inc. Chicago, USA). All continuous variables are expressed as 'mean ± standard deviation', and categorical data was expressed as frequencies and/or percentages. Continuous variables were assessed for their distribution with the Shapiro-Wilk Test.

Reliability can be described by a number of different statistical techniques. It is often considered a multi-factorial problem that is open to interpretation and is therefore assessed by multiple measures.¹⁴⁻¹⁶ In the present study test-retest and inter-observer reliability (i.e. reproducibility) were evaluated by the coefficient of variation (CV) and the intraclass correlation coefficient.

In addition to reproducibility of the segmentation factors like VOI size and I-123 MIBG uptake in surrounding organs may also influence quantification of counts within the heart. If a dependency exists between measured counts and either the size of the VOI or uptake in surrounding organs, the measurements are also considered less reliable. The relationship between VOI size and measured counts is determined by Pearson correlation coefficients (PCC). Stepwise multivariable regression analysis was used to determine the effects of I-123 MIBG uptake in the surrounding organs on the cardiac values. Regression analysis is described by the coefficient (*B*), standard error (*se*) and the total model fit (*R*²). The global SPECT uptake ratios and WORs were compared to the widely used planar indices. Correlations between the planar and SPECT values were expressed by Pearson correlation or Spearman's rank correlation, when appropriate.

RESULTS

Reproducibility of VOI size and count densities

In all acquisitions the segmentation was performed twice to assess the test-retest reliability. Size differences between the first and second segmentation were found for all VOIs, as could be expected. The reproducibility of the box-shaped VOI-size was considered relatively low (ICC ranging from -0.17 to 0.03 and CV ranging from 12.2 to 18.4%). In general, the elliptical cardiac VOIs (i.e. heart and lumen) had high ICC values indicating a good correlation, but also relatively high CV values suggesting high levels of variability between the segmentations. The size differences and the corresponding ICC or CV values are provided in Table 2a.

A low reproducibility of VOI size could result in poor reliability of the measured count densities. Nonetheless, the variability in count densities derived from the box-shaped VOIs was moderate, suggesting that the count densities obtained by the box-shaped VOI can be reliable. The cardiac VOIs provide highly reliable count densities in the test-retest evaluation (see Table 2b). The ICCs and CVs of the uptake ratios determined based on the three VOI combinations (heart-to-mediastinum, myocardial wall-to-mediastinum and myocardial wall-to-lumen) are provided in Table 2c. The inter-observer variability of the count densities for the cardiac VOIs was also considered low, as can be seen in Table 3. Both the CV and ICC suggest a high degree of consistency in the values produced by the two raters. The variation among the uptake ratios is higher, as was also demonstrated in the test-rest analysis.

When the total population is subdivided into the three patient groups, the test-retest ICC for the heart counts is 0.99 for each of the groups, and the ICC for the ventricular counts VOI ranges from 0.90 to 0.98. The inter-rater ICC for the heart counts ranges from 0.97 to 0.99 and for the ventricular lumen from 0.88 to 0.99. So, both in the affected and near normal populations SPECT segmentation of the heart can be considered reproducible.

The effect of VOI size on count densities

The results of the test-retest analysis already suggest that there is no clear relationship between the VOI size and the count densities. Mean VOI sizes for all measurements are provided in Table 2a. When assessing the correlation between size and counts in all segmentations, no significant correlations were found in both early and delayed SPECT

TABLE 2A. TEST-RETEST REPRODUCIBILITY OF VOI SIZE

		Mean	Difference †	CV	ICC	95% CI
Early	Liver	13.1 ± 1.3	2.52 ± 1.6	13.7	-0.14	-0.40 – 0.14
	Lung	13.0 ± 1.3	2.32 ± 1.5	12.5	-0.09	-0.36 – 0.19
	Mediastinum	12.7 ± 1.5	2.32 ± 1.7	18.4	0.00	-0.27 – 0.28
	Heart	522.0 ± 237.5	77.2 ± 76.0	10.5	0.90	0.84 – 0.94
	Lumen	10.4 ± 6.9	4.38 ± 4.7	29.8	0.65	0.46 – 0.78
Delayed	Liver	13.2 ± 1.3	2.27 ± 1.7	12.2	-0.13	-0.39 – 0.15
	Lung	13.3 ± 1.3	2.58 ± 1.8	13.7	-0.17	-0.43 – 0.11
	Mediastinum	12.7 ± 1.5	2.39 ± 1.8	13.3	0.03	-0.25 – 0.29
	Heart	519.0 ± 232.2	83.3 ± 107.1	11.5	0.84	0.75 – 0.91
	Lumen	10.4 ± 6.9	4.03 ± 4.4	27.6	0.70	0.52 – 0.81

TABLE 2B. TEST-RETEST REPRODUCIBILITY OF COUNT DENSITIES

		Mean	Difference †	CV	ICC	95% CI
Early	Liver	28.0 ± 7.7	4.14 ± 3.6	10.4	0.79	0.63 – 0.87
	Lung	12.8 ± 3.6	0.94 ± 0.9	5.2	0.93	0.88 – 0.96
	Mediastinum	4.8 ± 1.3	1.25 ± 1.0	18.4	0.47	0.20 – 0.66
	Heart	9.3 ± 3.6	0.20 ± 0.2	1.5	0.99	0.99 – 1.00
	Lumen	5.0 ± 1.7	0.33 ± 0.3	4.7	0.96	0.93 – 0.98
Delayed	Liver	26.6 ± 9.0	3.03 ± 2.5	8.1	0.91	0.81 – 0.95
	Lung	10.5 ± 3.0	0.69 ± 0.6	4.6	0.95	0.91 – 0.97
	Mediastinum	4.1 ± 1.0	0.50 ± 0.4	8.7	0.84	0.72 – 0.90
	Heart	8.2 ± 4.4	0.23 ± 0.2	1.9	0.99	0.99 – 1.0
	Lumen	4.4 ± 2.2	0.34 ± 0.3	5.4	0.97	0.95 – 0.99

TABLE 2C. TEST-RETEST REPRODUCIBILITY OF UPTAKE RATIOS

		Mean	Difference †	CV	ICC	95% CI
Early	HM ratio	1.92 ± 0.4	0.48 ± 0.3	17.8	0.37	0.09 – 0.59
	MM ratio	0.86 ± 0.3	0.25 ± 0.2	20.1	0.57	0.23 – 0.77
	ML ratio	0.82 ± 0.2	0.13 ± 0.2	11.2	0.60	0.37 – 0.75
Delayed	HM ratio	1.98 ± 0.7	0.26 ± 0.2	9.4	0.90	0.82 – 0.95
	MM ratio	0.89 ± 0.4	0.15 ± 0.1	12.0	0.89	0.81 – 0.93
	ML ratio	0.81 ± 0.2	0.14 ± 0.1	12.5	0.61	0.40 – 0.76

† One sample T-test of the **absolute** differences between the two measurements, all differences were $p < 0.001$.

TABLE 3. INTER-RATER REPRODUCIBILITY

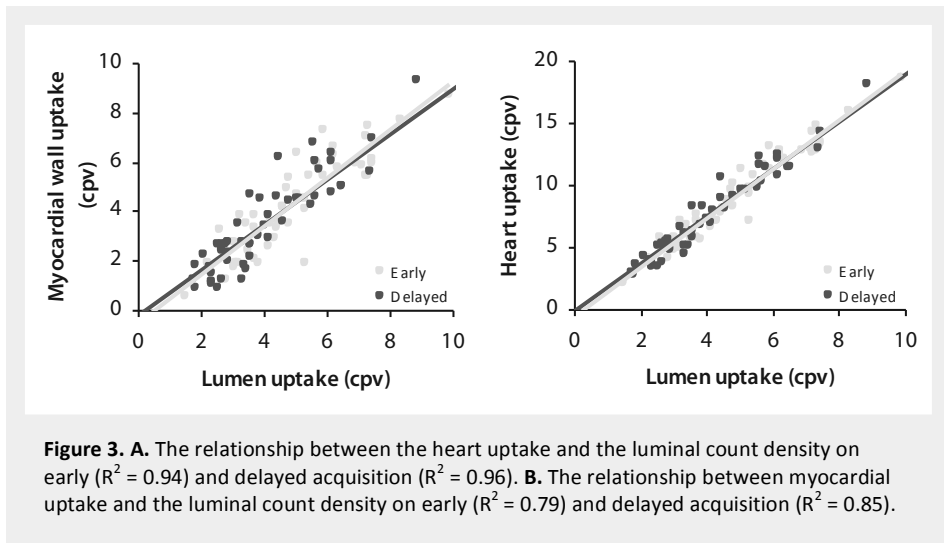
		Mean	Difference †	CV	ICC	95% CI
Early	Mediastinum	4.2 ± 0.9	0.73 ± 0.5	12.2	0.63	0.25 – 0.81
	Heart	9.1 ± 3.5	0.35 ± 0.3	2.7	0.99	0.98 – 1.00
	Lumen	4.8 ± 1.7	0.46 ± 0.3	6.7	0.94	0.89 – 0.97
	HM ratio	2.17 ± 0.6	0.34 ± 0.3	11.0	0.80	0.57 – 0.90
	MM ratio	1.01 ± 0.4	0.20 ± 0.2	14.0	0.77	0.58 – 0.87
	ML ratio	0.87 ± 0.3	0.19 ± 0.1	14.9	0.52	0.29 – 0.69
Delayed	Mediastinum	3.9 ± 1.0	0.42 ± 0.3	13.4	0.66	0.30 – 0.82
	Heart	8.1 ± 4.3	0.21 ± 0.2	1.8	0.99	0.99 – 1.00
	Lumen	4.4 ± 2.2	0.74 ± 0.6	6.8	0.97	0.94 – 0.98
	HM ratio	2.08 ± 0.9	0.43 ± 0.5	14.6	0.75	0.52 – 0.87
	MM ratio	0.95 ± 0.5	0.23 ± 0.3	17.2	0.74	0.56 – 0.84
	ML ratio	0.84 ± 0.2	0.20 ± 0.2	17.3	0.51	0.28 – 0.69

† One sample T-test of the **absolute** differences between the two measurements, all differences were $p < 0.001$.

TABLE 4. RELATION BETWEEN PLANAR AND SPECT INDICES

		Correlations †		Mean values for clinical populations ‡			
		PCC [†]	p-value	ICD	NDD	RCT	p-value
Early	Planar HM	-		1.53 ± 0.3	1.44 ± 0.3	1.71 ± 0.2	0.024
	SPECT HM	0.795	<0.001	1.95 ± 0.5	1.70 ± 0.8	2.52 ± 0.3	0.001
	SPECT MM	0.771	<0.001	0.91 ± 0.3	0.73 ± 0.5	1.20 ± 0.2	0.006
	SPECT ML	0.578	<0.001	0.87 ± 0.2	0.69 ± 0.3	0.93 ± 0.2	0.011
Delayed	Planar HM	-		1.40 ± 0.2	1.38 ± 0.4	1.75 ± 0.2	<0.001
	SPECT HM	0.851	<0.001	1.69 ± 0.6	1.63 ± 1.1	2.54 ± 0.3	<0.001
	SPECT MM	0.842	<0.001	0.79 ± 0.3	0.71 ± 0.5	1.22 ± 0.2	0.001
	SPECT ML	0.497	<0.001	0.85 ± 0.2	0.74 ± 0.3	0.92 ± 0.2	0.139
Washout	Planar HM	-		0.49 ± 0.38	0.48 ± 0.35	0.15 ± 0.13	<0.001
	SPECT HM	0.706	<0.001	0.41 ± 0.65	0.97 ± 1.32	0.04 ± 0.32	0.002
	SPECT MM	0.359	0.010	-0.71 ± 2.47	0.10 ± 0.56	1.38 ± 4.30	0.044
	SPECT ML	-0.145	0.315	0.18 ± 2.06	-0.65 ± 1.90	1.56 ± 2.40	0.163

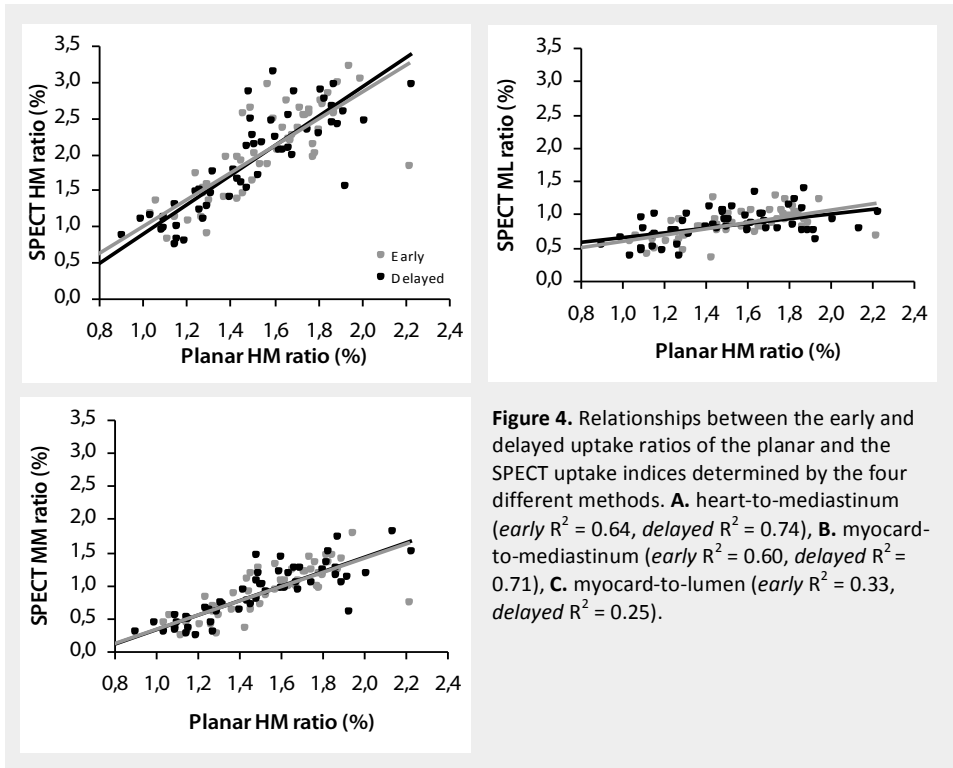
† Pearson correlation analysis or Spearman's rank correlation between the planar and the SPECT for uptake and washout indices. ‡ Anova or Kruskal-Wallis analysis to determine the difference between the mean values. HM, heart-to-mediastinum ratio; MM, myocardial wall-to-mediastinum ratio; ML, myocardial wall-to-lumen ratio



for liver (*early* PCC 0.179, p -value = 0.066; *delayed* PCC -0.015, p -value = 0.876), long (*early* PCC 0.131, p -value = 0.182; *delayed* PCC 0.155, p -value = 0.112), heart (*early* PCC -0.123, p -value = 0.209; *delayed* PCC -0.143, p -value = 0.144) and mediastinal VOIs (*early* PCC 0.030, p -value = 0.759; *delayed* PCC -0.063, p -value = 0.524). Only for the lumen VOI moderate correlations were found in both early and delayed segmentations (*early* PCC -0.344, p -value < 0.001; *delayed* PCC -0.227, p -value = 0.020) suggesting a relationship between VOI size and measured counts.

The effect of organ uptake on quantification

The effect of I-123 MIBG uptake in the surrounding organs was evaluated by multivariable regression analysis. The mediastinal uptake was an independent predictor of uptake within the entire heart (*early* $B = 2.06$, $se = 0.38$, $R^2 = 0.36$; *delayed* $B = 2.74$, $se = 0.448$, $R^2 = 0.43$) and in the myocardial wall (*early* $B = 0.96$, $se = 0.22$, $R^2 = 0.28$; *delayed* $B = 1.27$, $se = 0.248$, $R^2 = 0.37$). The lung washout was found to be an important explanatory variable of the organ washout in the entire heart ($B = 0.58$, $se = 0.10$, $R^2 = 0.38$) and the myocardial wall ($B = 0.69$, $se = 0.14$, $R^2 = 0.33$). For both cardiac uptake and washout, changes in liver uptake were not considered an important factor. The luminal count densities, although not included in the multivariate analysis, did show a strong relation to the uptake and washout in the heart or myocardial wall (Figure 3).



Relationship between planar and SPECT indices

The values for the planar and SPECT indices for the three different populations are provided in Table 4, as are the correlation between the SPECT and planar indices. Especially the cardiac uptake ratios determined based on the SPECT data had a good correlation with the planar uptake values, as can be seen in Figure 4. The method using the myocard-to-lumen ratio had the lowest regression coefficients, whereas the heart-to-mediastinum and myocardial wall-to-mediastinum had a moderate, to good relationship with the planar indices. Using these latter two methods, it was also possible to discriminate between the three clinical patient populations (see Table 4).

DISCUSSION

In this study a simple volumetric based segmentation of I-123 MIBG SPECT data was introduced to determine global uptake and washout in the entire heart and myocardial

wall. Both the test-retest and the inter-observer reproducibility of the measured count densities were high, despite the low reproducibility of the VOI sizes. In both the affected and near normal populations SPECT segmentation of the heart can be performed and was found to be reproducible. The correlations between the widely used planar and SPECT indices was high for the uptake ratios determined based on the heart-to-mediastinum and myocardial wall-to-mediastinum regions. The differences between the three clinical patient populations were most profound when using the heart-to-mediastinum SPECT indices, which may suggest that this method has the best discriminatory value.

Effects of extra cardiac I-123 MIBG uptake

The extent to which external factors influence a measurement can be just as important for the clinical value of a technique as the reproducibility or the discriminatory value. Verberne et al.¹⁷ demonstrated that cardiac organ washout on planar images can be explained by a model containing mediastinum and lung washout. This implies that changes in myocardial count densities overtime are, to some extent, related to count changes in the surrounding organs.

Since cardiac segmentation can be performed more precisely on SPECT images due to the three-dimensional information content, it was anticipated that cardiac count densities determined on SPECT images were less prone to influences from surrounding organs. The results of the current study suggest that mediastinal uptake was an important explanatory variable of cardiac uptake on both early and delayed images. Lung washout, on the other hand, was an independent predictor of the cardiac washout. Even though, the inclusion of mediastinal and lung counts into the cardiac VOI is limited when applying SPECT segmentation; these count densities do seem to correlate with the cardiac uptake and washout measures. Whether these effects are caused by technical problems in the segmentation, or reflect a true relation in the innervation processes within these organs remains unclear.

Liver uptake or washout had a smaller impact on quantification of cardiac counts, as was shown by both the study of Verberne et al.¹⁷ and our study. Still, it is described that liver uptake has to be reckoned with when visually assessing I-123 MIBG SPECT images.^{13,18} Most often, uptake in the liver causes areas of reduced myocardial count densities, especially in inferior wall. In severe cases, the liver will superimpose on the myocardial wall making the entire inferior wall non-assessable.

Lumen, myocardial wall or entire left ventricle

In advance, it was hypothesized that SPECT imaging could be more suitable for global quantification as it is feasible to distinguish between myocardial wall, lumen and surrounding organs. When using separate VOIs to describe the myocardial wall and lumen, it is possible to use the lumen-counts as non-specific uptake measure that can be calibrated using a blood sample. This methodology was previously described by Somsen et al.¹⁹. Their study concluded that this is an accurate method to assess MIBG uptake.

The results of our study (Figure 3) demonstrate a strong positive relationship between the cardiac and lumen count densities. This correlation is most likely the result of the spillover-effect from the myocardial wall, and probably does not reflect a true relation between myocardial counts and the non-specific I-123 MIBG uptake. Additionally, the gathered experience suggests that lumen VOIs are more difficult to position than heart VOIs, especially in patients with small heart sizes or severely reduced cardiac uptake. These observations are supported by the reproducibility analysis, in which variability of lumen counts is higher than the variability of cardiac counts. Furthermore, a moderate correlation between the VOI size and count densities was found for the lumen, suggesting that lumen counts are partly dependent on VOI size. All these findings suggest that lumen-based quantification of non-specific uptake may be less reliable, than for instance the mediastinal counts. Additionally, a recent study demonstrated in planar images that cardiac and mediastinal count densities are unrelated to changes in vascular I-123 MIBG activity, making a blood pool correction somewhat redundant.²⁰

Uptake ratios as well as washout determined by the myocardial wall-to-mediastinum or heart-to-mediastinum regions showed a good relationship with the planar indices (Figure 4). The measurements based on the heart-to-mediastinum regions were considered to be more reproducible than the myocardial wall-to-mediastinum measures, and had a better discriminatory value. Still, more research has to be performed to establish the clinical value of both of these SPECT based quantification methods.

Other methods to assess innervation based on SPECT data

The majority of the studies visually score cardiac uptake based on either the standard tomographic cardiac views or a polarmap display.^{6,8,10-13,22-24} Automated evaluation, or comparisons to a normal database, are possible when polarmaps are used. All these methods rely on the principle that segmental uptake is scaled to the maximum counts

within the heart. However, I-123 MIBG uptake can be abnormal throughout the entire myocardium creating a false representation of the uptake. Additionally, discrepancies in delineation or orientation between early and delayed images can result in an erroneous washout. So, it is important to relate visual scoring to the count-based indices such as the HM ratio.⁵ At present, there are only a few studies that describe count-based indices derived from I-123 MIBG SPECT data. Druschky et al.²¹ placed thirty-three small square ROIs in six short axis slices to assess global and regional myocardial uptake. Results were expressed as percentage of the maximum ROI, and were used to calculate an inhomogeneity index. Since counts in each ROI are scaled to the maximum uptake, one expects that the scaling problem can arise in patients with overall reduced I-123 MIBG uptake. However, the idea of an inhomogeneity index is probably more suitable to described I-123 MIBG abnormalities in SPECT, because there is no need to scale the data. Somsen et al.¹⁹ used single- and multi-slice SPECT data in which cardiac counts were related to either lumen or organ uptake. Their findings indicate that the single-slice SPECT method had a poor reproducibility, making it less suitable for global quantification. The multi-slice method, in which the entire cardiac volume is segmented, had a high reproducibility with CVs of less than 5%. The results found for the multi-slice method are comparable to the results found in our study.

Clinical application of I-123 MIBG SPECT

The regional assessment of cardiac innervation using SPECT is less established than planar I-123 MIBG imaging. In general, SPECT imaging is advisable in diseases where cardiac innervation is affected in a heterogeneous manner. There are, at present, a few clinical indications described for SPECT imaging which include ischemic heart disease, ventricular arrhythmias and diabetes mellitus.⁹

The areas of sympathetic denervation often exceed beyond that of the perfusion defects, because sympathetic neurons are considered to be more sensitive to ischemic events than cardiac myocytes. Furthermore, it is thought that chronic repetitive ischemia may induce long term sympathetic nerve dysfunction.²⁵ These mechanisms also ensure that in the early stages of coronary artery disease or during frequent vasospastic events, sympathetic neurons can be affected without the presence of obvious perfusion defects.^{11,22,26} This heterogenic cardiac sympathetic innervation, in otherwise viable myocardium, is thought to be the source of electrical instability which is associated with the development of ventricular arrhythmias.^{12,27} The role of SPECT I-123 MIBG imaging

in ischemic heart disease and ventricular arrhythmias is therefore mainly focused on describing the regional sympathetic innervation status and detecting areas with perfusion/innervation mismatch.^{10,28} Cardiac autonomic neuropathy (CAN) in patients with diabetes mellitus, on the other hand, is associated with regional hyperactivity of the sympathetic nervous system, resulting in an electrical instability.^{8,29} It is recognized that planar I-123 MIBG imaging is useful to detect CAN and provide prognostic information on future cardiac events.³⁰⁻³² However, planar indices are less sensitive in detecting small regional abnormalities which are often associated with diabetic neuropathy. Therefore, it was suggested by Hattori et al.⁸ that I-123 MIBG SPECT imaging should be used to detect CAN. Still, the additive role of SPECT imaging in diabetes needs to be established.

Study limitations

In the present study a straightforward volumetric technique was introduced that is able to provide reproducible global I-123 MIBG parameters. The initial results indicate that it is possible to distinguish between different patient populations using these SPECT indices, and that these indices relate to the planar measures. Still, this study does not provide a validation of this quantitative method. Such a validation will require the comparison of the new SPECT-based method to a golden standard. At present, there are no measures that can serve as a true golden standard, only the prognosis of the patient can be used as such. The only other imaging technique that is able to directly assess cardiac sympathetic innervation is C-11 meta-hydroxyephedrine (HED) positron emission tomography (PET).³³ This technique is, however, only available in a limited number of centres and is not yet considered to be standard clinical practice. Accordingly, more research has to be performed to establish the value of I-123 MIBG SPECT imaging over planar imaging in specific patient populations.

CONCLUSION

By applying a simple volumetric segmentation method we were able to determine global uptake and washout in the heart or myocardial wall in all patients. In general I-123 MIBG SPECT quantification was found to be reproducible, reliable and had a moderate to good correlation with the planar indices. Still, the additive value of I-123 MIBG SPECT quantification over planar imaging has to be established in specific patient populations.

REFERENCE LIST

- (1) Carrio I. Cardiac neurotransmission imaging. *J Nucl Med.* 2001;42:1062-1076.
- (2) Ji SY, Travin MI. Radionuclide imaging of cardiac autonomic innervation. *J Nucl Cardiol.* 2010;17:655-666.
- (3) Henneman MM, Bengel FM, van der Wall EE, Knuuti J, Bax JJ. Cardiac neuronal imaging: application in the evaluation of cardiac disease. *J Nucl Cardiol.* 2008;15:442-455.
- (4) Yamashina S, Yamazaki J. Neuronal imaging using SPECT. *Eur J Nucl Med Mol Imaging.* 2007;34:939-950.
- (5) Flotats A, Carrio I, Agostini D et al. Proposal for standardization of 123I-metaiodobenzylguanidine (MIBG) cardiac sympathetic imaging by the EANM Cardiovascular Committee and the European Council of Nuclear Cardiology. *Eur J Nucl Med Mol Imaging.* 2010;37:1802-1812.
- (6) Somsen GA, Verberne HJ, Fleury E, Righetti A. Normal values and within-subject variability of cardiac I-123 MIBG scintigraphy in healthy individuals: implications for clinical studies. *J Nucl Cardiol.* 2004;11:126-133.
- (7) Muxi A, Paredes P, Navales I et al. Diagnostic cutoff points for (1)(2)(3)I-MIBG myocardial scintigraphy in a Caucasian population with Parkinson's disease. *Eur J Nucl Med Mol Imaging.* 2011;38:1139-1146.
- (8) Hattori N, Tamaki N, Hayashi T et al. Regional abnormality of iodine-123-MIBG in diabetic hearts. *J Nucl Med.* 1996;37:1985-1990.
- (9) Flotats A, Carrio I. Cardiac neurotransmission SPECT imaging. *J Nucl Cardiol.* 2004;11:587-602.
- (10) Boogers MJ, Borleffs CJ, Henneman MM et al. Cardiac sympathetic denervation assessed with 123-iodine metaiodobenzylguanidine imaging predicts ventricular arrhythmias in implantable cardioverter-defibrillator patients. *J Am Coll Cardiol.* 2010;55:2769-2777.
- (11) Matsunari I, Aoki H, Nomura Y et al. Iodine-123 metaiodobenzylguanidine imaging and carbon-11 hydroxyephedrine positron emission tomography compared in patients with left ventricular dysfunction. *Circ Cardiovasc Imaging.* 2010;3:595-603.
- (12) Simoes MV, Barthel P, Matsunari I et al. Presence of sympathetically denervated but viable myocardium and its electrophysiologic correlates after early revascularised, acute myocardial infarction. *Eur Heart J.* 2004;25:551-557.
- (13) Tsuchimochi S, Tamaki N, Tadamura E et al. Age and gender differences in normal myocardial adrenergic neuronal function evaluated by iodine-123-MIBG imaging. *J Nucl Med.* 1995;36:969-974.
- (14) Chinn S. Statistics in respiratory medicine. 2. Repeatability and method comparison. *Thorax.* 1991;46:454-456.

- (15) Bruton A, Conway JH, Holgate ST. Reliability: What is it, and how is it measured? *Physiotherapy*. 2000;86:94-99.
- (16) McGraw KO, Wong SP. Forming inferences about some intraclass correlation coefficients. *Psychological methods*. 1996;1:30-46.
- (17) Verberne HJ, Somsen GA, Povinec P, van Eck-Smit BL, Jacobson AF. Impact of mediastinal, liver and lung (123)I-metaiodobenzylguanidine ((123)I-MIBG) washout on calculated (123)I-MIBG myocardial washout. *Eur J Nucl Med Mol Imaging*. 2009;36:1322-1328.
- (18) Gill JS, Hunter GJ, Gane G, Camm AJ. Heterogeneity of the human myocardial sympathetic innervation: in vivo demonstration by iodine 123-labeled meta-iodobenzylguanidine scintigraphy. *Am Heart J*. 1993;126:390-398.
- (19) Somsen GA, Borm JJ, de Milliano PA, van VB, Dubois EA, van Royen EA. Quantitation of myocardial iodine-123 MIBG uptake in SPET studies: a new approach using the left ventricular cavity and a blood sample as a reference. *Eur J Nucl Med*. 1995;22:1149-1154.
- (20) Verberne HJ, Verschure DO, Somsen GA, van Eck-Smit BL, Jacobson AF. Vascular time-activity variation in patients undergoing (123)I-MIBG myocardial scintigraphy: implications for quantification of cardiac and mediastinal uptake. *Eur J Nucl Med Mol Imaging*. 2011;38:1132-1138.
- (21) Druschky A, Hilz MJ, Platsch G et al. Differentiation of Parkinson's disease and multiple system atrophy in early disease stages by means of I-123-MIBG-SPECT. *J Neurol Sci*. 2000;175:3-12.
- (22) Simula S, Vanninen E, Viitanen L et al. Cardiac adrenergic innervation is affected in asymptomatic subjects with very early stage of coronary artery disease. *J Nucl Med*. 2002;43:1-7.
- (23) Wakabayashi T, Nakata T, Hashimoto A et al. Assessment of underlying etiology and cardiac sympathetic innervation to identify patients at high risk of cardiac death. *J Nucl Med*. 2001;42:1757-1767.
- (24) Yukinaka M, Nomura M, Ito S, Nakaya Y. Mismatch between myocardial accumulation of 123I-MIBG and 99mTc-MIBI and late ventricular potentials in patients after myocardial infarction: association with the development of ventricular arrhythmias. *Am Heart J*. 1998;136:859-867.
- (25) Fallavollita JA, Canty JM, Jr. Dysinnervated but viable myocardium in ischemic heart disease. *J Nucl Cardiol*. 2010;17:1107-1115.
- (26) Sakata K, Iida K, Kudo M, Yoshida H, Doi O. Prognostic value of I-123 metaiodobenzylguanidine imaging in vasospastic angina without significant coronary stenosis. *Circ J*. 2005;69:171-176.
- (27) Chen LS, Zhou S, Fishbein MC, Chen PS. New perspectives on the role of autonomic nervous system in the genesis of arrhythmias. *J Cardiovasc Electrophysiol*. 2007;18:123-127.

- (28) Nishisato K, Hashimoto A, Nakata T et al. Impaired cardiac sympathetic innervation and myocardial perfusion are related to lethal arrhythmia: quantification of cardiac tracers in patients with ICDs. *J Nucl Med*. 2010;51:1241-1249.
- (29) Stevens MJ, Raffel DM, Allman KC et al. Cardiac sympathetic dysinnervation in diabetes: implications for enhanced cardiovascular risk. *Circulation*. 1998;98:961-968.
- (30) Nagamachi S, Fujita S, Nishii R et al. Prognostic value of cardiac I-123 metaiodobenzylguanidine imaging in patients with non-insulin-dependent diabetes mellitus. *J Nucl Cardiol*. 2006;13:34-42.
- (31) Scholte AJ, Schuijf JD, Delgado V et al. Cardiac autonomic neuropathy in patients with diabetes and no symptoms of coronary artery disease: comparison of 123I-metaiodobenzylguanidine myocardial scintigraphy and heart rate variability. *Eur J Nucl Med Mol Imaging*. 2010;37:1698-1705.
- (32) Vinik AI, Ziegler D. Diabetic cardiovascular autonomic neuropathy. *Circulation*. 2007;115:387-397.
- (33) Bengel FM, Schwaiger M. Assessment of cardiac sympathetic neuronal function using PET imaging. *J Nucl Cardiol*. 2004;11:603-616.

Chapter 8

Summary and conclusions

GENERAL SUMMARY

Early diagnosis and risk stratification of ischemic heart diseases by non-invasive imaging techniques are nowadays the main focus of cardiovascular medicine. Nuclear imaging, and myocardial perfusion scintigraphy in particular, have a well established role in diagnosing and evaluating ischemic heart diseases.¹⁻³ Although evaluation of myocardial perfusion will remain the mainstay, developments over the last decades have shifted the field of nuclear cardiology beyond visual assessment of perfusion.⁴ *Chapter 1* of this thesis provides an overview of the evolution of the clinical single photon emission computed tomography (SPECT) based quantitative nuclear cardiology. Extensive research over the last years has led to new developments in the quantification of perfusion, function and innervation. At present some ambiguities in SPECT-based quantification still remain, which form the focus of this thesis. In Part 1, new aspects of perfusion and function quantification based on MPS are discussed, and Part 2 focuses on the quantification of sympathetic innervation in both planar and SPECT acquisitions.

Part I – Myocardial Perfusion Scintigraphy

Quantification has proven to be an objective method to stratify patients and communicate findings. Several studies underline the added value of this quantitative functional analysis; however, the value of these measures depends on the accuracy of the parameter estimates.⁴⁻⁸ The relationship between functional indices and the software self is an important issue, which is addressed in *Chapter 2*. In this study two widely used commercially available software systems were compared with respect to linearity and parameter outcomes.^{9,10} A Bland-Altman study indicates that, although the correlations between the systems are very good, the parameter values are software dependent. The found discrepancies are clinically relevant, depend on the heart size and could be related to the underlying algorithms of the two software systems.

A second factor that is known to influence the visual evaluation of MPS is image quality itself.¹¹ Extracardiac tracer accumulation in the hepatobiliary system can directly influence the evaluation of the perfusion patterns in the myocardium. As excretion and accumulation of the Tc-99m labelled perfusion tracers in the hepatobiliary system changes over time, the image quality may also be time dependent.¹²⁻¹⁴ In *Chapter 3* the effects of early (15 minutes post-injection) and late (50 minutes post-injection) imaging on the quantitative analysis is evaluated. The results indicate that in the majority of the

patients extracardiac accumulation is lower in the late acquisition, resulting in a better image quality. In the early acquisition, errors in the functional quantification were more frequently observed. The main reason for this inaccuracy was incorrect border segmentation due to extracardiac tracer uptake. Consequently, it is imperative to check the myocardial segmentation before the quantitative indices are interpreted.

New quantitative indices

Recent developments in the automated functional quantification of MPS have led to the introduction of a couple of new parameters. The *Transient Ischemic Dilatation* (TID) ratio was introduced as an important global indicator for severe coronary artery disease.¹⁵⁻¹⁷ Though several studies underline the relationship between TID and the degree of ischemia, there is no clear explanation for this abnormal post-stress dilatation of the ventricle. In *Chapter 4* the TID is related to various other functional MPS parameters to better understand the meaning of an abnormal TID. The outcomes of this study in part disagree with the current literature, as only a modest relation between TID and summed perfusion scores was found. The relationship between the TID and the heart rate during acquisition, on the other hand, was profound. These results indicate a dependency of the TID on the heart rate, which is also suggested by several case studies.¹⁷⁻²⁰

The *Ventricular Dyssynchrony* is another recently introduced parameter, which provides information on the contraction timing in ventricular segments.^{21,22} To quantify dyssynchrony in MPS data there are different algorithms available. One of these algorithms, the geometrical approach, was assessed in a feasibility study in *Chapter 5*. In all included patients with a normal MPS the dyssynchrony analysis was possible. No clear dependence of the dyssynchrony indices on the gender or method of stress induction was observed. Furthermore, it was possible to distinguish this normal population from a population with proven dyssynchrony. These results suggest that dyssynchrony analysis by the geometrical approach is feasible, though more research has to be preformed on the factors that might influence these estimates.

Part II – Myocardial Innervation Scintigraphy

At present, I-123 MIBG imaging is the most widely used scintigraphic technology to visualize the sympathetic nerve activity in the myocardium.²³⁻²⁵ Quantification of the planar or SPECT images is an important addition to the visual analysis. In general, quantification is performed on the anterior planar images; however, there is not yet

complete concordance on the acquisition protocols and quantification methods that are to be used.^{26,27} Therefore, *Chapter 6* provides a systematic evaluation of the methods that are used to assess planar I-123 MIBG images. Within the included manuscripts a great diversity was found in the acquisition protocols and quantification methods. Especially the washout rate (i.e. the change in I-123 MIBG accumulation over time) showed a large heterogeneity in calculation methods and normal values used in different studies. These findings clearly underline the need for protocol standardization.

SPECT imaging, although less frequently used for quantification, could be better suited for the assessment of sympathetic nerve activity due to its 3-dimensional nature.²⁸ In *Chapter 7* a simple volumetric quantification method for I-123 MIBG SPECT was introduced. Overall, volumetric segmentation was highly reproducible in various clinical I-123 MIBG images. Furthermore, a clear relationship between planar and SPECT indices was present, and using SPECT it was possible to distinguish between different populations. Still, the added clinical value of this volumetric SPECT quantification method has to be established in different patient populations.

CONCLUSION

The outcomes of this thesis underline the importance of understanding the impact of technical-, procedural- and patient-related factors on both the visual and quantitative evaluation of myocardial SPECT acquisitions. Based on the research described in this thesis the following conclusions can be drawn;

- Parameter estimates, and the factors that may influence quantification, are highly software dependent. Therefore, transitions between software systems can be clinically relevant and should always be evaluated.
- Transient ischemic dilatation is influenced by the heart rate during acquisition and is probably not suitable as independent indicator of severe coronary artery disease.
- The geometrical approach for assessing ventricular dyssynchrony in myocardial perfusion imaging using gated-SPECT is a feasible method.
- Great diversity is present in quantification methods to determine global I-123 MIBG parameters, which may limit the exchangeability and comparability of patient data and normal values.
- Volumetric quantification of I-123 MIBG SPECT can be a reliable method to assess global cardiac innervation status.

REFERENCE LIST

- (1) Clark AN, Beller GA. The present role of nuclear cardiology in clinical practice. *Q J Nucl Med Mol Imaging*. 2005;49:43-58.
- (2) Marcassa C, Bax JJ, Bengel F et al. Clinical value, cost-effectiveness, and safety of myocardial perfusion scintigraphy: a position statement. *Eur Heart J*. 2008;29:557-563.
- (3) Underwood SR, Anagnostopoulos C, Cerqueira M et al. Myocardial perfusion scintigraphy: the evidence. *Eur J Nucl Med Mol Imaging*. 2004;31:261-291.
- (4) Ficaro EP, Corbett JR. Advances in quantitative perfusion SPECT imaging. *J Nucl Cardiol*. 2004;11:62-70.
- (5) Petix NR, Sestini S, Coppola A et al. Prognostic value of combined perfusion and function by stress technetium-99m sestamibi gated SPECT myocardial perfusion imaging in patients with suspected or known coronary artery disease. *Am J Cardiol*. 2005;95:1351-1357.
- (6) Travin MI, Heller GV, Johnson LL et al. The prognostic value of ECG-gated SPECT imaging in patients undergoing stress Tc-99m sestamibi myocardial perfusion imaging. *J Nucl Cardiol*. 2004;11:253-262.
- (7) Xu Y, Hayes S, Ali I et al. Automatic and visual reproducibility of perfusion and function measures for myocardial perfusion SPECT. *J Nucl Cardiol*. 2010;17:1050-1057.
- (8) Abidov A, Germano G, Hachamovitch R, Berman DS. Gated SPECT in assessment of regional and global left ventricular function: major tool of modern nuclear imaging. *J Nucl Cardiol*. 2006;13:261-279.
- (9) Ficaro EP, Lee BC, Kritzman JN, Corbett JR. Corridor4DM: the Michigan method for quantitative nuclear cardiology. *J Nucl Cardiol*. 2007;14:455-465.
- (10) Germano G, Kavanagh PB, Slomka PJ, Van Kriekinge SD, Pollard G, Berman DS. Quantitation in gated perfusion SPECT imaging: the Cedars-Sinai approach. *J Nucl Cardiol*. 2007;14:433-454.
- (11) Ficaro EP, Corbett JR. Technical Considerations in Quantifying Myocardial Perfusion and Function. *Nuclear Cardiology: Technical Applications*. McGraw-Hill Medical; 2008.
- (12) Baggish AL, Boucher CA. Radiopharmaceutical agents for myocardial perfusion imaging. *Circulation*. 2008;118:1668-1674.
- (13) Heo J, Iskandrian AS. Technetium-labeled myocardial perfusion agents. *Cardiol Clin*. 1994;12:187-198.
- (14) Hambye AS, Delsarte P, Vervaet AM. Influence of the different biokinetics of sestamibi and tetrofosmin on the interpretation of myocardial perfusion imaging in daily practice. *Nucl Med Commun*. 2007;28:383-390.
- (15) Abidov A, Bax JJ, Hayes SW et al. Transient ischemic dilation ratio of the left ventricle is a significant predictor of future cardiac events in patients with otherwise normal myocardial perfusion SPECT. *J Am Coll Cardiol*. 2003;42:1818-1825.

- (16) Duarte PS, Smanio PE, Oliveira CA, Martins LR, Mastrocolla LE, Pereira JC. Clinical significance of transient left ventricular dilation assessed during myocardial Tc-99m sestamibi scintigraphy. *Arq Bras Cardiol.* 2003;81:474-482.
- (17) Hardebeck CJ. Transient ischemic dilation. *J Am Coll Cardiol.* 2004;44:211-212.
- (18) Choong KK, Russell PA. Transient left ventricular dilatation in the absence of epicardial disease on angiography. *Clin Nucl Med.* 2004;29:348-351.
- (19) Kirkpatrick ID, Leslie WD. Erroneous Left ventricular cavity size measurements on myocardial perfusion SPECT resulting from transient arrhythmias. *Clin Nucl Med.* 2005;30:783-786.
- (20) Robinson VJ, Corley JH, Marks DS et al. Causes of transient dilatation of the left ventricle during myocardial perfusion imaging. *AJR Am J Roentgenol.* 2000;174:1349-1352.
- (21) Bax JJ, Marwick TH, Molhoek SG et al. Left ventricular dyssynchrony predicts benefit of cardiac resynchronization therapy in patients with end-stage heart failure before pacemaker implantation. *Am J Cardiol.* 2003;92:1238-1240.
- (22) Boogers MM, Chen J, Bax JJ. Myocardial perfusion single photon emission computed tomography for the assessment of mechanical dyssynchrony. *Curr Opin Cardiol.* 2008;23:431-439.
- (23) Carrio I. Cardiac neurotransmission imaging. *J Nucl Med.* 2001;42:1062-1076.
- (24) Henneman MM, Bengel FM, van der Wall EE, Knuuti J, Bax JJ. Cardiac neuronal imaging: application in the evaluation of cardiac disease. *J Nucl Cardiol.* 2008;15:442-455.
- (25) Patel AD, Iskandrian AE. MIBG imaging. *J Nucl Cardiol.* 2002;9:75-94.
- (26) Flotats A, Carrio I, Agostini D et al. Proposal for standardization of 123I-metaiodobenzylguanidine (MIBG) cardiac sympathetic imaging by the EANM Cardiovascular Committee and the European Council of Nuclear Cardiology. *Eur J Nucl Med Mol Imaging.* 2010;37:1802-1812.
- (27) Verberne HJ, Habraken JB, van Eck-Smit BL, Agostini D, Jacobson AF. Variations in 123I-metaiodobenzylguanidine (MIBG) late heart mediastinal ratios in chronic heart failure: a need for standardisation and validation. *Eur J Nucl Med Mol Imaging.* 2008;35:547-553.
- (28) Yamashina S, Yamazaki J. Neuronal imaging using SPECT. *Eur J Nucl Med Mol Imaging.* 2007;34:939-950.

Samenvatting en conclusies

ALGEMENE SAMENVATTING

Voor de diagnostiek en risicostratificatie van patiënten met hart- en vaatziekten wordt veel gebruik gemaakt van niet-invasieve beeldvormende technologieën. Nucleaire beeldvorming met behulp van radioactieve stoffen, ook wel ‘tracers’ genoemd, wordt vooral toegepast in de evaluatie van patiënten met ischemische hartziekten.¹⁻³ Het myocard perfusiescintigram (MPS), waarbij de doorbloeding van het hart visueel wordt beoordeeld, is nog altijd het meest uitgevoerde nucleair cardiologisch onderzoek in Nederland.⁴ Echter, de introductie van nieuwe camera technologieën, geautomatiseerde software systemen en nieuwe tracers hebben het vakgebied veranderd.⁵ Kwantificatie speelt in toenemende mate een rol in de beoordeling van deze onderzoeken. Eerdere studies benadrukken de klinische meerwaarde van kwantificatie als aanvulling op de gebruikelijke visuele beoordeling van de afbeeldingen.⁵⁻⁹

In de introductie van dit proefschrift (*Hoofdstuk 1*) wordt een uiteenzetting gegeven van de belangrijkste technologische ontwikkelingen die bijgedragen hebben aan de evolutie van kwantitatieve nucleaire cardiologie. De daaropvolgende hoofdstukken richten zich op nieuwe inzichten en ontwikkelingen in de kwantificatie van perfusie, functie en innervatie.

Deel I – Myocard perfusie scintigrafie

Er zijn diverse commerciële en niet-commerciële software systemen beschikbaar voor de geautomatiseerde kwantificatie van ‘single-photon’ emissie computer tomografie (SPECT) MPS.⁶ Deze systemen kunnen onder andere volumina, wandbewegingen en wandverdikkingen van het hart bepalen. Echter, de toegevoegde waarde van dergelijke metingen hangt, onder meer, af van de mate waarin de waarden afhankelijk zijn van het software system zelf. In *Hoofdstuk 2* worden daarom de lineariteit, het functioneren en de parameterwaarden van twee klinisch gevalideerde systemen met elkaar vergeleken.^{10,11} De uitkomsten tonen goede correlaties tussen de waarden afkomstig van deze twee systemen. De gevonden verschillen in deze waarden zijn echter klinische relevant, en blijken afhankelijk van de hartgrootte. Over het algemeen zijn de gevonden discrepanties te herleiden tot de onderliggende algoritmen van de software systemen.

De visuele beoordeling van MPS beelden is afhankelijk van de hoeveelheid en locatie van extracardiale activiteit. Perfusie tracers (tetrofosmin en sestamibi) verlaten het lichaam via het hepatobiliaire systeem, wat kan leiden tot een extracardiale stapeling

van radioactiviteit nabij het hart. Het feit dat deze klaring tijdsafhankelijk is doet vermoeden dat de beeldkwaliteit ook tijdsafhankelijk kan zijn.^{12,13} De mate waarin de beeldkwaliteit en vooral de kwantificatie beïnvloed worden door het interval tussen de injectie van de tracer en de acquisitie is beschreven in *Hoofdstuk 3*. De resultaten laten zien dat de hoeveelheid extracardiale activiteit in de vroege scan (15 min na tracer injectie) aanzienlijk hoger is dan in de late scan (50 min na tracer injectie). Ook worden in de vroege scan vaker artefacten geïnduceerd waardoor de kwantitatieve analyse niet mogelijk is. Een onjuiste segmentatie van het myocard door het software systeem blijkt de belangrijkste reden voor de onbetrouwbare kwantificatie.

Nieuwe kwantitatieve parameters

'*Transient Ischemic Dilatation*' (TID) en *Ventriculaire Dissynchronie* zijn twee recent geïntroduceerde parameters die twee verschillende facetten van het hartfunctie beschrijven. In de literatuur wordt een abnormale TID beschreven als een belangrijke bevinding dat kan duiden op uitgebreid coronairia lijden.¹⁴⁻¹⁶ Toch zijn de mechanismen die verantwoordelijk zijn voor deze stress gebonden dilatatie nog altijd niet uitgekristalliseerd. In *Hoofdstuk 4* is de TID daarom gerelateerd aan andere functionele parameters om zo de onderliggende mechanismen beter te begrijpen. In tegenstelling tot de huidige opvattingen over de TID, bleek dat de relatie tussen de perfusie scores en de TID matig. Er was wel een sterke relatie aanwezig tussen de TID en het verschil in hartfrequentie tijdens de rust en post-stress acquisitie. Deze resultaten duiden op een afhankelijkheid van de hartfrequentie, waarmee de TID niet geschikt zou zijn als onafhankelijke marker voor uitgebreid coronairia lijden.

Ventriculaire dissynchronie analyse geeft inzicht in het moment van de regionale contractie van het hart.^{17,18} Onlangs is een geometrische methode geïntroduceerd die gebruik maakt van de regionale wandbeweging om de contractie-timing te bepalen. In *Hoofdstuk 5* is deze geometrische dissynchronie analyse gevalideerd. In een normale populatie bleek dat de geometrische kwantificatie uitvoerbaar in alle patiënten, en waren de parameters niet geslachtsafhankelijk. Deze normale dissynchronie metingen zijn vervolgens vergeleken met data van patiënten met bewezen ventriculaire dissynchronie. De resultaten geven aan dat de geometrische methode een haalbare methode is voor ventriculaire dissynchronie analyse in MPS. Echter, een goede segmentatie van het myocard blijkt zeer belangrijk voor deze analyse methode.

Deel II – Myocard innervatie scintigrafie

Momenteel is innervatie scintigrafie met radioactief gelabeld meta-iodobenzylguanidine (MIBG) de belangrijkste technologie om de sympathische innervatie status van het hart af te beelden.¹⁹⁻²¹ De kwantificatie van deze innervatie wordt voornamelijk uitgevoerd op basis van planaire opnamen. In de praktijk worden verschillende protocollen en berekeningen gehanteerd om de opname van I-123 MIBG in het hart te bepalen. *Hoofdstuk 6* geeft een uitgebreid overzicht van de verschillende methoden en normaalwaarden die gehanteerd worden. De resultaten van deze systematische evaluatie van de literatuur laten een grote variatie zien in zowel de acquisitie protocollen als kwantificatie methoden die gehanteerd worden. Deze variatie blijkt klinisch relevant en is zeer waarschijnlijk het gevolg van het ontbreken van standaardisatie.²²

Naast de planaire kwantificatie kan de globale sympathische innervatie ook geëvalueerd worden op basis van SPECT.²³ Ondanks dat deze werkwijze veel minder gebruikelijk is, geeft SPECT 3-dimensionele informatie waardoor het waarschijnlijk mogelijk is het hart met grotere precisie te segmenteren. In *Hoofdstuk 7* is daarom een volumetrische kwantificatie methode geïntroduceerd om de I-123 MIBG opname in SPECT data te kunnen bepalen. Uit de resultaten valt af te leiden dat de volumetrische kwantificatie zeer reproduceerbaar is. Ook wordt er een duidelijke correlatie gevonden tussen planaire en SPECT parameters. De klinische meerwaarde van een dergelijke SPECT kwantificatie zal in de toekomst nog bepaald moeten worden.

CONCLUSIES

Kwantificatie is een belangrijke rol gaan spelen binnen de nucleaire cardiologie. In tegenstelling tot het gemak waarmee kwantificatie uitgevoerd kan worden, zijn de algoritmen die verantwoordelijk zijn voor de berekeningen vaak complex. Daarom is het van belang om goed gevalideerde software systemen en parameters te gebruiken voor de diagnostiek en risicostratificatie van patiënten. Deze thesis benadrukt daarnaast het belang van kennis over de effecten die protocol en patiënt gerelateerde factoren kunnen hebben. De belangrijkste conclusies die op basis van het onderzoek in dit proefschrift gesteld kunnen worden zijn;

- Functionele meetwaarden van MPS zijn deels afhankelijk van het gebruikte software systeem, waarbij de verschillen tussen systemen klinisch relevant zijn.

- De bepaling van de '*Transient Ischemic Dilatation*' wordt beïnvloed door de hartfrequentie, waardoor deze parameter als onafhankelijke marker voor uitgebreid coronairia ongeschikt is.
- De evaluatie van ventriculaire dissynchronie in MPS data door middel van het geometrische algoritme geeft een betrouwbare benadering van de contractie.
- Er bestaat een grote diversiteit in de methoden die gebruikt worden voor de evaluatie van innervatie op basis van planaire I-123 MIBG scintigrafie. Verschillen in de diverse methoden kunnen als klinisch relevant beschouwd worden.
- Volumetrische kwantificatie van globale I-123 MIBG opname in SPECT data is reproduceerbaar en relateert aan de planaire metingen.

REFERENCE LIST

- (1) Clark AN, Beller GA. The present role of nuclear cardiology in clinical practice. *Q J Nucl Med Mol Imaging*. 2005;49:43-58.
- (2) Underwood SR, Anagnostopoulos C, Cerqueira M et al. Myocardial perfusion scintigraphy: the evidence. *Eur J Nucl Med Mol Imaging*. 2004;31:261-291.
- (3) Marcassa C, Bax JJ, Bengel F et al. Clinical value, cost-effectiveness, and safety of myocardial perfusion scintigraphy: a position statement. *Eur Heart J*. 2008;29:557-563.
- (4) RIVM. Overzicht nucleair geneekundige onderzoeken. Informatiesysteem Medische Stralingstoepassingen. 2010. Internet Communication
- (5) Ficaro EP, Corbett JR. Advances in quantitative perfusion SPECT imaging. *J Nucl Cardiol*. 2004;11:62-70.
- (6) Abidov A, Germano G, Hachamovitch R, Berman DS. Gated SPECT in assessment of regional and global left ventricular function: major tool of modern nuclear imaging. *J Nucl Cardiol*. 2006;13:261-279.
- (7) Petix NR, Sestini S, Coppola A et al. Prognostic value of combined perfusion and function by stress technetium-99m sestamibi gated SPECT myocardial perfusion imaging in patients with suspected or known coronary artery disease. *Am J Cardiol*. 2005;95:1351-1357.
- (8) Travin MI, Heller GV, Johnson LL et al. The prognostic value of ECG-gated SPECT imaging in patients undergoing stress Tc-99m sestamibi myocardial perfusion imaging. *J Nucl Cardiol*. 2004;11:253-262.
- (9) Xu Y, Hayes S, Ali I et al. Automatic and visual reproducibility of perfusion and function measures for myocardial perfusion SPECT. *J Nucl Cardiol*. 2010;17:1050-1057.
- (10) Ficaro EP, Lee BC, Kritzman JN, Corbett JR. Corridor4DM: the Michigan method for quantitative nuclear cardiology. *J Nucl Cardiol*. 2007;14:455-465.
- (11) Germano G, Kavanagh PB, Slomka PJ, Van Kriekinge SD, Pollard G, Berman DS. Quantitation in gated perfusion SPECT imaging: the Cedars-Sinai approach. *J Nucl Cardiol*. 2007;14:433-454.
- (12) Heo J, Iskandrian AS. Technetium-labeled myocardial perfusion agents. *Cardiol Clin*. 1994;12:187-198.
- (13) Baggish AL, Boucher CA. Radiopharmaceutical agents for myocardial perfusion imaging. *Circulation*. 2008;118:1668-1674.
- (14) Abidov A, Bax JJ, Hayes SW et al. Transient ischemic dilation ratio of the left ventricle is a significant predictor of future cardiac events in patients with otherwise normal myocardial perfusion SPECT. *J Am Coll Cardiol*. 2003;42:1818-1825.
- (15) Duarte PS, Smanio PE, Oliveira CA, Martins LR, Mastrocolla LE, Pereira JC. Clinical significance of transient left ventricular dilation assessed during myocardial Tc-99m sestamibi scintigraphy. *Arq Bras Cardiol*. 2003;81:474-482.

- (16) Hardebeck CJ. Transient ischemic dilation. *J Am Coll Cardiol.* 2004;44:211-212.
- (17) Bax JJ, Marwick TH, Molhoek SG et al. Left ventricular dyssynchrony predicts benefit of cardiac resynchronization therapy in patients with end-stage heart failure before pacemaker implantation. *Am J Cardiol.* 2003;92:1238-1240.
- (18) Boogers MM, Chen J, Bax JJ. Myocardial perfusion single photon emission computed tomography for the assessment of mechanical dyssynchrony. *Curr Opin Cardiol.* 2008;23:431-439.
- (19) Carrio I. Cardiac neurotransmission imaging. *J Nucl Med.* 2001;42:1062-1076.
- (20) Henneman MM, Bengel FM, van der Wall EE, Knuuti J, Bax JJ. Cardiac neuronal imaging: application in the evaluation of cardiac disease. *J Nucl Cardiol.* 2008;15:442-455.
- (21) Patel AD, Iskandrian AE. MIBG imaging. *J Nucl Cardiol.* 2002;9:75-94.
- (22) Verberne HJ, Habraken JB, van Eck-Smit BL, Agostini D, Jacobson AF. Variations in 123I-metaiodobenzylguanidine (MIBG) late heart mediastinal ratios in chronic heart failure: a need for standardisation and validation. *Eur J Nucl Med Mol Imaging.* 2008;35:547-553.
- (23) Yamashina S, Yamazaki J. Neuronal imaging using SPECT. *Eur J Nucl Med Mol Imaging.* 2007;34:939-950.

Curriculum Vitae and Publications

CURRICULUM VITAE

The author of this thesis was born on the 20th of august 1984 in Yde (Drenthe). She graduated at the Zernike College high school, first for the HAVO degree in 2001 and later for the VWO degree in 2003. In 2003 she was selected for the study Technical Medicine at the University of Twente (Enschede). In the following years she continued this study and chose for the master-specialisation '*Robotics & Imaging*'.

As part of the Technical Medicine master she performed clinical-research internships at different surgical and imaging departments in academic centres. The research performed at these departments covered diverse aspects of medical imaging. Her graduation research was performed at the Department of Radiology (head: prof. dr. J.L. Bloem), section Nuclear Medicine of the Leiden University Medical Hospital (LUMC). The focus of this project was on the quantification of function and innervation within the nuclear cardiology. After graduating Technical Medicine in 2010, receiving her MSc. degree, she continued doing research at the section Nuclear Medicine of the LUMC as PhD-student. The results of this research are presented in this thesis.

FULL PUBLICATIONS

B.J. van der Veen, N. Kuperij, M.P. Stokkel. Transient Ischemic Dilatation ratio derived from myocardial perfusion scintigraphy; What are we looking at? *J Nucl Cardiol* 2010; 17(2):207-215

B.J. van der Veen, A.J. Scholte, M.P. Stokkel. Mathematical methods to determine quantitative parameters of myocardial I-123 MIBG studies: a review of the literature. *Nucl Med Comm* 2010; 31(7):617-628

B.J. van der Veen, A.J. Scholte, P. Dibbets-Schneider, M.P. Stokkel. The consequences of a new software package for the quantification of gated-SPECT myocardial perfusion studies. *Eur J Nucl Med Mol Imaging* 2010; 37(9):1736-1744

I. Albutaihi, **B.J. van der Veen**, A.J. Scholte, M.P. Stokkel. The effects of early and late scanning on image quality and functional parameters in myocardial perfusion imaging. *Clin Nucl Med* 2010; 35(10):764-769

B.J. van der Veen, I. Al Younis, N. Ajmone-Marsan, J.J. Westenberg, J.J. Bax, M.P. Stokkel, A. de Roos. Ventricular dyssynchrony assessed by gated myocardial perfusion SPECT using a geometrical approach: a feasibility study. *Eur J Nucl Med Mol Imaging* 2012; 39(3):421-429

B.J. van der Veen, I. Al Younis, A. de Roos, M.P. Stokkel. Assessment of global cardiac I-123 MIBG uptake and washout using volumetric quantification of SPECT acquisitions. *J Nucl Cardiol* – Accepted

ABSTRACTS FOR PROCEEDINGS

B.J. van der Veen, A.J. Scholte, P. Dibbets-Schneider, M.P. Stokkel. The clinical consequences of a software package for the quantification of gated-SPECT myocardial perfusion studies. *European Association of Nuclear Medicine Barcelona 2009* – Oral poster presentation

B.J. van der Veen, N. Kuperij, M.P. Stokkel. The dependence of the Transient Ischemic Dilatation ratio on the heart rate during myocardial perfusion scintigraphy. *European Association of Nuclear Medicine Vienna 2010* – Poster

B.J. van der Veen, A.J. Scholte, M.P. Stokkel. The relationship between quantitative functional parameters derived with post-adenosine myocardial perfusion scintigraphy and I-123 MIBG. *European Association of Nuclear Medicine Vienna 2010* – Poster

B.J. van der Veen, N. Kuperij, M.P. Stokkel. Transient ischemic dilatation ratio derived from myocardial perfusion scintigraphy: What are we looking at? *Scientific meeting of the Dutch Society of Nuclear Medicine 2010* – Oral presentation

B.J. van der Veen, A.J. Scholte, M.P. Stokkel. The relation between quantitative parameters derived with I-123 MIBG and post-adenosine myocardial perfusion scintigraphy. *European Association of Nuclear Medicine Vienna 2010* – Poster

B.J. van der Veen, I. Al Younis, N. Ajmone-Marsan, J.J. Westenberg, J.J. Bax, M.P. Stokkel, A. de Roos. The assessment of dyssynchrony in gated myocardial perfusion scintigraphy using a geometrical approach. *European Association of Nuclear Medicine Birmingham 2011* – Oral presentation

B.J. van der Veen, I. Al Younis, N. Ajmone-Marsan, J.J. Westenberg, J.J. Bax, M.P. Stokkel, A. de Roos. The feasibility of dyssynchrony assessment in gated myocardial perfusion scintigraphy using a geometrical approach. *Scientific meeting of the Dutch Society of Technical Medicine 2011* – Oral Presentation

Acknowledgements

Looking back, I am surprised that after only two-and-a-half year I finished my PhD-thesis. During those years working at the section Nuclear Medicine of the LUMC I have been given many opportunities, for this I am grateful! And, because nobody can complete a PhD-program on one's own, it is a pleasure to thank all the people who made the successful realization of this thesis possible.

First and foremost, I would like to thank my copromotor dr. Marcel Stokkel for giving me the opportunity to start a PhD-program at the Leiden University Medical Hospital. He has been supportive and encouraging since the day I began working at the LUMC on my graduation thesis as a Master student. I would also like to show my gratitude to my promotor prof. dr. Albert de Roos for the helpful advice and critical comments in the second half of my PhD-program.

In my daily work I was surrounded by friendly and cheerful colleagues. So, I am indebted to all my colleagues of the Nuclear Medicine section for providing a stimulating and fun work environment. Special credits to Petra and Imad for their help in the time-consuming and sometimes dull process of data collection and reviewing.

I also want to say thanks to my dear friend and fellow PhD-student at the LUMC Bernardine, not only for the statistical advice, but also for the chatty lunchtime and afternoon-tea breaks.

For more reasons than one, I would also like to express thanks to my family and all my friends. Above all, I would like to thank my husband, Joost, and my parents, Jan en Janny, for stimulating me during my study, supporting me in my decisions and for their never-dying belief in me.

Thanks to each and everyone!

Linda

